1970

The ultrastructure of meiotic chromosomes of Lilium longiflorum

James Peyton Braselton
Iowa State University

THE ULTRASTRUCTURE OF MEIOTIC CHROMOSOMES OF *LILIUM LONGIFLORUM*

by

James Peyton Braselton

A Dissertation Submitted to the
Graduate Faculty in Partial Fulfillment of
The Requirements for the Degree of
DOCTOR OF PHILOSOPHY

Major Subject: Botany (Plant Cytology)

Approved:

Signature was redacted for privacy.

In Charge of Major Work

Signature was redacted for privacy.

Head of Major Department

Signature was redacted for privacy.

Dean of Graduate College

Iowa State University
Of Science and Technology
Ames, Iowa

1970

TABLE OF CONTENTS

INTRODUCTION

After Robert Brown discovered the nucleus in 1833, the early cytologists emphasized the general morphological changes that occur in it during cell divisions. Nuclear division (karyokinesis or mitosis) and its relation to cell division (cytokinesis) were described by 1880 (Hughes, c1959), but the concept of meiosis as being somehow complementary to fertilization did not develop until around 1890. Chromosomes were so named by Waldeyer in 1888 (De-Robertis, et al. 1954).

New importance was placed on chromosomes in 1903 when the fields of cytology and genetics were joined by the Sutton-Boveri Hypothesis. Emphasis shifted from the general total nuclear cycle to the structure of the individual chromosomes. Cytological and genetic data were correlated to the extent that genetic loci were matched with specific sites on chromosomes.

As modern molecular biology developed, biochemical, biophysical, and genetic information, often obtained from viruses and prokaryotes, established the molecular basis for heredity and cellular control almost independently of eukaryotic chromosome morphology. The typical prokaryotic chromosome consists of a single DNA double helix usually arranged in a ring, perhaps structurally involved with one or a few protein molecules. In contrast, the eukaryotic

chromosome is a relatively larger, more complex structure with a high proportion of protein and other non-nucleic acid constituents. It is obviously important that we understand the architecture of these important genetic structures. A lack of such an understanding has been a handicap to many areas of research in the life sciences.

The role of chromosomes as packages and means of distribution of genetic material during cell divisions is as significant as the function of chromatin in cellular control. We cannot minimize the importance of the eukaryotic chromosome in maintaining both the genetic continuity and diversity of higher living systems. For this reason, it is necessary to understand the morphological changes of chromosomes during mitosis and meiosis.

The purpose of this dissertation is to elucidate chromosome structure and behavior by studying the elementary chromosome fibril and its organization into other structural units in the course of meiosis.

LITERATURE REVIEW

Classical Meiosis and Chromosome Morphology

Classical cytologists believed that chromosomes consisted of one or more coiled threads, the "chromonemata", embedded in a "matrix", which was separated from the surrounding nucleoplasm by a "delicate interfacial membrane", the "pellicle" (cf. Kaufmann, 1948).

The meiotic stages and the characteristic morphology of the chromosomes during each stage are discussed in most cytology and cytogenetics textbooks (cf. Brown and Bertke, 1969; DeRobertis, et al. 1954; and Swanson, et al. 1967), and have been reviewed extensively over the years (John and Lewis, 1965; Kaufmann, 1948; Kaufmann, et al. 1960; Manton, 1950; Nebel, 1939; Rhoades, 1950, 1961; Sax and Humphrey, 1934; and Taylor, 1967a). The stages of the first meiotic division and their salient features as seen in light microscopy appear below.

Leptotene

The chromosomes appear as long, twisted, beaded filaments.

Zygotene

Homologous chromosomes begin to pair (synapsis). Each chromosome still appears single, but Rhoades (1961) on theoretical grounds believes the chromosomes to be divided at the time of synapsis.

Pachytene

Synapsis has been completed and the paired chromosomes contract longitudinally and appear thicker. Each pair of synapsed homologues is called a bivalent, even though chromatids within each chromosome can sometimes be distinguished (cf. Rhoades, 1950).

Diplotene

The homologues contract more extensively and the forces of synapsis cease and homologues separate except for chiasmata, which in many species begin to terminalize. Chromatids of each chromosome can be seen clearly.

During diplotene a period often occurs in which the bivalents lose their morphological identity and the nucleus fills with a interphase-like network of chromatin threads. Consequently this period is called "diffuse diplotene" or "dictyotene". This stage often is not considered in general discussions of meiosis. For reasons that will become apparent in the DISCUSSION, it is necessary to review diffuse diplotene in more detail than the other meiotic stages.

The diffuse stage in animal meiosis occurs in late diplotene (Ohno, et al. 1962; Ris, 1945; Seshachar and Bagga, 1963; and Teplitz and Ohno, 1963). The purpose and importance of the stage was summarized by Swanson (1958, p. 71): "In most instances the diffusion of chromatin is correlated with a growth in the cytoplasm; the phenomenon is generally observed in eggs that go through a long period of development to store

reserve materials in the form of yolk".

The diffuse stage in plant meiosis occurs at the onset of diplotene (Barry, 1969; Carr and Oliver, 1958; Ekberg and Eriksson, 1967; Ekberg, et al. 1968; Ghidoni, 1967; Mergen and Lester, 1961; Moens, 1964, 1968a; and Sen, 1969). However, Dill (1964) reported dictyotene in mosses to occur at the end of diplotene and indicated that there is no increase in cell size during dictyotene in plants.

Barry (1969) indicated that the diffuse stage in plants does not necessarily reflect increased gene activity as generally occurs in animals. Sen (1969, p. 125) with limited experimental verification, proposed that ". . . a gradual developmental reorganization of the chromatin into the individual chromatids takes place during and after 'diffuse stage'".

Ekberg and Eriksson (1967) reported that microsporocytes of Larix remain in diffuse diplotene over the winter. The earlier stages occur in the preceding fall, and the divisions go to completion in the following spring. However, in some locales in Sweden, poor seed set occurs (Ekberg, et al. 1968). Pollen sterility was suspected, and therefore microsporocyte meiosis was studied. In pollen-sterile plants meiosis proceeds beyond diffuse diplotene in the fall. When this occurs, no cell walls are formed at the end of meiosis. The first post meiotic mitosis is characterized by multipolar spindles, bridges, and lagging chromosomes. Their conclusion was that

". . . further development from the diplotene stage during the autumn is not favorable for a proper pollen formation" (p. 431).

Diakinesis

The chromosomes continue to contract by becoming tightly coiled. The bivalents become distributed throughout the nuclear area, the nuclear envelope breaks down, and the nucleolus disappears, or in some species detaches from its organizing chromosome.

Metaphase I

The spindle forms and the chromosomes orient on the metaphase plate equidistance from the poles. With special treatments (e.g., KCN, high temperature, or ammonia vapor) major and minor coils become evident. The chromatids are paranemically coiled which is in contrast to the plectonemic coiling of chromatids in mitotic chromosomes (cf. Manton, 1950).

Anaphase I

The chromosomes proceed from the metaphase plate toward the poles. Each anaphase group contains a haploid set of chromosomes. The two chromatids of each chromosome become relaxed and separate from each other except for their attachment at the kinetochore. Structures appearing to be half-chromatids, plectonemically coiled, have frequently been described (cf. Kaufmann, 1948; and Nebel, 1939).

Telophase I

When this stage occurs in most species, the nuclear envelope reconstructs and the coiled structures of the chromosomes relax.

Biochemistry

DNA

Taylor, et al. (1957) established that DNA constitutes a permanent, continuous part of the chromosome by following ^{3}H-thymidine labeled chromatids in Vicia mitosis. Filner (1965) demonstrated semi-conservative DNA replication in tobacco, as Meselson and Stahl (1958) had classically done with Escherichia coli.

DNA synthesis occurs in interphase 24-36 hours before prophase in Lilium meiosis (Taylor, 1953, 1959a). But Moses and Taylor (1955) observed that DNA synthesis in Tradescantia continues into prophase. Wimber and Prensky (1963) likewise reported that a slow DNA synthesis occurs during part of meiotic prophase I in the newt, Triturus; and postulated that it could be necessary for the "reunion" of broken chromatids at crossover or that the chromosomes had not completed replication by the beginning of prophase.

Hotta, et al. (1966) have more recently demonstrated that 0.3% of the total cellular DNA synthesis in both Lilium and Tradescantia occurs in zygotene and pachytene. When the prophase DNA synthesis is inhibited with deoxyadenosine in

leptotene-early zygotene the cells halt development; cells treated in early-mid zygotene undergo delayed and abortive first divisions; and cells treated in late zygotene and pachytene have chromosome breakage and abnormal second meiotic divisions (Ito, et al. 1967).

Roth and Ito (1967) correlated the inhibition of DNA synthesis with the formation of the synaptinemal complex. They concluded that late leptotene or early zygotene DNA synthesis is required to initiate synaptinemal complex formation, a special class of DNA is synthesized in late zygotene and is necessary for normal disjunction of the homologues at diplotene, and pachytene DNA synthesis is necessary for normal anaphase II separation of sister chromatids.

RNA

RNA synthesis extends into meiotic prophase (Das, 1965; Das and Alfert, 1966; Heslop-Harrison, 1969; Hotta and Stern, 1963; Stern and Hotta, 1963; and Taylor, 1967a).

The synthesis of RNA in animal meiosis is exemplified by Seshachar and Bagga (1963) who demonstrated that RNA synthesis in the dragonfly, Pantala flavescens, increases during the dictyotene stage when the cells and nuclei of the oocytes enlarge.

The results from plant meiosis (in microsporocytes) have been inconsistent. Hotta and Stern (1963) demonstrated in Trillium that RNA synthesis occurs in two intervals:

pachytene-diplotene and tetrad formation. Taylor (1967a) reported RNA synthesis rises in leptotene, decreases and remains low during zygotene, and increases during pachytene (the latter attributed to synthesis within the nucleolus). Heslop-Harrison (1969) reported a reduced ribosome population and a minimum of ribosomal RNA during diplotene-diakinesis. Das (1965) and Das and Alfert (1966) showed that RNA labeling decreases during prophase in Zea mays microsporocytes. Nucleolar RNA decreases much more rapidly than chromosomal RNA; diplotene and diakinesis label is due entirely to chromosomal RNA.

Protein

Protein does not distribute semi-conservatively during mitosis as does DNA; nor does it, including histone, appear to remain a permanent, fixed part of the nucleus (Prescott, 1964; Prescott and Bender, 1963; and Prescott and Stone, 1965).

Protein synthesis is rapid during premeiotic interphase and leptotene, and continues through prophase (Hotta and Stern, 1963; Hotta, et al. 1968; Parchman and Stern, 1969; Stern and Hotta, 1963; and Taylor, 1959a). Hotta and Stern (1963) demonstrated that protein synthesis in Trillium occurs in two intervals that parallel RNA synthesis: pachytene-diplotene and tetrad formation.

Hotta, et al. (1968) inhibited protein synthesis in Lilium longiflorum microsporocyte meiotic prophase. If

inhibition occurs at the end of zygotene, there is a failure of chiasmata formation. If cells are inhibited during very late zygotene-early pachytene, chiasmata are formed.

Parchman and Stern (1969) extended Hotta's work and summarized their results (see Table 1) by stating, "What is clear from this table and from preceding discussion is that continuous synthesis throughout meiotic prophase is essential to normal meiotic development" (p. 307).

Radiation induced chromosomal aberrations

Radiation induced chromosomal aberrations during plant meiosis have been shown by Crouse (1954, 1961), Mitra (1958), and Sparrow, et al. (1952).

Sparrow, et al. (1952) showed in Trillium microsporocytes that diplotene is the most sensitive meiotic stage to X-radiation. Likewise, Mitra (1958) demonstrated in Lilium longiflorum that there is a sensitivity peak at diplotene-diakinesis, and that there is a sudden increase of subchromatid type aberrations after irradiation at pachytene. Crouse (1954), also working with Lilium longiflorum, observed chromatid aberrations when irradiation takes place at pachytene, but half-chromatid aberrations when irradiation occurs during diakinesis and metaphase I. Swanson and Young (1965, p. 120) summarized the irradiation experiments of both meiosis and mitosis by stating, "The appearance of half-chromatid aberrations following irradiation in prophase (post-pachytene

Table 1. Cytological effects of cycloheximide on meiotic cells (modified from Parchman and Stern, 1969)

	Cytological abnormality	
Initial stage	Type	Stage becomes apparent
leptotene	arrest[a]	early prophase
early-mid zygotene	arrest	late prophase
mid zygotene	chromosome[b]	metaphase I
late zygotene	achiasmata	metaphase I
early pachytene	achiasmata	metaphase I
early-mid pachytene	chromosome and disjunction[c]	anaphase I
late pachytene	chromosome and disjunction	diakinesis and metaphase I
early diplotene	chromosome and disjunction	metaphase I and anaphase I
late diplotene	arrest	anaphase I through prophase II
diakinesis	arrest and disjunction	prophase II and metaphase II

[a]Arrest means the cells failed to develop beyond the stage indicated in the Stage column.

[b]Chromosome abnormalities indicate stickiness or fusion of bivalents and (or) contraction of metaphase arms more or less than normal.

[c]Disjunction abnormalities refer to failures in segregation of otherwise normal chromosomes.

in meiotic cells) poses a problem, therefore, since no new round of DNA synthesis has taken place. Why the chromatid behaves single to X rays in one instance and double in another is unclear".

Ultrastructure: Accessory Structures

The synaptinemal complex

Moses (1956) and Fawcett (1956) independently discovered in synapsed homologues a tripartite structure which is now referred to as the synaptinemal complex. It has been shown to occur during synapsis of homologues in meiotic prophase of a variety of animals, plants, and fungi (Aldrich, 1967; Carroll and Dykstra, 1966; Chardard, 1962; Coleman and Moses, 1964; Engles and Croes, 1968; Gassner, 1969; Lu, 1967; Moens, 1968a, 1968b, 1969a, 1969b; Moses, 1960, 1964; Moses and Coleman, 1964; Nebel, 1960; Nebel and Coulon, 1962a; Roth, 1966; Roth and Ito, 1967; Schin, 1965; Sheridan and Barrnet, 1969; Sotelo and Trujillo-Cenoz, 1958; Sotelo and Wettstein, 1966; Underbrink, et al. 1967b; Wolstenholm and Meyer, 1966; and Woollam and Ford, 1966). Menzel and Price (1966) observed synaptinemal complexes in a tomato-potato hybrid. Meiosis in these plants involves synapsis of homeologous chromosomes which seldom form chiasmata.

Only slight variation in the ultrastructural morphology of the complex has been shown (e.g., Sotelo and Wettstein, 1966). The majority of reports have agreed as to both the

structure and behavior of the synaptinemal complex. The following description has been largely derived from a review by Moses (1968) and an extensive study of synaptinemal complex formation in Lilium longiflorum by Moens (1968a).

The synaptinemal complex lies longitudinally in the axis between the two synapsed homologues of a bivalent, and in cross section it is completely surrounded by the chromatin of the bivalent. The structure is formed in early zygotene and is at its maximum expression during pachytene. It looses its axial orientation and is eliminated from the bivalent at the end of pachytene and at the onset of diffuse diplotene.

The most commonly presented plane of view is the "frontal plane" in which the synaptinemal complex consists of three regions: (1) the lateral elements, two parallel electron-dense ribbons (each 30-50 nm across) which are 65-100 nm apart and in contact with the chromatin; (2) a less electron-dense central region (65-100 nm across, the space between the lateral elements) which contains fine filaments perpendicular to the lateral elements; and (3) the central element, the electron-dense medial component of the complex.

Two hypotheses on the role of the synaptinemal complex are being debated. The more established hypothesis (cf. Moses, 1968) is that once chromosome pairing has occurred, the synaptinemal complex then operates at the "effective" level of pairing (molecular pairing) leading to crossing-over. As emphasized by Moses and Coleman (1964, p. 37), "The key to

such a hypothesis resides in knowing where DNA and related proteins are localized in the axial complex".

The second hypothesis (Comings and Okada, 1969; Menzel and Price, 1966; and Schin, 1965) is that the synaptinemal complex functions in chromosome pairing (synapsis), but is not specifically involved in the actual molecular pairing and crossing-over occurring in the bulk of the chromatin surrounding the synaptinemal complex.

Schin (1965) inferred from self-assembled multiple core complexes that the synaptinemal complex is protein. Comings and Okada (1969) showed with enzyme digestions on whole-mount chromosomes that all components of the synaptinemal complex are sensitive to proteolytic enzymes, but not so with DNase. On the contrary, Moses (1968, p. 387) in summarizing the ultracytochemistry of the synaptinemal complex stated that ". . . DNA is scarce or absent in the central region and central element, while it is present together with protein in the lateral elements, but in a lower concentration than in chromatin. The possibility of DNA filaments in the central region is thus not excluded".

Nucleolus

The interphase nucleolus is spherical; several microns in diameter; and composed of fibrils, granules, and electron-transparent "vacuoles" (Allen and Bowen, 1966; Brinkley, 1965; Brown and Ris, 1959; Chardard, 1962; Hay, 1968; Hsu,

et al. 1965; Hyde, 1966; Hyde, et al. 1965; Jacob and Sirlin, 1963, 1964; Kalnins, et al. 1964; Lafontaine, 1968; Lafontaine and Chouinard, 1963; Lafontaine and Lord, 1966; Marinozzi and Bernhard, 1963; Porter, 1960; Schoefl, 1964; Stevens, 1965; Swift, 1959, 1966; Swift and Stevens, 1966; and Underbrink, et al. 1967a).

The fibrils range from 5-10 nm in diameter; are densely packed in amorphous-appearing areas; and occur in the central area of the nucleolus (Allen and Bowen, 1966; Brinkley, 1965; Chouinard, 1966; Hyde, 1966; Hyde, et al. 1965; Jacob and Sirlin, 1964; Kalnins, et al. 1964; Lafontaine, 1968; Lafontaine and Chouinard, 1963; Lafontaine and Lord, 1966; Marinozzi and Bernhard, 1963; Porter, 1960; Stevens, 1965; Swift, 1959, 1966; and Swift and Stevens, 1966), uniformly distributed throughout the nucleolus (Brinkley, 1965; Brown and Ris, 1959; and Hsu, et al. 1965), or in twisting strands (the nucleolonema) approximately 40-100 nm in diameter (Brinkley, 1965; Schoefl, 1964; Stevens, 1965; Swift, 1966; and Underbrink, et al. 1967a).

The granules (15-20 nm in diameter) resemble cytoplasmic ribosomes except for being smaller and less regular in outline. These granules generally occur on the periphery of the nucleolus (Allen and Bowen, 1966; Brinkley, 1965; Hyde, 1966; Hyde, et al. 1965; Jacob and Sirlin, 1964; Lafontaine, 1968; Lafontaine and Lord, 1966; Marinozzi and Bernhard, 1963; Stevens, 1965; Swift, 1959, 1966; and Swift

and Stevens, 1966); but they also appear in 40-100 nm diameter strands (Brinkley, 1965; Chouinard, 1966; Lafontaine and Chouinard, 1963; Porter, 1960; Stevens, 1965; and Underbrink, et al. 1967a), or scattered throughout the nucleolus (Brinkley, 1965; Hsu, et al. 1965; and Swift, 1966).

The "vacuoles" are electron-transparent areas that occur in the amorphous-appearing fibrillar areas and contain loosely scattered granules and (or) fibrils (Allen and Bowen, 1966; Brinkley, 1965; Chouinard, 1966; Hyde, 1966; Lafontaine and Chouinard, 1963; and Swift, 1966).

Variations in nucleolus ultrastructure during mitosis include the dispersion of the nucleoli into smaller masses (Brinkley, 1965), the disintegration into surrounding nucleoplasm (Chouinard, 1966; Lafontaine, 1968; and Lafontaine and Chouinard, 1963), the loosening of the components with a loss of the granular areas and persistance of the fibrillar areas (Hsu, et al. 1965; and Underbrink, et al. 1967a), and the loosening of the granular zone accompanied by the loss of the fibrillar regions (Allen and Bowen, 1966).

Moens (1968a) followed the general position and shape of the nucleolus in Lilium longiflorum meiotic prophase. The nucleolus is spherical and separate from the nuclear envelope during leptotene, appressed to the nuclear envelope during zygotene, and separate from the nuclear envelope and spherical in pachytene through diffuse diplotene. His micrographs did not show any fine structural changes. All stages had dense,

amorphous appearing nucleoli which contained electron-transparent "vacuoles" scattered throughout.

Nucleolar organizer

Lafontaine and Chouinard (1963) described the nucleolar secondary constriction of mitotic Vicia chromosomes as fibrillar and of low electron density. Chardard (1962) presented micrographs of orchid meiosis that showed a less electron-dense region of the chromosome attached to the nucleolus.

Jacob and Sirlin (1964) described finely granular (10-15 nm particles) nucleolar organizers in salivary gland cells of Smittia. A study by Kalnins, et al. (1964) showed that Chironomid salivary gland chromosomes have nucleolar organizers consisting of groups of parallel 10 nm diameter fibrils. Hsu, et al. (1967) extensively studied the nucleolar organizer of the rat kangaroo (Potorous tridactylis) and found it consists of 5-8 nm diameter fibrils that are less electron-dense than the rest of the chromosome. They interpreted this loosely condensed state in mitotic metaphase as an intermediate step in condensation, indicating some metabolic activity.

The kinetochore

The various descriptions of kinetochore ultrastructure in the literature may be arbitrarily classified into the following groups.

Animal types

"Undifferentiated" The ultrastructure of kinetochores of a variety of organisms did not appear to differ from the rest of the chromatin, and these kinetochores were recognized only by the attachment of spindle microtubules (DuPraw, 1965c; Kane, 1962; Mota, 1962; Roth and Daniels, 1962; Roth, et al. 1966; and Wettstein and Sotelo, 1965).

"Granular" The diffuse kinetochore of Rhodnius appeared to consist of fine granules that stained less densely than the rest of the chromatin (Buck, 1967).

"Dense plate" Harris (1962, 1965) described the kinetochore of the sea urchin as an electron-opaque plate, 50 nm thick and 150 nm in diameter.

"Layered" Bernhard and de Harven (1960), George, et al. (1965), Krishan and Buck (1965), Murray, et al. (1965), and Robbins and Gonatas (1964) observed kinetochores similar to that described by Harris, except that the dense area is separated from the chromosome by a clear zone approximately 15 nm wide. Nebel and Coulon (1962b) reported pigeon spermatocyte chromosomes to have acorn-shaped kinetochores with several layers of varying electron-density. Luykx (1965) observed Urechis chromosomes with kinetochores consisting of a thin electron-transparent layer with thicker electron-dense areas on each side. Mitotic rat kinetochores appeared disk-shaped with an outer electron-dense layer of fine fibrils or granules, a middle electron-transparent layer, and an inner

electron-dense layer continuous with the chromatin (Jokelainen, 1967).

"Lampbrush configuration" Chinese hamster kinetochores were described as having a dense core (20-30 nm diameter) surrounded by a less dense zone (20-60 nm wide) that contained microfibrils (5-9 nm diameter) looping out perpendicularly from the core (Brinkley and Stubblefield, 1966; and Stubblefield and Brinkley, 1967). This configuration was interpreted to be an indication of synthetic activity, presumably because the kinetochore, in contrast to the rest of the chromosome, remains active in cell division.

Plant types Descriptions of plant kinetochore ultrastructure are not as diverse as animal types, and may be placed in the following four classes.

"Undifferentiated" As in animals, this type was recognized only by the attachment of spindle microtubules (Ichida and Fuller, 1968; Pickett-Heaps and Northcote, 1966; Roth, et al. 1966; and Underbrink, et al. 1967a). Cronshaw and Esau (1968) reported Nicotiana kinetochores as undifferentiated depressed areas with granular regions on both sides.

"Granular" Bajer (1968a), Harris and Bajer (1965), and Wilson (1967, 1968) described the kinetochore as a ball consisting of 7-8 nm diameter granules and less electron-dense than the rest of the chromosome.

"Fibrillar" Manton (1964b) reported fibrillar kinetochores in Equisetum meiosis that appear less electron-

dense than the rest of the chromosomes. Allen and Bowen (1966) indicated a fibrillar nature in Psilotum mitotic kinetochores when they referred to ". . . a finer texture . . . than the rest of the chromosome" (p. 305).

"Undecided" This class includes three studies that showed a differentiation of structure from the rest of the chromosome, but which made no mention as to the nature of the structural components. Dietrich (1966, 1968) described Lilium candidum kinetochores as less dense than the rest of the chromosome. Bajer (1968b), working with Haemanthus, reported the kinetochore as a ball-shaped body consisting of bands of lighter and darker material, with the spindle microtubules embedded in the lighter material.

The spindle

Classical cytologists have recognized two types of spindle fibers in both mitosis and meiosis: the pole-to-pole "continuous fibers" and the pole-to-kinetochore "chromosomal fibers" (cf. Schrader, 1953). Both types of fibers are composed of bundles of 14-30 nm diameter microtubules (Allen and Bowen, 1966; Bajer, 1968a, 1968b, 1968c; Bernhard and de Harven, 1960; Bowen, 1959; Brinkley and Stubblefield, 1966; Buck, 1967; Chardard, 1962; Cronshaw and Esau, 1968; Dietrich, 1966, 1968; George, et al. 1965; Harris, 1961, 1962, 1965; Harris and Bajer, 1965; Harris and Mazia, 1962; Ichida and Fuller, 1968; Jensen and Bajer, 1969; Jokelainen, 1967; Kane,

1962; Krishan and Buck, 1965; Ledbetter and Porter, 1963; Luykx, 1965; Manton, 1964a, 1964b; Moor, 1967; Mota, 1962; Murray, et al. 1965; Newcomb, 1969; Pickett-Heaps and Northcote, 1966; Robbins and Gonatas, 1964; Roth, 1964, 1967; Roth and Daniels, 1962; Roth, et al. 1966; Sakai, 1968; Sato, 1958, 1960; Stubblefield and Brinkley, 1967; and Wilson, 1967, 1968).

The number of microtubules attached to the kinetochore ranges from 4-7 in rat mitosis (Jokelainen, 1967), 10 in sea urchin (Harris, 1965), and 16 in yeast (Moor, 1967), to 70-150 in Haemanthus mitosis (Bajer, 1968b).

Microtubules of the continuous fibers usually do not involve chromosomes (e.g., Allen and Bowen, 1966; Jensen and Bajer, 1969; and Manton, 1964b); but Bajer (1968b), Buck (1967), Pickett-Heaps and Northcote (1966), and Robbins and Gonatas (1964) have also shown individual microtubules piercing the chromosome arms.

Cronshaw and Esau (1968) postulated that observed undulations of the spindle microtubules are due to microwaves traveling along the microtubules at the time of fixation. Jensen and Bajer (1969) and Bajer (personal communication, University of Oregon, Eugene, Oregon) attributed the waviness of the spindle microtubules in Haemanthus to shrinkage of the chromosome arms during dehydration in preparation for electron microscopy, and maintained that the microtubules are straight in the living state.

Ultrastructure: The Chromatin

The elementary chromosome fibril

The most definitive statement about chromosome ultrastructure is that chromosomes basically consist of fibrils of varying thickness (generally 10-30 nm in diameter) and of undetermined length (Abuelo and Moore, 1969; Allen and Bowen, 1966; Amano, et al. 1956; Ambrose, et al. 1956; Bopp-Hassenkamp, 1959; Brinkley, 1965; Chardard, 1962; DuPraw, 1965a, 1965b, 1965c, 1966, 1968; DuPraw and Bahr, 1968, 1969; DuPraw and Rae, 1966; Faberge', 1967; Hsu, et al. 1967; Kaufmann and De, 1956; Kaufmann and McDonald, 1956; Nebel, 1959, 1960; Ris, 1956, 1961, 1962, 1966a, 1966b; Ris and Chandler, 1963; Shinke, 1959; Sparvoli, et al. 1965; Swift, 1965; Underbrink, et al. 1967a; Wolfe, 1965a, 1965b, 1967; Wolfe and Grim, 1967; Wolfe and Hewitt, 1966; Wolfe and John, 1965; and Wolfe and Martin, 1967). The extremes in diameter range from 5 nm (DeRobertis, 1956; and Hay and Revel, 1963) through 50 nm (Davies and Tooze, 1964; Gay, 1956; and Ris, 1955).

DuPraw (1965c, 1966) observed an increase in diameter of the fibrils from 23 nm at interphase to greater than 30 nm at mitotic metaphase, and also showed via quantitative electron microscopy (DuPraw and Bahr, 1968, 1969) an increase in the packing ratio of DNA to fibril length from 56:1 in interphase to 100:1 in metaphase. A similar situation was shown in grasshopper meiosis (DeRobertis, 1956) where the mean diameters

of the fibrils increase from 4.7 nm at early prophase to 7 nm during late prophase and 10 nm at metaphase.

Wolfe and Grim (1967) attributed the observed difference in diameters of whole-mount (25 nm) and sectioned (10 nm) fibrils to the rupturing of the cell membranes during the spreading technique, and maintained that the elementary chromosome fibrils in the living state are nearer to the 10 nm diameter. Jensen and Bajer (1969) showed an overall shrinkage of the chromosome arms during dehydration in preparation for embedding for thin-sectioning. Bajer (personal communication, University of Oregon, Eugene, Oregon) emphasized that the diameters of the elementary chromosome fibrils are also likely to change during dehydration procedures, but he did not predict whether their diameters would increase or decrease.

Substructure of the elementary chromosome fibril

The substructure of the elementary chromosome fibril has been variously described throughout the literature.

Kaufmann and De (1956) and Kaufmann and McDonald (1956) described in Tradescantia mitosis and meiosis respectively, the formation of the 12.5 nm diameter fibril from the coiling of two 4 nm threads around a 4 nm core. Amano, et al. (1956) observed 2-3 nm diameter "protochromonema" spiraled into 26-30 nm diameter "subchromonema" in interkinetic lymphocytes, monocytes, and plasma cells; Bopp-Hassenkamp (1959) reported 2-3 nm diameter subunits in the elementary chromosome fibril

from a variety of plant meiotic cells; Shinke (1959) saw electron-dense fibrils 3-5 nm diameter in plant interphase material; and Nebel (1959) likewise reported a 3 nm thread in mouse meiotic metaphase. Nebel said, however, that four of these strands are paranemically coiled to form the 20-50 nm threads. Ris (1956) observed electron-dense 6 nm parallel threads in Lilium meiotic prophase, but he interpreted them as the edges of a 20 nm fibril with an electron-transparent core. Wettstein and Sotelo (1965) reported that the 10 nm elementary chromosome fibril consists of irregularly coiled 1.5-2.0 nm diameter subunits.

Using the whole-mount technique developed by Gall (1963), Ris (1966a) speculated that a 20 nm fibril forms from the supercoiling of a 10 nm fibril and that each 10 nm fibril contains two parallel DNA strands with associated proteins. However, in reviewing and updating his previous work, he (Ris, 1966b) stated that the 25 nm fibrils are composed of two parallel 10 nm fibrils (possibly the same fibril folded back onto itself), each of which contains a pronase-resistant, DNase-sensitive fibril about 2.5 nm thick. Abuelo and Moore (1969), on the contrary, showed that the elementary chromosome fibril consists of a single 2.5-5 nm diameter trypsin-resistant core surrounded by a trypsin-sensitive sheath 20-25 nm in diameter. DuPraw (1965a, 1965b, 1968) and DuPraw and Bahr (1968, 1969) described the elementary chromosome fibril as a "type B" fibril, 20-50 nm in diameter, which in turn consists

of a coiled "type A" fibril, 5-11 nm in diameter, which is formed from the coiling and packing of a single DNA strand with proteins.

Higher organization of the elementary chromosome fibril

Faberge' (1967), Hay and Revel (1963), Luykx (1965), Wettstein and Sotelo (1965), and Wolfe (1965b) saw no apparent organization of the elementary chromosome fibril into intermediate units within the chromosomes.

Ris (1956) reported that 20 nm fibrils occur in parallel pairs in Lilium meiotic prophase, and Barnicot (1967) reported many parallel fibrils in newt mitotic chromosomes. Wolfe and Hewitt (1966) observed many parallel fibrils in Oncopeltus meiotic prophase chromosomes, and attributed the increase in number of these fibrils between zygotene and diakinesis to an increase in parallel folding. DuPraw (1965a, 1966, 1968) proposed a "folded-fiber" model for the chromosome, in which an elementary chromosome fibril ". . . is repeatedly folded back on itself both longitudinally and transversely to make up the body of the chromatid . . ." (DuPraw, 1968, p. 558).

As indicated by Peveling (1968) in a review, the most commonly reported observation has been the coiling of the elementary chromosome fibril into several higher orders.

Amano, et al. (1956) observed interkinetic nuclei of lymphocytes, monocytes, and plasma cells and described spiralization of the 26-30 nm diameter "subchromonemata"

into 120 nm diameter "chromonemata", which in turn spiral to form the 500 nm diameter chromosomes. The diameters of the gyres in these spirals were said to increase during "contraction" of the chromosomes, and to decrease during "loosening". Kaufmann and De (1956) in Tradescantia mitosis, Kaufmann and McDonald (1956) in Tradescantia meiosis, and Bopp-Hassenkamp (1959) in meiotic prophase of several plant species observed 35-100 nm "chromonemata" and reported that these "chromonemata" consist of spiraled 10-12.5 nm diameter fibrils. Nebel (1959, 1960) described a hierarchy of coils in mouse meiotic chromosomes in which the elementary fibril forms a coil with a 200 nm diameter gyre. In turn, this unit coils again yielding the "major" coil of meiosis, a 1-3 μm diamter gyre.

Shinke (1959), using interphase plant material, assigned the term "elementary helices" to the 30-50 nm diameter units that are formed from coiled 20 nm fibrils. The "elementary helices" then spiral into 100-130 nm diameter "subchromonema" which likewise spiral into 400-500 nm "chromonema". Allen and Bowen (1966) similarly reported in Psilotum mitosis parallel 10 nm fibrils that give the appearance of a 40 nm diameter helix.

Chardard (1962) reported that coiled 8-10 nm diameter fibrils constitute 30-70 nm diameter helices in first meiotic metaphase in orchids. The helices are often separated by clear areas (approximately 50 nm across) that appear similar

to the nucleoplasm surrounding the chromosomes. The clear areas are more obvious in diplotene and diakinesis and were interpreted as areas of separation between the chromatids as well as the axes of coiling of the chromonema. The units of chromatin between the clear areas decrease from diameters of 120 nm and 50-100 nm diameters in diplotene and diakinesis, respectively to the 30-70 nm unit of metaphase. The decrease was attributed to the "contraction" of the chromosomes.

Lafontaine and Chouinard (1963) and Lafontaine (1968) also observed "light zones" in Vicia mitosis, and interpreted them as spaces between chromonemal coils. The light zones are prominent in prophase but decrease in number and size as prophase progresses. Metaphase chromosomes are condensed to the extent that the only observed structural elements are granules and convoluted tubules. The only evidence of chromosome gyres are the undulating contours of the chromosome mass. Lafontaine (1969, p. 164) postulated that ". . . a matrixlike substance is responsible for the masking of their coiled organization under the electron microscope". Other "light areas" were observed in the center of cross sectioned anaphase chromosomes and were interpreted as chromosome "cores".

Steffensen (1959) and Kaufmann, et al. (1960) proposed a "rope" model for the chromosome that starts with a DNA-protein complex which pairs and coils with an identical partner. This pattern is repeated, each subsequently-formed unit pairing and coiling with an identical partner, until half-chromatids,

chromatids, and chromosomes are formed. Such a chromosome would contain 64 parallel strands of DNA.

Cole (1962) predicted different levels of coiling from the interactions between DNA and protein. The attachment of protein (presumably histone) to the DNA molecule would produce a 13.8 nm diameter coil, which would associate with additional protein to form a 140 nm diameter coil (the "chromonema"), which again would associate with protein to form the coils observed in chromatids. This model, in contrast to Steffensen's and Kaufmann's, contains only one DNA strand per chromatid.

Chromosome models

In addition to the models by Cole, DuPraw, Steffensen, and Kaufmann, et al. presented in the preceding section, several other chromosome models have been discussed in the literature.

The "centipede" model is characterized by a core consisting of two parallel side-by-side, ribbon-shaped units of unspecified chemical composition, with DNA molecules attached to and radiating perpendicularly from the core (Taylor, 1957, 1958a, 1958b). Nebel and Coulon (1962a) and Painter (1964) interpreted meiotic prophase chromosomes to fit this model, and reported "lateral loops" of chromatin fibrils connected to the core (the lateral element of the synaptinemal complex). Stubblefield and Wray (1969) and Wray and Stubblefield (1969) isolated what they consider to be the ribbon-shaped cores of

Chinese hamster mitotic chromosomes, supporting the original Taylor model. The core was presumed to consist of parallel deoxyribonucleoprotein fibrils which differ in histone composition from the chromatin attached to the core.

The "linker model" was proposed by Schwartz (1955) and Freese (1958), and eventually modified into a "ladder" model by Taylor (1963). The essence of the model is that the chromosome consists of tandem DNA double helices connected by "linkers" which are presumably histone or some special type of DNA. Uhl (1965a, 1965b) modified this model to explain crossing-over with both single-stranded and multi-stranded chromatids. Taylor (1967b) again revised the model, eliminating the tandem situation in favor of one continuous DNA double helix with replication guides (former "linkers") connected along the DNA molecule.

De (1964) proposed a model in which DNA molecules associated with histone are arranged like rungs on a ladder with parallel, spirally-coiled protein backbones analogous to the ladder sidepieces.

Peacock (1965) proposed a "bineme" chromosome model in which the chromatids contain two parallel strands of DNA, each equivalent to a subchromatid. The like strands of the two helices were postulated to be connected to each other by some type of unidentified bond, possibly in the kinetochore region. The like DNA strands would therefore act as one unit, so that semi-conservative DNA distribution would be maintained during

mitosis. The two-subchromatid condition would allow for the radiation-induced subchromatid aberrations as well as for the light microscopic observations which indicate subunits within chromatids (cf. Kaufmann, 1948).

MATERIALS AND METHODS

Lilium longiflorum var. Arai (2n=24) bulbs were obtained from a commercial supplier, potted in soil, and grown in the Iowa State University botany greenhouses or in growth chambers with 15.5°C, 11 hour nights, and 22°C, 13 hour days.

Stages of meiosis were roughly correlated with bud length by measuring from the base to the top of the longest petal with vernier calipers (Erickson, 1948). The stage of each flower bud to be fixed was determined by squashing one of the anthers in lacto-acetic orcein (modified Darlington and LaCour, 1950) and examining it in the light microscope (Figures 1-8). The remaining five anthers of each bud were prepared for electron microscopy.

Electron Microscopy

Fixation, dehydration, and embedment

Anthers were longitudinally halved (two locules per half), each half transversely quartered, and then fixed in 3% v/v glutaraldhyde (Sabatini, *et al.* 1963) or 3% v/v glutaraldehyde-3% v/v acrolein (Sanborn, *et al.* 1964) in 0.05-0.1 M phosphate buffer, pH 6.8-7.4 at 4°C for 12 hours or 23°C for one hour. The material was rinsed thoroughly in the buffer, postfixed in 1% w/v buffered osmium tetroxide (Millonig, 1961) for one-half to one hour, dehydrated in an ethanol-propylene oxide series, and embedded in Epon-Araldite (modified Anderson and

Ellis, 1965). These procedures are given in detail in Appendix A.

Sectioning and staining

Embedded material was trimmed with a single edge razor blade to a truncated pyramid with a face that contained in cross section the two locules of the halved anther. Thick sections 1 µm were cut with glass knives on the LKB Ultratome III ultramicrotome and examined with phase-contrast light microscopy to locate cells at desired stages and orientations. By adjusting the light and microscope on the ultramicrotome, the same cells seen in the thick section could be located in the block. The block was trimmed to the desired cell(s) by using the ultramicrotome equipped with glass knives.

Thin sections (40-80 nm) were cut on the same ultramicrotome using a DuPont diamond knife. Serial sections were picked up on Formvar-carbon coated 75 or 100 mesh copper grids. The sections were stained with 10% uranyl acetate in methanol (Appendix A) for 20 minutes (Stempak and Ward, 1964).

Freeze-etching

Many trials with numerous variations were attempted. Variations in the procedures were concentration, temperature, and pH of the fixative (including non-fixed material); type, concentration, and length of infiltration of cryoprotective agent; length and type of etching; ultimate vacuum at time of fracture; type of shadowing material; and type of replica

cleaning solution. The procedure described in the following paragraph, and described in detail Appendix B, was the only procedure that gave satisfactory results for the material used in this study.

Sporocytes were squeezed directly into 3% v/v glutaraldehyde in 0.1 M phosphate buffer, pH 6.8, and fixed for one hour at room temperature. The suspension was loosely pelleted using a clinical centrifuge, rinsed three times with the phosphate buffer, infiltrated with 30% ethylene glycol and frozen in liquid propane cooled with liquid nitrogen.

Fracturing, etching, and shadowing were carried out utilizing a Berkley Freeze-Etch Device (C. W. French) fitted to a Varian VE-30M vacuum evaporator equipped with modified Ladd electrodes. Replicas were cleaned with standard laboratory dichromate cleaning solution, rinsed six times with double distilled water, and picked up on 400 mesh copper grids.

Specimen examination

Specimens were examined with an Hitachi HU-11C electron microscope. Micrographs were recorded on DuPont Cronar Ortho S litho film which was developed in Kodak D-19. Enlargements of micrographs of sectioned material were made from the negatives using standard photographic techniques, but micrographs from freeze-etched replicas required additional processing.

Due to the nature of shadowing in freeze-etching (platinum is electron-opaque), the film that comes directly

from the electron microscope contains a positive image, i.e., the platinum deposits appear light, and the areas without platinum appear dark. The platinum appears and acts as a pseudo-light source. If prints were to be made directly from these negatives, the images formed would yield erroneous information, i.e., the light areas (areas without platinum) would not appear as natural illumination and the dark areas (platinum deposits) would not have the characteristics of true shadows.

Internegatives were made by contacting the original negatives onto Kodak Panatomic-X sheet film, which was developed in Kodak D-76 using standard photographic techniques. Enlargements from the internegatives gave prints that contained, as the original negative, correct illumination (platinum acting as a pseudo-light source) with undistorted shadows (areas with no platinum deposits). All shadowed prints have been presented with the direction of platinum (pseudo-light source) coming from the upper left (indicated by an arrow) so that concave and convex areas are perceived as such.

Light Microscopy

Squashes and 1 μm plastic sections were used as described earlier to determine stages of cell division. Squashes were made permanent by freezing with liquid carbon dioxide, popping off the cover slip, dehydrating in 95% ethanol, and mounting

with Diaphane (Bowen, 1956). Plastic sections were dried onto a slide and mounted with Piccolyte. Some thick sections were stained with one percent aqueous safranin O prior to mounting.

Squashes were studied in bright field, and plastic sections were studied under phase-contrast with either a Leitz Labolux or Leitz Ortholux microscope. Micrographs were recorded on Kodak Panatomic-X 35 mm film using a Leitz Orthomat Microscope Camera mounted on the Ortholux. Panatomic-X was developed in Microdol-X and prints were made using standard photographic procedures.

OBSERVATIONS

Accessory Structures

The synaptinemal complex

Synaptinemal complexes appear in early zygotene (Figures 9 and 24), are most obvious during pachytene (Figures 10, 28, and 29), and are not observable in any stage thereafter. They lie in the axes between the homologues of the bivalents (Figures 9, 10, 24, and 29), and in cross section are completely surrounded by the chromatin of the bivalent (Figure 28).

When observed in the frontal plane, each synaptinemal complex is 200-250 nm across, and can be seen to consist of the three components previously reviewed by Moses (1968). The outermost component, the lateral complex, is in contact with the chromatin, and consists of two electron-dense parallel strips (each 50-60 nm wide) which are separated by the central region. The less electron-dense central region is 100 nm across and contains fine filaments (5-8 nm in diameter) perpendicular to the lateral complex. The electron-dense central element (25-30 nm wide) is the median component of the central region as well as of the entire complex.

Nucleolar organizer

The chromatin attached to the nucleolus, the nucleolar organizer, is less electron-dense than the rest of the chromatin, and consists of fine 7.5-12.5 nm diameter fibrils (Figures 11 and 12). These fibrils are more distinct than those in the kinetochores (see Kinetochore, p. 38) and are not as tightly appressed to each other as those in the bulk of the chromatin or in the nucleoli (see Nucleolus).

Nucleolus

Nucleoli are appressed to the nuclear envelope during zygotene and in sections form spindle-shaped profiles (Figures 13 and 21). They are separate from the nuclear envelope and circular in profile from pachytene (Figure 14) through diplotene (Figures 15 and 16). No nucleoli were observed after diplotene until late anaphase I (Figure 116). Nothing that could be interpreted as nucleolar degeneration or fragmentation was observed.

At low magnification the nucleoli are electron-dense and appear amorphous, with relatively electron-transparent 50-100 nm diameter "vacuoles" scattered throughout (Figures 13-16). Occasionally large "vacuoles" up to 750 nm in diameter occur (Figure 14). The possibility exists that some of these "vacuoles" are profiles of portions of the nucleolar organizers embedded in the nucleoli.

At higher magnification the amorphous portion of the nucleolus can be seen to consist of very densely packed 10-15 nm diameter fibrils (Figure 9). No granular areas were observed.

Kinetochore

Metaphase I and anaphase I kinetochores are less electron-dense than the majority of the chromatin, roughly circular in profile (1 μm in diameter), and composed of 7-20 nm diameter fibrils with indistinct boundaries (Figures 85-88, 99, 103, and 117). Some chromatin fibrils project into the lighter kinetochore region (Figures 87 and 88). The fibrils of the kinetochores are more distinct in telophase I when despiralization of the chromosomes, including the kinetochores, occurs (Figure 117).

By counting the profiles of microtubules in serial sections of kinetochores, approximately 150-200 microtubules are estimated to end in each metaphase I kinetochore. However, no specific attachment sites can be detected.

The spindle

Spindle microtubules are observable in abundance only in the material fixed at room temperature and pH 6.8.

Two types of spindle microtubules occur in metaphase I and anaphase I: chromosomal (Figures 52, 85-88, and 103) and continuous (Figures 53 and 54). Both type are 20-30 nm in diameter, of undetermined length, and slightly undulating (Figures 53, 54, and 85-88).

Chromosomal microtubules end in the kinetochores (see Kinetochore, p. 38). Continuous microtubules extend through the metaphase plate, passing between the bivalents (Figure 54) and between homologues of a given bivalent (Figures 53 and 54), with some even piercing the chromosome arms (Figures 54 and 86).

The Chromatin

Superficially, the Lilium chromatin at meiosis appears granular, but critical examination reveals that the fundamental structural units are fibrillar. The elementary chromosome fibrils are electron-dense, 20 nm in diameter, and of undetermined length. No structures that could be interpreted as either chromosomal cores ("backbones"), matrices, or pellicles were ever observed in any of the stages of first division. It appears that chromosome morphology consists entirely of the elementary chromosome fibrils.

These 20 nm fibrils are present in all of the stages of the first meiotic division, but the larger units that the fibrils form vary in texture, compactness, and size among the various stages. Consequently the chromatin of each stage has its own characteristic appearance which has developed from the preceding stages and will develop into the following stages.

Leptotene

The 20 nm fibrils form units 80-120 nm wide in profile, and in favorable sections can be seen to have parallel curved arrays that suggest coiling (Figures 18 and 19). The 80-120 nm units have twisted profiles which are loosely paired into units 300-500 nm wide (Figure 20). Each 300-500 nm unit is considered to be a chromosome (the threads seen with the light microscope), and each of the 80-120 nm elements is therefore considered a chromatid.

Zygotene

Zygotene is characterized by the appearance of the synaptinemal complex (see The synaptinemal complex, p. 36) and the nucleolus appressed to the nuclear envelope (see Nucleolus, p. 37).

The 20 nm fibrils form configurations indicating that they coil into 80-120 nm elements as in leptotene (Figures 22 and 23). The zygotene chromatids, however, are 200-250 nm in diameter, and each chromatid appears to consist of a super-coiled 80-120 nm element (Figure 24). The chromosomes which consist of the paired chromatids are 500-600 nm in diameter, and the bivalents, including the synaptinemal complex, are 800-1000 nm in diameter.

In zygotene, as will be noted in later stages, as the units of chromatin become appressed to each other, the fibrils of each of the appressed units interdigitate to the extent

that the boundaries between the units are concealed except for clear spaces (Figure 24). The clear spaces appear similar to the relatively electron-transparent nucleoplasm surrounding the chromatin, and can be shown with serial sections (see Metaphase, p. 44) to be continuous with this surrounding nucleoplasm.

Pachytene

Pachytene chromatin (Figures 10 and 26-29) is more tightly packed than the previous stages. The 20 nm fibrils as in previous stages appear in configurations that suggest they are coiled into the 80-120 nm elements (Figures 26 and 27). The 80-120 nm elements likewise appear coiled very tightly into the 300 nm chromatids (Figures 26 and 27).

The most striking aspect of pachytene chromatin is its overall amorphous appearance in contrast to the granular appearance of the preceding and following stages. In cross section (Figure 28) the homologues of the bivalent cannot be distinguished; instead the chromatin is compactly arranged, and often appears to be uniformly distributed around the axial synaptinemal complex. Occasionally a clear space delineates a 300 nm chromatid (Figures 28 and 29). The bivalents (1-1.5 μm in diameter, including the synaptinemal complex) have undulating outlines which suggest a coiled arrangement of the chromatids and chromosomes (Figures 28 and 29).

Diffuse diplotene

Immediately after pachytene, in both the light and electron microscope studies, the chromatin changes from the compact arrangement of pachytene to a loosely arranged state in which the individual bivalents are difficult to distinguish (compare Figures 2 and 3, 25 and 30, and 28 and 31). Neither synaptinemal complexes nor remnants of them were observed from this stage on.

The 20 nm fibrils are arranged into 80-120 nm elements (Figures 40-43) which are loosely twisted into 175-250 nm profiles (Figure 32). In turn the 175-250 nm profiles are loosely twisted into 500-600 nm units which occasionally occur in pairs and often are loosely aggregated into masses of chromatin 2-2.5 μm across (Figure 31). These large masses are interpreted as areas at or near chiasmata, i. e., they are large because portions of each homologue of the bivalent are closely associated and intertwined.

The standard units of chromosomal organization can be more easily distinguished near the end of diffuse when the typical bivalents and chromosomes begin to reappear. Each chromosome (1.5-1.75 μm in maximum diameter) then consists of two loosely associated 500-600 nm chromatids (Figure 32). The most drastic change from pachytene is that now two structures, apparently subchromatids (each 175-250 nm in diameter), are seen side-by-side in the chromatids (Figures 32 and 33).

Profiles of this size were seen in earlier stages of diffuse diplotene, but their relation to the higher order units were not evident at that time.

Freeze-etch preparations (Figures 34-37) show 80-120 nm, 200-300 nm, and 600-800 nm profiles of chromatin, but the interrelations of these units into chromosomes, chromatids, and subchromatids are not apparent. The profiles of the elementary chromosome fibrils in freeze-etch preparations are 10 nm in diameter in contrast to the 20 nm fibril profiles seen in thin sections.

Late diplotene

In late diplotene, the units seen at the end of diffuse diplotene are more clearly recognizable (Figure 39). The homologues are separated (except in the vicinity of chiasmata) by a large clear space continuous with the surrounding nucleoplasm, and prominent clear spaces between chromatids indicate that the chromatids are not tightly coiled together (Figure 39).

Profiles of the 20 nm fibrils suggest that the fibrils are still coiled into 80-120 nm elements (Figures 44-47). The 80-120 nm elements apparently are coiled forming the 300-400 nm subchromatids. The subchromatids pair to form the 500-800 nm chromatids which in turn pair, resulting in the 1.5 μm profiles of the chromosomes (Figure 39).

The homologues are difficult to distinguish in areas of chiasmata because the chromatin fibrils between homologues and chromatids interdigitate and no definite boundaries can be followed. Occasionally, however, units of chromatin in the subchromatid size range can be observed passing between homologues (Figure 39).

Diakinesis

Chromatin in diakinesis (Figures 49 and 50) is more dense than in diplotene, presumably because the chromosomes are more contracted. Large clear spaces separate the homologues (each homologue is 1.5-2.0 μm in diameter) which are associated only at the chiasmata. Less conspicuous clear spaces separate profiles of the 700-900 nm chromatids and also those of the 400-500 nm subchromatids.

As in diplotene the units of each homologue are difficult to resolve in the chiasmata (Figures 49 and 50) because the masses of chromatin blend together. However, profiles of both chromatid and subchromatid sizes can occasionally be seen to pass between the homologues (Figures 49 and 50).

Metaphase I

Metaphase I bivalents are easily recognized by their orientation on the metaphase plate and by the presence of spindle fiber microtubules (Figure 52). The bivalents are at the most contracted state of the meiotic cycle, with their undulating profiles (Figures 52 and 55) suggesting the gyres

observable through the light microscope in many species at metaphase I.

Except where concealed by interdigitating chromatin fibrils, boundaries between the several units of the bivalent are delineated by electron-transparent clear spaces (Figures 53, 61-63, 68, 69, and 86). Although in many sections the clear spaces appear isolated within the chromatin (Figures 61, 63, and 68), they can often be followed through serial sections and many are seen to be continuous with the surrounding nucleoplasm (Figures 60 and 69).

No specific terminating structures are seen at the telomeres (Figures 76-84). The chromatin is frequently continuous between sister chromatids and also between the homologues suggesting terminalized chiasmata. Where this is seen, serial sections (Figures 76-84) reveal that at least two chromatid-size units (800-1000 nm in diameter) are continuous between the homologues.

Other areas of chromatin exchange, presumably chiasmata, occur in areas removed from the telomeres. Subchromatid size (400-600 nm) and chromatid size units are continuous between the homologues (Figures 76-84). Other areas have the chromatin from both homologues so arranged that no boundaries of any type are evident (Figures 61 and 64-75).

The subchromatids are so appressed that they are generally difficult to distinguish as such. In favorable sections, particularly in serial sections, units of subchromatid size

can be seen side-by-side within chromatids (Figures 60-63 and 64-73).

The profiles of the 20 nm fibrils as in earlier stages appear in configurations that indicate the fibrils have coiled into the 80-120 nm diameter elements (Figures 89-96). At the edges of the chromosomes the 80-120 nm elements have wavey profiles that suggest their coiling into higher units (Figures 56-59).

Anaphase I

Anaphase I chromosomes are not as tightly coiled as those in metaphase I. The profiles are contoured (Figures 98 and 99) which suggest the gyres seen via light microscopy.

The anaphase I chromosome consists of two chromatids held together only at the kinetochore. Therefore each anaphase chromosome has four arms if metacentric and only two apparent if the kinetochore is nearly terminal. No distinction can be made between the individual chromatids in the kinetochore region. As for the rest of the chromosome, chromatids are not only separate, but units that appear to be subchromatids are easily observed (Figures 98-100).

As in the previous stages, the 20 nm diameter fibrils and their 80-120 nm coils appear in anaphase I (Figures 109-114). The 80-120 nm elements can be seen to form wavey profiles (indicating coiling) at the edges of the chromatin masses (Figures 100-102 and 108).

Freeze-etch preparations of anaphase I chromatid arms in cross section (Figures 106 and 107) compare in general outline and size to those in thin-section preparations (Figures 105 and 108). The various levels of organization in thin-sectioned chromatin are not as evident in freeze-etched chromatin, although areas that may correspond to the clear spaces are present (Figure 107). The most noticeable difference between the two preparations is that the profiles of freeze-etched chromatin fibrils are 10 nm in diameter in contrast to the 20 nm thin-sectioned fibrils (also see Diffuse diplotene).

Telophase I

When the chromosomes are despiralizing in early telophase I, the 80-120 nm profiles can be seen to be loosely coiled into 400 nm units (Figure 117). These larger profiles likewise are twisted into the 1-2 μm chromosome arms (Figures 116 and 117).

DISCUSSION

Accessory Structures

The purpose of this dissertation is to gain insight into the organization of the eukaryotic chromosome by studying the organization of chromatin in Lilium longiflorum in the course of first meiotic division. Incidental observations were also made on the kinetochore, spindle, nucleolus, nucleolar organizer, and synaptinemal complex. These accessory structures are compared and contrasted to those reported in the literature, and when possible are used to gain insight into the organization and behavior of chromosomes in general.

Kinetochore

The fundamental structure of the kinetochores in the first meiotic division in Lilium is seen to be fibrillar. However, the profiles of the seemingly irregularly arranged fibrils often appear as granules. Granules described in kinetochores in other studies (Bajer, 1968a; Harris and Bajer, 1965; and Wilson, 1967, 1968) have profiles similar to the granular appearing profiles of the fibrils observed in Lilium. Also, the reports that have not been definite about the kinetochore structural components (Bajer, 1968b; and Dietrich, 1966, 1968) show micrographs of kinetochores that appear to be consistant with the fibrillar organization.

Similarly, the fibrous "lampbrush" configuration

described by Brinkley and Stubblefield (1966) may be resolved only at high magnifications and with careful examination of serial sections. At low magnifications these kinetochores appear to consist of several layers as described in other organisms by Bernhard and de Harven (1960), George, et al. (1965), Jokelainen (1967), Krishan and Buck (1965), Luykx (1965), Murray, et al. (1965), Nebel and Coulon (1962b) and Robbins and Gonatas (1964).

Variations in the observations of kinetochore structure may also be due to variations in fixation procedures. The earliest workers (e.g., Harris, 1961, 1962) who used osmium tetroxide alone showed a "dense plate" with no substructures, while the latest workers (e.g., Brinkley and Stubblefield, 1966; and Jokelainen, 1967) used glutaraldehyde prior to osmium tetroxide and their results may be interpreted as showing fibrillar structure.

Higher plant kinetochores generally are ball-shaped and less electron-dense than the rest of the chromatin. In contrast, the higher animal kinetochores generally consist of several layers, with one or more of the layers more electron-dense than the rest of the chromatin. These general differences suggest that there may be phylogenetic differences in kinetochore structure between the Kingdoms. It may be safe to assume that phylogenetic differences in kinetochore structure (in addition to the differences caused by interpretation and fixation) also occur within each Kingdom. To

what extent this occurs is unknown because of the lack of systematic study of the kinetochores in either Kingdom.

It is evident that the role of the kinetochore is the attachment of the chromosome to the spindle, and possibly the formation or control of formation of chromosomal spindle microtubules (Bajer, 1968b). Exactly how either of these functions is performed is not understood. One prerequisite to such an understanding is the clarification of kinetochore morphology. This must wait until the observed variations in kinetochore structure are specifically determined as differences in interpretation, differences in fixation-embedment procedures, or genuinely reflect differences in phylogenetic origins.

The spindle

The spindle microtubules in Lilium meiotic first division exhibit typical microtubule morphology. Their behavior in relation to pH and temperature (i.e., being apparent only in material fixed at room temperature and relatively low pH, 6.8) is also typical.

The estimated number of microtubules connected to a kinetochore of a Lilium meiotic metaphase chromosome (150-200) compares favorably to the estimated number (70-150) connected to a Haemanthus mitotic metaphase kinetochore (Bajer, 1968b).

Continuous spindle microtubules have been described by other workers as extending across the metaphase plate both

between bivalents (chromosomes in mitosis) and actually passing through the chromatin masses. Such are observed in Lilium meiotic metaphase. There have been no other reports, however, showing continuous spindle microtubules passing in between the homologues of a bivalent as observed here. The significance of continuous spindle fibers in relation to spindle function, let alone the significance of these three locations, is not known.

Nucleolar organizer

Both plant and animal (except those described as "granular" by Jacob and Sirlin, 1964) nucleolar organizers reported in the literature and those seen in this study appear to consist of fibrils that are finer in texture and less electron-dense than the rest of the chromatin.

Hsu, et al. (1965) suggested that the less dense appearance of the organizer region in mitotic chromosomes may be an indication of an active or semi-active metabolic state since ribosomal RNA is synthesized during mitotic prophase. The same could be said about the meiotic nucleolar organizer described here in Lilium since RNA synthesis in the nucleolus (presumably ribosomal RNA) has been reported during meiotic prophase (Taylor, 1967a).

Nucleolus

The structure and behavior of the nucleoli in this study confirm Moen's (1968a) observations of Lilium. The appression

of the nucleolus to the nuclear envelope during zygotene and its subsequent separation is not understood. This behavior, however, provides a convenient method of determining the early meiotic stages.

The fibrillar and "vacuolar" components of the nucleolus in Lilium meiotic prophase are similar to those reported throughout the literature. However, no granular region, also a standard nucleolar component of most organisms (cf. Swift, 1966), was observed in Lilium.

No direct precursor-product relationship has been proven, but Jones (1965) concluded from the absence of the nucleolar granules in a ribosome-deficient mutant of Xenopus (normals had granules in the nucleoli) that the nucleolar granules and cytoplasmic ribosomes are part of the same biosynthetic pathway. If this is correct, then the absence of nucleolar granules in Lilium meiotic prophase would suggest there is a reduced ribosomal RNA synthesis during this period as suggested by Heslop-Harrison (1969) and Das and Alfert (1966). This is inconsistent with the postulated structure-function relationship involving synthetic activity just presented for the nucleolar organizer, which was based on the nucleolar RNA synthesis in pachytene reported by Taylor (1967a). These conflicting circumstances make it difficult to speculate any further on nucleolar ultrastructure in relation to nucleolar function in meiotic prophase. Radioautography at the electron microscope level could aid in resolving this problem.

Synaptinemal complex

The most studied, and the most controversial, meiotic structure is the synaptinemal complex. Those observed here in Lilium are consistent with the established structure as described in Lilium by Moens (1968a) and in a number of higher plants, higher animals, and fungi as reviewed by Moses (1968).

Controversy in the literature arises as to the role of the synaptinemal complex in synapsis. The original idea, and still the most generally accepted (cf. Moses, 1968), is that the synaptinemal complex is the actual site of molecular pairing and crossing-over. The support for this view is the presence of DNA in the lateral elements (cf. Moses, 1968), and the evidence of Roth and Ito (1967) that part of the prophase DNA synthesis is necessary for synaptinemal complex formation during zygotene and normal disjunction during diplotene. The weakness of this hypothesis is that DNA has not definitely been shown in the central region, presumably where molecular pairing and crossing-over occurs. An attractive aspect of this hypothesis is that the occurrence of the orderly arrangement of the synaptinemal complex correlates in time with the precise locus-by-locus synapsis followed by a precise molecular pairing and crossing-over in the chromosomes.

The second and more recent interpretation is that the synaptinemal complex functions as a bond in chromosome pairing, but has no specific role in molecular pairing and crossing-over. Schin (1965) inferred this, but Comings and Okada (1969)

gave the strongest evidence for this view by showing that none of the synaptinemal complex components are altered by DNase digestion, but all are subject to complete removal by proteolytic enzymes.

Other evidence that is consistent with the "indirect role" hypothesis is that somatic exchange (molecular crossing-over) occurs (e.g., Taylor, 1958b) where and when no synaptinemal complexes have ever been shown; and that synapsis with synaptinemal complex formation occurs in tomato-potato hybrids, but no genetic or cytological crossing-over takes place (Menzel and Price, 1966). The synaptinemal complex is not necessary for all types of crossing-over, nor does crossing-over and chiasmata formation always occur when the synaptinemal complex is present.

Both hypotheses have favorable aspects, but no proof for either hypothesis has been presented in the literature. Better techniques than are now available must be developed for determining the chemical nature and arrangements of the macromolecules in the synaptinemal complex. Once this has been accomplished, the relationship of the synaptinemal complex to synapsis and crossing-over may be more definitely defined.

The Chromatin

Two kinds of ultrastructural data regarding chromosome organization in the various stages of meiosis I have been

collected: (1) extensive observations of the profiles of the interfaces of the chromatin masses with the rest of the nucleoplasm have been made; and (2) local regions of anisotropic organization of the elementary fibrils have been studied and charted. Undulations of chromatin profiles or local regions of chromatin showing an apparently orderly array of fibrils in a single thin section have little significance. However, the examination of chromatin structure in many sections (including serial sections) of many different cells at each stage of meiosis I has yielded some observations which are consistent and reproducible. Only such observations have been reported here.

Ultrastructure

The organization of Lilium meiotic chromatin, except the accessory structures, appears to be based entirely on the 20 nm diameter elementary chromosome fibril. No matrices, pellicles, or cores were observed, nor have indications of matrices, pellicles, or cores been found in the majority of ultrastructural studies. The possibility of cores will be discussed in a later section (Chromosome models).

Occasional reports of "matrix-like" material (e.g., Lafontaine, 1968; and Peveling, 1968) suggest that matrices may occur in certain types of chromosomes. Therefore the possibility of a chromosome matrix cannot be completely ignored. The extent to which matrices exist, if at all,

remains to be answered.

Lilium meiotic chromosomes appear to consist of a hierarchy of coils, beginning with the coiling of the 20 nm diameter elementary chromosome fibril into a 80-120 nm diameter unit (hereafter referred to as the "first order coil"). The first order coils have undulating profiles that suggest they are coiled into larger units.

In leptotene the first order coil appears to be equivalent to the chromatid. In zygotene and pachytene it appears to be coiled (i.e., has regularly undulating profiles) into 200-250 nm and 300 nm chromatids respectively. The changes in thickness of the chromatids, and consequently the chromosomes and bivalents, in the course of meiosis seem to be due to differences in supercoiling of the first order coil.

During diffuse and late diplotene, the profiles of the first order coils are seen in the subchromatids, which have not been observable in the preceding stages (see Diffuse diplotene and chromatin reorganization). After diplotene, the first order coils cannot be seen forming specific higher elements, but the undulations of the edges of profiles of condensed chromatin (i.e., in metaphase I and anaphase I) suggest that the first order coils are supercoiled. Lilium meiotic metaphase I bivalents, unlike the anaphase I chromosomes, do not clearly exhibit the "major" coils seen by light microscopy in other plant species (e.g., Tradescantia and

Trillium). However, electron microscopy reveals large undulations of chromatid profiles which are suggestive of large gyres. Similar profiles are seen in electron micrographs of anaphase I chromosomes and are comparable with those seen through light microscopy. The previously mentioned undulating profiles of the first order coils ride on these large undulations similar to small perturbations on a wave.

Similarly formed coils were reported or suggested in mitosis of a lower vascular plant (Allen and Bowen, 1966), gymnosperm interphase (Shinke, 1959), both angiosperm mitosis (Kaufmann and McDonald, 1956) and meiosis (Bopp-Hassenkamp, 1959; Chardard, 1962; and Kaufmann and De, 1956), human interphase (Amano, et al. 1956), and mouse meiosis (Nebel, 1959, 1960). The diameters of these reported coils vary from 26-30 nm, and 35-100 nm, to 120 nm. It is difficult to determine if these variations in dimensions reflect phylogenetic differences, or whether they result from variations in interpretation or variations in preparative techniques. Even more perplexing, however, is the inconsistent terminology used to describe the various levels of coils. For example, Amano, et al. (1956) referred to 26-30 nm units as "subchromonemata", whereas Shinke (1959) termed 30-50 nm units as "elementary helices" and 100-130 nm units as "subchromonemata". "Chromonemata" has been the term for 35-100 nm units (Bopp-Hassenkamp, 1959), 120 nm units (Amano, et al. 1956), and 400-500 nm units (Shinke,

1959), as well as for the "threads" seen through light microscopy. Although this set of terminology has lent confusion to attempts to review and collate studies of chromosome ultrastructure, the basic organizational pattern, i.e., the hierarchy of coils, remains evident. The relation of this observed organizational pattern to the various chromosome models will be discussed in a later section (Chromosome models).

Variations in chromatin fine structure and the preparative techniques

Little argument arises concerning the concept that the fundamental units of eukaryotic chromosomes are the elementary chromosome fibrils. Likewise, little issue is made of the reported variations in their diameters from study-to-study. It is simple, and logical, to assume slight variations between organisms, slight variations in magnification calibrations, and the variation introduced by the whole-mount and thin-sectioning procedures. Although there is agreement that the various procedures yield different diameters of the fibrils, no agreement exists on which effect results from which suspected cause.

Wolfe and Grim (1967) believe sectioned fibrils are closer to the living dimensions than are whole-mount fibrils. Yet Bajer (personal communication, Department of Biology, University of Oregon, Eugene, Oregon) maintains that dehy-

dration for thin-sectioning introduces many dimensional artifacts which are unpredictable and probably vary depending upon the degree of chromatin contraction.

Added to these two views are the differences in fibril diameters between freeze-etched and sectioned chromatin of Lilium as observed here. Certainly it is easy to point out the possible sources of artifacts in thin-sectioning procedures: (1) osmium fixation; (2) alcohol dehydration; (3) plastic polymerization; and (4) stresses in thin sectioning. Although the intention of freeze-etching is to eliminate the most obvious artifact-inducing steps of embedding procedures (osmium fixation and alcohol dehydration), in doing so, new possible sources of artifacts are encountered: (1) cryoprotective agent infiltration; (2) freezing; (3) abrupt fracturing; and (4) warming during etching.

The ideal situation would be to have thin-sectioning, whole-mount, and freeze-etching techniques give exactly the same results. Or if this were not possible, have the separate techniques give such drastic results that one or two of the techniques could be judged as inadequate. Neither of these situations, however, occurs. The results from the three techniques yield fibril diameters within the same magnitude, so that subtle preparation-induced artifacts are difficult, in fact at this time impossible, to determine.

Related to this problem is the variation in dimensions of the elementary chromosome fibrils during the division

cycles. The diameters of the fibrils in Lilium first meiotic division remain consistently around 20 nm (except those in freeze-etched preparations). The majority of studies in the literature also reported constant fibril diameters throughout the various stages of the division cycles. DeRobertis (1956), however, described an increase in fibril diameter in grasshopper meiosis from 4.7 nm in early prophase to 10 nm at metaphase. Likewise, DuPraw (1965a, 1966) observed increases in diameters of mitotic fibrils from interphase to metaphase. DuPraw and Bahr (1968, 1969) elegantly correlated this with an increase in DNA packing ratios from interphase to metaphase.

It is difficult to assign any reason(s) why there are these descrepancies in observations. As discussed in the preceding paragraphs, preparation procedures may be the sources of these varied dimensions. This could be the case in DeRobertis' results. After all, his observations were made when preparation techniques (1956) for electron microscopy were in their infancy, and inconsistencies in so-called "standard" procedures resulted in variations of fine structural detail. Assuming that this is an adequate explanation of DeRobertis' observations, we still must contend with DuPraw's and Bahr's elegant and most convincing results. No satisfactory explanation can be given for the changes in size reported by DuPraw and Bahr compared to the constant

diameter seen in Lilium meiosis, unless there are differences between the mechanisms of contraction between animal mitosis and plant meiosis. This problem will probably remain unsolved until variations in chromatin fine structure induced by the respective preparative techniques are determined.

Diffuse diplotene and chromatin reorganization

A diffuse stage in plant meiosis has been described in Abies (Mergen and Lester, 1961), corn (Ghidoni, 1967), Larix (Ekberg and Eriksson, 1967), Lilium (Moens, 1968a; Sen, 1969; and this study), tomato (Moens, 1964), several mosses (Dill, 1964), as well as in several fungi (Carr and Oliver, 1958; and Barry, 1969). The majority of reports indicated that this diffuse stage occurs at the onset of diplotene. This is in contrast to the diffuse stage at the end of diplotene as occurs in oogenesis in many animals.

The dispersion of chromatin in developing eggs in animals has been explained as a period of increased RNA synthesis during a growth and food accumulation phase (Seshachar and Bagga, 1963). This is consistent with the general idea that chromatin must be dispersed (as opposed to condensed) in order to perform metabolic functions (Swanson, 1958). However, there is no specific evidence linking this brief diffuse stage in plant microsporocyte meiosis to increased genetic activity of the chromatin.

Diffuse diplotene in plants has been described in microsporocytes at a time when no increases in cell size are evident. Similarly, although RNA synthesis has been reported in microsporocytes, there is little agreement as to the stage of meiotic prophase when it occurs (Das, 1965; Das and Alfert, 1966; Hotta and Stern, 1963; Stern and Hotta, 1963; and Taylor, 1967a). In general there is little or no support for the notion that the primary function of the cell in diffuse diplotene is increased synthetic activity.

The diffuse state may well be a symptom of another sort of event, the reorganization of nuclear material. This was suggested when Mitra (1958, p. 783) pointed out that increases in irradiation-induced aberrations during diplotene-diakinesis and the shift from chromatid to subchromatid aberrations in Lilium microsporocyte meiosis could be due to the fact that this is a period ". . . where a reorganization of nuclear material is known to occur". Other irradiation experiments on microsporocyte meiosis (Crouse, 1954, 1961; and Sparrow, et al. 1952) have indicated that the pachytene-diplotene period is the most sensitive period to radiation in meiosis, as well as the swivel point for the change from chromatid to subchromatid aberrations. Although the various workers may disagree on the exact stage of maximum sensitivity to X-radiation, there is no doubt that the change from chromatid to subchromatid aberrations is during late pachytene or immediately after. The appearance of structures interpreted

as subchromatids during Lilium diffuse diplotene as seen in this study is consistent with these irradiation experiments.

The change in the general behavior of the chromatin between pachytene and diplotene also suggests that the chromatin is undergoing some type of reorganization during this time. In pachytene the homologues are tightly attracted to each other, but in diplotene the homologues behave as if they are strongly repelling each other, with the only contact of the homologues being at the chiasmata. Certainly the behavior of the synaptinemal complex (i.e., axial to the homologues in pachytene, but removed from the bivalents in diplotene) is related to this change in attraction of the homologues. It remains to be seen if this is the cause of the behavior of the chromatin, or if it is another symptom of a more general process, the reorganization of chromatin.

Sen (1969) proposed that the chromatin is reorganized into individual chromatids during diffuse diplotene. It is true that diplotene is the first time that chromatids are regularly visible through light microscopy; however, the irradiation data and ultrastructural observations suggest that this is rather the time of the formation (or at least the appearance) of subchromatids. This appearance of a new level of organizational units is perplexing from both morphological and genetical viewpoints. The nature of the problem was

indicated by Crouse (1961, p. 211): "Whether the shift from the chromatid to the two-half-chromatid condition involves a change in spatial relation of pre-existing units or a synthesis of new materials is not known".

The majority of DNA synthesis occurs in the premeiotic interphase (Taylor, 1953, 1959a). From this standpoint, the formation of subchromatids (or half-chromatids) would involve spatial reorganization of pre-existing units. Ultrastructurally, no indications of subchromatids were observed prior to diffuse diplotene. So the pre-existing units apparently are organized in some manner that conceals their morphological identity as well as their susceptibility to X-radiation.

In addition to the massive DNA and protein synthesis occurring in premeiotic interphase, much smaller amounts of DNA and protein are synthesized at several points in meiotic prophase. This prophase DNA synthesis (Hotta, et al. 1966; and Roth and Ito, 1967) and protein synthesis (Parchman and Stern, 1969) are necessary for normal development of bivalent morphology. Leptotene-early zygotene DNA synthesis and protein synthesis are necessary for synaptinemal complex formation and normal synapsis. Late zygotene DNA synthesis is necessary for normal diplotene bivalent development, as is late zygotene-early pachytene protein synthesis. Normal anaphase II chromosome morphology and behavior depend

on pachytene DNA synthesis and pachytene-diplotene protein synthesis. The synthesis of these new materials is closely correlated in time with the changes in irradiation induced aberrations and the appearance of subchromatids in electron micrographs. This suggests that these prophase syntheses could be involved in chromatin reorganization. There is not enough DNA synthesis or protein synthesis, however, to account for the formation of new units. Wimber and Prensky (1963) speculated that prophase DNA synthesis may be necessary for a "reunion" of broken chromatids. The functional significance of meiotic prophase DNA synthesis and protein synthesis appears to be more involved than this, and remains to be clarified.

The observations of pollen sterility made by Ekberg and his group (Ekberg and Eriksson, 1967; and Ekberg, et al. 1968) might be explained in terms of a reorganzation of chromatin during diffuse diplotene. Under normal environmental conditions the microsporocytes remain in diffuse diplotene through the winter, and meiosis continues to completion in the following spring. However, if environmental conditions are not normal, then meiosis continues to completion prematurely in the fall. This results in various abnormalities (bridges, lagging chromosomes, and multipolar spindles) which presumably cause pollen sterility. The environmental conditions trigger control mechanisms that initiate the

the completion of the divisions, perhaps prematurely and before full expression of the normal events in diffuse diplotene (presumably chromatin reorganization).

The observations reported here suggest that microsporocyte meiotic chromatin undergoes a reorganization associated with the appearance of subchromatids during or near diffuse diplotene. But it is difficult to assign a functional role to this purported reorganization. The most difficult aspect of reorganization is to explain the appearance of subchromatids. Although the existence of subchromatids in late prophase I is supported by evidence from several experimental approaches, they do not fit into the generally accepted scheme of "classical" meiosis.

None of the single-stranded chromosome models (see Chromosome models) which are consistent with genetic data can account for subchromatids. On the other hand, the "bineme" model proposed by Peacock (1965) fails to explain crossing-over unless complicated behavior of the linkers is introduced. It is capable, however, of reconciling the observed subchromatids to the reported semi-conservative DNA distribution during mitosis.

Before we can better evaluate this suggested chromatin reorganization, more must be known about the nature and behavior of all the subchromosomal units, the role of both prophase DNA synthesis and protein synthesis in chromosome

structure, the mechanism of synapsis and crossing-over, and the arrangement of DNA in the elementary chromosome fibrils during each stage of meiosis.

Chromosome models

Eukaryotic chromosomes appear far more complex than the "naked" single strands of DNA double helices generally believed to compose the prokaryotic chromosomes (cf. Ris, 1966a). The prokaryotic systems have been useful in elucidating the role of DNA in cellular metabolism and genetic control, but they have not contributed to the understanding of eukaryotic chromosome structure.

The various eukaryotic chromosome models presented in the literature are attempts to visualize arrangements of DNA and protein that could explain semi-conservative DNA distribution (Taylor, et al. 1957) and the various classical genetic phenomena during meiosis. Added to these, the models must also explain general chromosome morphology and cytogenetic behavior as seen through light microscopy, as well as observations on chromosome fine structure as seen through electron microscopy. None of the models proposed in the literature completely satisfy all of these requirements, but they are useful because they give us a working foundation from which we can strive to better understand eukaryotic chromosome structure and function.

The "coil" model proposed by Cole (1962) fits the many ultrastructural observations, including those reported here of Lilium, and the classical observations through light microscopy (cf. Manton, 1950) that indicate that chromosomes consist of a hierarchy of coils. This model, which is very similar to that proposed by the classical "torsion" school of chromosome coiling (Darlington, 1937), explains the morphological units from a biophysical point-of-view. DuPraw's studies (1965a, 1965b) support Cole's notion that the elementary chromosome fibril consists of a single strand of DNA coiled with proteins.

Contrary to Cole's views, however, DuPraw (1965a, 1966, 1968) does not believe that the elementary chromosome fibril forms supercoils resulting in higher chromosomal units. Instead, DuPraw has proposed a "folded-fiber" model in which the elementary chromosome fibril irregularly folds to form the chromatids. This model is inconsistent with the many ultrastructural studies, as well as the classical observations through light microscopy, that indicate chromosomes are basically coiled. The "folded-fiber" model could, however, be an adequate explanation for some chromosomes (e.g., the minute honey bee chromosomes) that do not exhibit any of the typical gyres as seen in many chromosomes (e.g., Tradescantia and Trillium).

Both the "coil" and the "folded-fiber" models are

single-stranded (i.e., only one DNA double helix, or one series of tandemly-linked DNA double helices, occurs in each chromatid) and are consistent with the observed semi-conservative DNA distribution during mitosis (Taylor, et al. 1957) and the majority of the genetic events during meiosis.

Although a single-stranded chromatid fits well with the genetic data, all such models are inconsistent with the subchromatids observed in many species through light microscopy (Kaufmann, 1948), the radiation induced subchromatid aberrations during meiotic prophase (Crouse, 1954, 1961; Mitra, 1958; and Sparrow, et al. 1952), and the post-pachytene subchromatid-like structures seen here in Lilium. Peacock (1965) attempted to resolve this conflict by proposing a "bineme" chromatid (not to be confused with the multi-stranded "rope" model discussed below) that requires a mechanism for holding like strands of DNA together within a chromatid, so that the two morphological units (i.e., the subchromatids, each which is equivalent to one DNA double helix) act as one unit. This idea has appeal in that it appears to bring together the genetic data and the morphological observations as well as certain cytogenetic behavior as discussed earlier (Diffuse diplotene and chromatin reorganization, p. 66). The "bineme" model, however, has difficulty in explaining crossing-over unless additional assumptions are made on the behavior of the linkers. Indeed,

as attempts are made to modify the "bineme" model to fit certain genetic data, the added suppositions become more burdensome than the original inconsistency (i.e., single-strandedness versus subchromatids) that prompted the proposal of the model. The question of single-stranded versus double-stranded ("bineme") chromosome structure remains unanswered, and more studies must be performed to determine the relation of DNA strands to chromatid (or subchromatid) structure.

The "rope" model (Kaufmann, et al. 1960; and Steffensen, 1959) was an attempt to explain some of the early thin-section studies that inferred that the elementary chromosome fibril consists of two (Kaufmann and De, 1956; and Kaufmann and McDonald, 1956) or four (Nebel, 1959) strands of DNA-protein complexes coiled together. The visualization of chromatid doubleness in light microscopy studies (Kaufmann, 1948), the subchromatid-like structures observed in this study of Lilium meiosis, as well as presumed subchromatid irradiation-induced aberrations (Crouse, 1954, 1961; Mitra, 1958; and Sparrow, et al. 1952) could be used as support for this model. However, the purported subchromatids have not yet been proven to be identical "halves" of the chromatids. A number of other explanations are possible. For example, the subchromatids could be the chromatid coiled back onto itself. And even if the subchromatids are identical "halves",

they could be used as evidence for Peacock's "bineme" model. There have been no suggestions in the whole-mount studies in the literature (e.g., Abuelo and Moore, 1969; DuPraw, 1965a, 1966; and Wolfe and John, 1965) that the elementary chromosome fibrils twist together in a rope-like manner. In addition, the multi-stranded condition of this model cannot be used to explain semi-conservative distribution of DNA during mitosis (Taylor, et al. 1957), or any of the genetic events during meiosis.

The "centipede" model was originally proposed as one of the possible explanations for semi-conservative DNA distribution during mitosis (Taylor, 1957, 1958a, 1959b). Occasionally the lateral elements of the synaptinemal complex have been interpreted as "backbones" (Nebel and Coulon, 1962a; and Painter, 1964). In view of the more recent, thorough studies of synaptinemal complex behavior (cf. Moses, 1968), it is questionable if any part of the synaptinemal complex can be considered as a permanent chromosome "backbone". The "cores" described in Vicia mitotic chromosomes (Lafontaine and Chouinard, 1963) do not serve as evidence for this model either. These "cores" appear similar to the clear spaces observed here in Lilium meiotic chromosomes, and could similarly be interpreted as either the axes of coiling of the chromatids or as the boundaries between units within the chromatids. Except for this weak

support, the "centipede" model had dropped almost completely out of consideration as a chromosome model until Stubblefield and Wray (1969) revived it with their isolation of ribbon-like structures, supposingly chromosome "backbones". More studies must be made before the significance of the latter study can be determined.

The other chromosome models discussed in the literature (the "linker", the "ladder", and modifications thereof) are usually single-stranded models and can account for, as well as aid in visualizing, semi-conservative DNA replication, semi-conservative DNA distribution, and crossing-over (Freese, 1958; Schwartz, 1955; Taylor, 1963, 1967b; and Uhl, 1965a, 1965b). These models are mainly concerned with the arrangement of DNA and protein in relation to each other. Since it is generally agreed that the elementary chromosome fibrils contain both the DNA and protein of the chromosomes, these models could be considered as attempts to explain the arrangement of DNA and protein within the elementary chromosome fibrils. More must be known about the organization of DNA and protein within the elementary chromosome fibrils before the validity of any of these models can be determined.

Conclusion

It is obvious that the structure and behavior of meiotic chromatin is complex. The observations here and as reported elsewhere suggest that the basic organizational pattern of chromosomes is a hierarchy of coils. Now the problem is to elucidate the mechanisms that govern the observed organizational pattern. We can use the various models for chromosome structure already proposed (e.g., the "coil", the "ladder", and the "linker") as our hypotheses from which to base future experiments. Such experiments will probably require refinements in the present techniques for electron microscopy as well as many of the sophisticated biochemical and biophysical procedures.

Perhaps the most significant aspect of this dissertation is the reported behavior of the chromatin during diffuse diplotene. Diffuse diplotene has been relatively ignored in most studies of plant meiosis. Consequently, little is known about the structure or behavior of the chromatin during this period. The purported reorganization of the chromatin during diffuse diplotene serves as a starting point for future experiments on the distribution of DNA during nuclear divisions in general. This reorganization during diffuse diplotene suggests that DNA is not distributed when it is synthesized during premeiotic interphase. Any explanation for

the behavior of the chromatin during diffuse diplotene must be consistent with any proposed mechanism for explaining the hierarchy of coils.

Although emphasis was not placed on the accessory structures, they also must be understood before we can completely understand the distribution of genetic material during the cell divisions. The various discriptions of the kinetochores point out that we must be aware that phylogenetic differences may account for variations in chromosome ultrastructure. In addition, the actual mechanisms of the roles of the kinetochores and spindle in chromosome movement await elucidation. The synaptinemal complex, despite the emphasis placed on it in the past, still requires additional study before its role in synapsis and crossing-over can be completely understood. The nucleoli and nucleolar organizers are the most little understood nuclear structures in relation to meiosis. The nucleolar organizer must eventually be explained in terms of a modified portion of chromatin. The nucleolus possibly has some role in the biochemical events that control the nuclear divisions.

The observations and interpretations presented in this dissertation can serve as foundations for future experiments to test hypotheses based on these observations. The author is confident that these future experiments will soon lead to the development of an acceptable theory on chromosome structure.

SUMMARY

Meiotic first divisions of Lilium longiflorum microsporocytes were studied with the electron microscope using both thin-sectioning and freeze-etching techniques.

1. Synaptinemal complexes were observed in zygotene and pachytene, and consist of the three components (lateral elements, central region, and central element) previously described by many workers.

2. Kinetochores of metaphase I through early telophase I are less electron-dense than the rest of the chromatin, and consist of fibrils 7-20 nm in diameter.

3. Chromosomal spindle microtubules in metaphase I and anaphase I are connected to the kinetochore. Continuous spindle microtubules extend across the metaphase plate, sometimes passing between the bivalents, sometimes between homologues, and sometimes piercing the chromosome arms.

4. Nucleoli are appressed to the nuclear envelope during zygotene and separated from it during pachytene through diplotene. The nucleoli consist of tightly-packed electron-dense fibrils 10-15 nm in diameter and relatively electron-transparent "vacuoles". No granular regions were observed.

5. Nucleolar organizers are less electron-dense than the rest of the chromatin and consist of fine fibrils 7.5-12.5 nm in diameter.

6. In thin sections chromosome morphology at all stages

appears to be based entirely on electron-dense, 20 nm diameter, chromosome fibril. Profiles of freeze-etched fibrils, however, are only 10 nm in diameter. No chromosomal matrices, pellicles, or backbones were observed in any stages of division.

7. The elementary chromosome fibrils appear to form a 80-120 nm first order coil in all observed stages of division. This first order coil likewise appears to form higher coils, depending upon the specific stage of division (see Figures 118-125 for a diagramatic summary).

8. At the onset of diplotene a diffuse stage occurs in which subchromatid-like structures become visible for the first time, and remain visible through the remaining stages of the first division. When these ultrastructural observations are collated with cytological observations from other sources, it seems apparent that the diffuse diplotene stage in microsporocytes is a period of chromatin reorganization.

9. The various chromosome models proposed in the literature are considered in relation to these fine structural studies. A coiled "unineme" model fits observations reported here and is compatible with the majority of the genetic data. However, the single-stranded nature of this model is inconsistent with the subchromatid-like structures seen. A "bineme" model explains subchromatids and some aspects of chromosome behavior, but has difficulty in explaining genetic crossing-over.

LITERATURE CITED

Abuelo, J. G. and D. E. Moore. 1969. The human chromosome. Journal of Cell Biology 41: 73-90.

Aldrich, H. C. 1967. The ultrastructure of meiosis in three species of Physarum. Mycologia 59: 127-148.

Allen, R. D. 1964. Fine structure of cell division in Psilotum nudum. Unpublished Ph.D. thesis. Ames, Iowa, Library, Iowa State University of Science and Technology.

Allen, R. D. and C. C. Bowen. 1966. Fine structure of Psilotum nudum cells during division. Caryologia 19: 299-342.

Amano, S., S. Dohi, H. Tanaka, F. Uchino, and M. Hanaoka. 1956. The structure of the nucleus studied by electron microscopy in ultrathin sections with special reference to the chromonema--an advocation of "subchromonema" and "protochromonema". Cytologia 21: 241-251.

Ambrose, E. J., F. W. Cuckow, and A. R. Gopal-Ayengar. 1956. The molecular organization and fine structure of chromosomes. Congress of Cell Biology, 8th, Leidon, 1954: 191-194.

Anderson, W. A. and R. A. Ellis. 1965. Ultrastructure of Tryponasoma lewisi: Flagellum, microtubules, and the kinetoplast. Journal of Protozoology 12: 483-499.

Bajer, A. 1968a. Behavior and fine structure of spindle fibers during mitosis in endosperm. Chromosoma 25: 249-281.

Bajer, A. 1968b. Chromosome movement and fine structure of the mitotic spindle. Society for Experimental Biology Symposium 23: 285-331.

Bajer, A. 1968c. Fine structure studies on phragmoplast and cell plate formation. Chromosoma 24: 383-417.

Barnicot, N. A. 1967. A study of newt mitotic chromosomes by negative staining. Journal of Cell Biology 32: 585-603.

Barry, E. G. 1969. The diffuse diplotene stage of meiotic prophase in Neurospora. Chromosoma 26: 119-129.

Behnke, O. 1964. A preliminary report on "microtubules" in undifferentiated and differentiated vertebrate cells. Journal of Ultrastructure Research 11: 139-146.

Bernhard, W. and E. de Harven. 1960. L' ultrastructure du centriole et d' autres elements de l' apporeil achromatique. International Conference on Electron Microscopy, 4th, Berlin, 1958, Proceedings 2: 217-227.

Bopp-Hassenkamp, G. 1959. Lichtmikroskopische und electronen-optische Untersuchungen uber den Aufbau pflanzlicher Chromosomen im Pachytan der Meiosis. Protoplasma 50: 243-268.

Bowen, C. C. 1956. Freezing by liquid carbon dioxide in making slides permanent. Stain Technology 31: 87-90.

Bowen, C. C. 1959. Fine structure of the mitotic spindle in Psilotum (Abstract). International Botanical Congress, 9th, Montreal, 1959, Proceedings 2: 43.

Brinkley, B. R. 1965. The fine structure of the nucleolus in mitotic divisions of Chinese hamster cells in vitro. Journal of Cell Biology 27: 411-422.

Brinkley, B. R. and E. Stubblefield. 1966. The fine structure of the kinetochore of a mammalian cell in vitro. Chromosoma 19: 28-43.

Brown, C. A. and H. Ris. 1959. Amphibian oocyte nucleoli. Journal of Morphology 104: 377-414.

Brown, W. V. and E. M. Bertke. 1969. Textbook of cytology. St. Louis, Missouri, The C. V. Mosby Company.

Buck, R. C. 1967. Mitosis and meiosis in Rhodnius prolixus: The fine structure of the spindle and diffuse kinetochore. Journal of Ultrastructure Research 18: 489-501.

Carr, A. J. H. and L. S. Oliver. 1958. Genetics of Sordaria fimicola. II. Cytology. American Journal of Botany 45: 142-150.

Carroll, G. C. and R. Dykstra. 1966. Synaptinemal complexes in Didymium iridis. Mycologia 58: 166-169.

Chardard, R. 1962. Recherches sur les cellules-meres des microspores des Orchidees. Etude au microscope electronique. Revue de Cytologie et de Biologie Vegetales 24: 1-148.

Chouinard, L. A. 1966. Nucleolar architecture in root meristematic cells of Allium cepa. National Cancer Institute Monograph 23: 125-143.

Cole, A. 1962. A molecular model for biological contractility: implications in chromosome structure and function. Nature 196: 211-214.

Coleman, J. R. and M. J. Moses. 1964. DNA and the fine structure of synaptic chromosomes in the domestic rooster (Gallus domesticus). Journal of Cell Biology 23: 63-78.

Comings, D. E. and T. A. Okada. 1969. Electron microscope study of well dispersed mammalian and avian chromosomes: a single DNA helix per chromatid model (Abstract). Journal of Cell Biology 43: 25a.

Cronshaw, J. and K. Esau. 1968. Cell division in leaves of Nicotiana. Protoplasma 65: 1-24.

Crouse, H. V. 1954. X-ray breakage of lily chromosomes at first meiotic metaphase. Science 119: 485-487.

Crouse, H. V. 1961. Irradiation of condensed meiotic chromosomes in Lilium longiflorum. Chromosoma 12: 190-214.

Darlington, C. D. 1937. Recent advances in cytology. 2nd ed. Philadelphia, Pennsylvania, Blakiston, Co.

Darlington, C. D. and L. F. LaCour. 1950. The handling of chromosomes. 2nd ed. London, George Allen and Unwin.

Das, N. K. 1965. Incactivation of the nucleolar apparatus during meiotic prophase in corn anthers. Experimental Cell Research 40: 360-364.

Das, N. K. and M. Alfert. 1966. Nucleolar RNA synthesis during mitotic and meiotic prophase. National Cancer Institute Monograph 23: 337-351.

Davies, H. G. and J. Tooze. 1964. Electron microscope observations on mitotic chromosomes in erythroblasts of the newt, Triturus cristatus. Nature 203: 990-992.

De, D. N. 1964. A new chromosome model. Nature 203: 343-346.

de Harven, E. 1968. The centriole and the mitotic spindle. In Dalton, A. J. and G. Haguenau, eds. The nucleus. Pp. 197-227. New York, New York, Academic Press, Inc.

DeRobertis, E. 1956. Electron microscope observations on the submicroscopic morphology of the meiotic nucleus and chromosomes. Journal of Biophysical and Biochemical Cytology 2: 785-796.

DeRobertis, E. D. P., W. W. Nowinski, and F. A. Saez. 1954. General cytology. 2nd ed. Philadelphia, Pennsylvania, W. B. Saunders Company.

Dietrich, J. 1966. Observations sur la structure fine de la fibre chromosomique: Formation et implantation dans la region du centromere. Comptes Rendes de L'Academie des Sciences, Serie D, 262: 1699-1701.

Dietrich, J. 1968. Organisation ultrastructurale du fuseau de caryocinese en prometaphase dans les allules-meres de microspores du Lis. Comptes Rendes de L'Academie des Sciences, Serie D, 266: 579-581.

Dill, F. J. 1964. Dictyotene stage of mosses. Science 144: 541-543.

DuPraw, E. J. 1965a. Macromolecular organization of nuclei and chromosomes: A folded fiber model based on whole-mount electron microscopy. Nature 206: 338-343.

DuPraw, E. J. 1965b. The organization of nuclei and chromosomes in honey bee embryonic cells. National Academy of Sciences Proceedings 53: 161-168.

DuPraw, E. J. 1965c. The ultrastructure of human chromosomes (Abstract). American Zoologist 5: 648a.

DuPraw, E. J. 1966. Evidence for a "folded-fibre" organization in human chromosomes. Nature 209: 577-581.

DuPraw, E. J. 1968. Cell and molecular biology. New York, New York, Academic Press, Inc.

DuPraw, E. J. and G. F. Bahr. 1968. The arrangement of DNA in human chromosomes, as determined by quantitative electron microscopy (Abstract). Journal of Cell Biology 39: 38a.

DuPraw, E. J. and G. F. Bahr. 1969. The arrangement of DNA in human chromosomes, as investigated by quantitative electron microscopy. Acta Cytologica 13: 188-205.

DuPraw, E. J. and P. M. M. Rae. 1966. Polytene chromosome structure in relation to the "folded-fibre" concept. Nature 212: 598-600.

Ekberg, I. and G. Eriksson. 1967. Development and fertility of pollen in three species of Larix. Hereditas 57: 303-311.

Ekberg, I., G. Eriksson, and A. Sulikova. 1968. Meiosis and pollen formation in Larix. Hereditas 59: 427-438.

Engles, F. M. and A. F. Croes. 1968. Synaptinemal complex in yeast. Chromosoma 25: 104-106.

Erickson, R. O. 1948. Cytological and growth correlations in the flower bud and anther of Lilium longiflorum. American Journal of Botany 36: 729-739.

Fabergé, A. C. 1967. Chromosome structure (Abstract). Genetics 56: 558-559.

Fawcett, D. W. 1956. The fine structure of chromosomes in the meiotic prophase of vertebrate spermatocytes. Journal of Biophysical and Biochemical Cytology 2: 403-406.

Filner, P. 1965. Semi-conservative replication of DNA in a higher plant cell. Experimental Cell Research 39: 33-39.

Freese, E. 1958. The arrangement of DNA in the chromosome. Cold Spring Harbor Symposia on Quantitative Biology 23: 13-18.

Gall, J. G. 1963. Chromosome fibers from an interphase nucleus. Science 139: 120-121.

Gassner, G. 1969. Synaptinemal complexes in the achiasmatic spermatogenesis of Bolbe nigra Giglio-Tos (Mantoidea). Chromosoma 26: 22-34.

Gay, H. 1956. Chromosome-nuclear membrane-cytoplasmic interrelations in Drosophila. Journal of Biophysical and Biochemical Cytology 2 (Suppl.): 407-414.

George, P., L. J. Journey, and M. M. J. Goldstein. 1965. Effect of vincristine on the fine structure of HeLa cells during mitosis. Journal of the National Cancer Institute 35: 355-375.

Ghidoni, A. 1967. The "diffuse stage" in meiotic prophase I of maize PMC. Maize Genetics Cooperation Newsletter 41: 84.

Harris, P. 1961. Electron microscope study of mitosis in sea urchin blastomeres. Journal of Biophysical and Biochemical Cytology 11: 419-431.

Harris, P. 1962. Some structural and functional aspects of the mitotic apparatus in sea urchin embryos. Journal of Cell Biology 14: 475-487.

Harris, P. 1965. Some observations concerning metakinesis in sea urchin eggs. Journal of Cell Biology 25 (Suppl.): 73-77.

Harris, P. and A. Bajer. 1965. Fine structure studies on mitosis in endosperm metaphase of Haemanthus kathernae Bak. Chromosoma 16: 624-636.

Harris, P. and D. Mazia. 1962. The finer structure of the mitotic apparatus. In Harris, R. J. C., ed. The interpretation of ultrastructure. Pp. 279-305. New York, New York, Academic Press, Inc.

Hay, E. D. 1968. Structure and function of the nucleolus in developing cells. In Dalton, A. J. and F. Haguenau, eds. The nucleus. Pp. 2-79. New York, New York, Academic Press, Inc.

Hay, E. D. and J. P. Revel. 1963. The fine structure of the DNP component of the nucleus: An electron microscope study utilizing autoradiography to locate DNA synthesis. Journal of Cell Biology 16: 29-51.

Heslop-Harrison, J. 1969. The cytoplasm during meiosis (Abstract). International Botanical Congress, Seattle, 1969, Proceedings 11: 90.

Hsu, T. C., F. E. Arrighi, R. R. Klevecz, and B. R. Brinkley. 1965. The nucleoli in mitotic divisions of mammalian cells in vitro. Journal of Cell Biology 26: 539-553.

Hsu, T. C., B. R. Brinkley, and F. E. Arrighi. 1967. The structure and behavior of the nucleolus organizers in mammalian cells. Chromosoma 23: 137-153.

Hotta, Y., M. Ito, and H. Stern. 1966. Synthesis of DNA during meiosis. National Academy of Sciences Proceedings 56: 1184-1191.

Hotta, Y., G. Parchman, and H. Stern. 1968. Protein synthesis during meiosis. National Academy of Sciences Proceedings 60: 575-582.

Hotta, Y. and H. Stern. 1963. Inhibition of protein synthesis during meiosis and its bearing on intracellular regulation. Journal of Cell Biology 16: 259-279.

Hughes, A. c1959. A history of cytology. New York, New York, Abelard-Schuman.

Hyde, B. B. 1966. Changes in nucleolar ultrastructure associated with differentiation in the root apex. National Cancer Institute Monograph 23: 39-52.

Hyde, B. B., K. Sankaranaryanan, and M. L. Birnstiel. 1965. Observations on fine structure in pea nucleoli in situ and isolated. Journal of Ultrastructure Research 12: 652-667.

Ichida, A. A. and M. S. Fuller. 1968. Ultrastructure of mitosis in the aquatic fungus Catenaria anguillulae. Mycologia 60: 141-155.

Ito, M., Y. Hotta, and H. Stern. 1967. Studies of meiosis in vitro. II. Effect of inhibiting DNA synthesis during meiotic prophase on chromosome structure and behavior. Developmental Biology 16: 54-77.

Jacob, J. and J. L. Sirlin. 1963. Electron microscope studies on salivary gland cells. I. The nucleus of Bradysia mycorum (Sciaridae), with special reference to the nucleolus. Journal of Cell Biology 17: 153-165.

Jacob, J. and J. L. Sirlin. 1964. Electron microscope studies on salivary gland cells. IV. The nucleus of Smittia parthenogenetica (Chironomidae) with special reference to the nucleolus and the effects of actinomycin thereon. Journal of Ultrastructure Research 11: 315-328.

Jensen, C. and A. Bajer. 1969. Effects of dehydration on the microtubules of the mitotic spindle. Journal of

Ultrastructure Research 26: 367-386.

John, B. and K. R. Lewis. 1965. The meiotic system. Protoplasmatologia 6 (F1): 1-335.

Jokelainen, P. T. 1967. The ultrastructure and spatial organization of the metaphase kinetochore in mitotic rat cells. Journal of Ultrastructure Research 19: 19-44.

Jones, K. W. 1965. The role of the nucleolus in the formation of the ribosomes. Journal of Ultrastructure Research 13: 257-262.

Kalnins, V. I., H. F. Stich, and S. A. Bencosme. 1964. Fine structure of the nucleolar organizer of salivary gland chromosomes of Chironomids. Journal of Ultrastructure Research 11: 282-291.

Kane, R. E. 1962. The mitotic apparatus. Fine structure of the isolated unit. Journal of Cell Biology 15: 279-289.

Kaufmann, B. P. 1948. Chromosome structure in relation to the chromosome cycle. II. Botanical Review 14: 57-109.

Kaufmann, B. P. and D. N. De. 1956. Fine structure of chromosomes. Journal of Biophysical and Biochemical Cytology 2 (Suppl.): 419-423.

Kaufmann, B. P. and M. R. McDonald. 1956. Organization of the chromosome. Cold Spring Harbor Symposia on Quantitative Biology 21: 233-246.

Kaufmann, B. P., H. Gay, and M. McDonald. 1960. Organizational patterns within chromosomes. International Review of Cytology 9: 77-127.

Krishan, A. and R. C. Buck. 1965. Structure of the mitotic spindle in L strain fibroblasts. Journal of Cell Biology 24: 433-444.

Lafontaine, J. G. 1968. Structural components of the nucleus in mitotic plant cells. In Dalton, A. J. and F. Haguenau, eds. The nucleus. Pp. 152-196. New York, New York, Academic Press, Inc.

Lafontaine, J. G. and L. A. Chouinard. 1963. A correlated light and electron microscope study of the nucleolar material during mitosis in Vicia faba. Journal of Cell Biology 17: 167-201.

Lafontaine, J. G. and Fr. A. Lord. 1966. Ultrastructure and mode of formation of the nucleolus in plant cells. National Cancer Institute Monograph 23: 67-75.

Ledbetter, M. C. and K. R. Porter. 1963. A "microtubule" in plant cell fine structure. Journal of Cell Biology 19: 239-250.

Lu, B. C. 1967. Meiosis in Coprinus lagopus: A comparative study with light and electron microscopy. Journal of Cell Science 2: 529-536.

Luft, J. 1961. Improvements in epoxy embedding methods. Journal of Biophysical and Biochemical Cytology 9: 409-414.

Luykx, P. 1965. The structure of the kinetochore in meiosis and mitosis in Urechis eggs. Experimental Cell Research 39: 643-657.

Manton, I. 1950. The spiral structure of chromosomes. Biological Reviews 25: 486-508.

Manton, I. 1964a. Observations with the electron microscope on the division cycle in the flagellate Prymnesium parvum Carter. Journal of the Royal Microscopical Society 83: 317-325.

Manton, I. 1964b. Preliminary observations on spindle fibers at mitosis and meiosis in Equisetum. Journal of the Royal Microscopical Society 83: 471-476.

Marinozzi, V. and W. Bernhard. 1963. Presence dans le nucleole de deux type de ribonucleoproteines morphologiquement distinctes. Experimental Cell Research 32: 595-598.

McAlear, J. H. and G. O. Kreutziger. 1967. Freeze etching with radiant energy in a simple cold block device. Electron Society of America Proceedings 25: 116-117.

Menzel, M. Y. and J. M. Price. 1966. Fine structure of synapsed chomosomes (sic) in F_1 Lycopersicon esculentum-Solanum lycopersicoides and its parents. American Journal of Botany 53: 1079-1086.

Mergen, F. and D. Lester. 1961. Microsporogenesis in Abies. Silvae Genetica 10: 146-156.

Meselson, M. and F. W. Stahl. 1958. The replication of DNA in Escherichia coli. National Academy of Sciences Proceedings 44: 671-682.

Millonig, G. 1961. Advantages of a phosphate buffer for OsO_4 solution in fixation. Journal of Applied Physics 32: 1637.

Mitra, S. 1958. Effects of x-rays on chromosomes of Lilium longiflorum during meiosis. Genetics 43: 771-789.

Moens, P. B. 1964. A new interpretation of meiotic prophase in Lycopersicon esculentum (tomato). Chromosoma 15: 231-242.

Moens, P. B. 1968a. The structure and function of the synaptinemal complex in Lilium longiflorum sporocytes. Chromosoma 23: 418-451.

Moens, P. B. 1968b. Synaptinemal complexes of Lilium tigrinum (triploid) sporocytes. Canadian Journal of Genetics and Cytology 10: 799-807.

Moens, P. B. 1969a. The fine structure of meiotic chromosome pairing in the triploid, Lilium tigrinum. Journal of Cell Biology 40: 273-279.

Moens, P. B. 1969b. Multiple core complexes in grasshopper spermatocytes and spermatid. Journal of Cell Biology 40: 542-551.

Moor, H. 1967. Der feinbau der Mikrotubuli in Hefe nach Gefrieratzung. Protoplasma 64: 89-103.

Moses, M. J. 1956. Chromosomal structures in crayfish spermatocytes. Journal of Biophysical and Biochemical Cytology 2: 215-218.

Moses, M. J. 1960. Patterns of organization in the fine structure of chromosomes. International Conference on Electron Microscopy, 4th, Berlin, 1958, Proceedings 2: 199-211.

Moses, M. J. 1964. The nucleus and chromosomes: A cytological perspective. In Bourne, G., ed. Cytology and cell physiology. 3rd ed. Pp. 423-558. New York, New York, Academic Press, Inc.

Moses, M. J. 1968. Synaptinemal complex. Annual Review of Genetics 2: 363-412.

Moses, M. J. and J. R. Coleman. 1964. Structural patterns and the functional organization of chromosomes. In Locke, M., ed. The role of chromosomes in development. Pp. 11-49. New York, New York, Academic Press, Inc.

Moses, M. J. and J. H. Taylor. 1955. Desoxypentose nucleic acid synthesis during microsporogenesis in Tradescantia. Experimental Cell Research 9: 474-488.

Mota, M. 1962. The ultrastructure of the centromere. International Conference for Electron Microscopy, 5th, Philadelphia, 1962, Proceedings 2: NN-11.

Murray, R. G., A. S. Murray, and A. Pizzo. 1965. The fine structure of mitosis in rat thymic lymphocytes. Journal of Cell Biology 26: 601-619.

Nebel, B. R. 1939. Chromosome structure. Botanical Review 5: 563-626.

Nebel, B. 1959. Observation of mammalian chromosome fine structure and replication with special reference to mouse testis after ionizing radiation. Radiation Research, Supplement 1: 431-452.

Nebel, B. R. 1960. On the structure of mammalian chromosomes during spermatogenesis and after radiation with special reference to cores. International Conference on Electron Microscopy, 4th, Berlin, 1958, Proceedings 2: 227-230.

Nebel, B. R. and E. M. Coulon. 1962a. The fine structure of chromosomes in pigeon spermatocytes. Chromosoma 13: 272-291.

Nebel, B. R. and E. M. Coulon. 1962b. Enzyme effects on pachytene chromosomes of the male pigeon evaluated with the electron microscope. Chromosoma 13: 292-299.

Newcomb, E. H. 1969. Plant microtubules. Annual Review of Plant Physiology 20: 253-288.

Ohno, S., H. P. Klinger, and W. B. Atkin. 1962. Human oogenesis. Cytogenetics 1: 42-51.

Painter, T. S. 1964. Chromosome structure. National Academy of Sciences Proceedings 51: 1282-1285.

Parchman, L. G. and H. Stern. 1969. The inhibition of protein synthesis in meiotic cells and its effect on chromosome behavior. Chromosoma 26: 298-311.

Peacock, W. J. 1965. Chromosome replication. National Cancer Institute Monograph 18: 101-123.

Peveling, E. 1968. Der gegenwartige Stand der Untersuchungen zur Aufklarung der Chromosomenstructur. Cytologia 33: 287-317.

Pickett-Heaps, J. D. and D. H. Northcote. 1966. Organization of microtubules and endoplasmic reticulum during mitosis and cytokinesis in wheat meristems. Journal of Cell Science 1: 109-120.

Porter, K. R. 1960. Problems in the study of nuclear fine structure. International Conference on Electron Microscopy, 4th, Berlin, 1958, Proceedings 2: 503-507.

Prescott, D. M. 1964. Turnover of chromosomal and nuclear proteins. In Bonner, J. and P. Ts'o, eds. The nucleohistones. Pp. 193-199. San Francisco, Holden-Day, Inc.

Prescott, D. M. and M. A. Bender. 1963. Synthesis and behavior of nuclear proteins during the cell life cycle. Journal of Cellular and Comparative Physiology 62: 175-194.

Prescott, D. M. and G. E. Stone. 1965. Synthesis and turnover of nuclear proteins. In Dawe, C. J., ed. The chromosome: structural and functional aspects. Pp. 72-77. Baltimore, Maryland, The Williams and Wilkins Company. c1967.

Rhoades, M. M. 1950. Meiosis in maize. Journal of Heredity 41: 58-67.

Rhoades, M. M. 1961. Meiosis. In Brachet, J. and A. E. Mirsky, eds. The cell. Vol. 3, Pp. 1-76. New York, New York, Academic Press, Inc.

Ris, H. 1945. The structure of meiotic chromosomes in the grasshopper and its bearing on the nature of "chromomeres" and lampbrush chromosomes. Biological Bulletin 89: 242-257.

Ris, H. c1955. The submicroscopic structure of chromosomes. Congress of Cell Biology, 8th, Leiden, 1954: 121-134.

Ris, H. 1956. A study of chromosomes with the electron microscope. In Porter, K. R., ed. Conference on tissue fine structure proceedings. Pp. 385-390. New York, New York, The Rockefeller Institute for Medical Research.

Ris, H. 1961. Ultrastructure and molecular organization of genetic systems. Canadian Journal of Genetics and Cytology 3: 95-120.

Ris, H. 1962. Interpretation of ultrastructure in the cell nucleus. In Harris, R. J. C., ed. The interpretation of ultrastructure. Pp. 69-88. New York, New York, Academic Press, Inc.

Ris, H. 1966a. Fine structure of chromosomes. Royal Society, London, Proceedings B164: 246-257.

Ris, H. 1966b. The organization of chromosomal nucleohistone fibrils. International Congress for Electron Microscopy, 6th, Kyoto, 1966, 2: 339-340.

Ris, H. and B. L. Chandler. 1963. The ultrastructure of genetic systems in prokaryotes and eukaryotes. Cold Spring Harbor Symposia on Quantitative Biology 28: 1-8.

Robbins, E. and N. K. Gonatas. 1964. The ultrastructure of a mammalian cell during the mitotic cycle. Journal of Cell Biology 21: 429-464.

Roth, L. E. 1964. Motile systems with continuous filaments. In Allen, R. D. and N. Kamiya, eds. Primitive motile systems in cell biology. Pp. 527-548. New York, New York, Academic Press, Inc.

Roth, L. E. 1967. Electron microscopy of mitosis in amebae. III. Cold and urea treatments: A basis for test of direct effects of mitotic inhibitors of microtubule formation. Journal of Cell Biology 34: 47-59.

Roth, L. E. and E. W. Daniels. 1962. Electon microscope studies of mitosis in amebae. II. The giant ameba Pelomyxa. Journal of Cell Biology 12: 57-78.

Roth, L. E., H. J. Wilson, and J. Chakraborty. 1966. Anaphase structure in mitotic cells typified by spindle elongation. Journal of Ultrastructure Research 14: 460-483.

Roth, T. F. 1966. Changes in the synaptinemal complex during meiotic prophase in mosquito oocytes. Protoplasma 61: 346-386.

Roth, T. F. and M. Ito. 1967. DNA-dependent formation of the synaptinemal complex at meiotic prophase. Journal of Cell Biology 35: 247-255.

Sabatini, D. D., K. Bensch, and R. J. Barrnett. 1963. Cytochemistry and electron microscopy: The preservation of cellular ultrastructure and enzymatic activity by aldehyde fixation. Journal of Cell Biology 17: 19-58.

Sakai, A. 1968. Electron microscopy of dividing cells. I. Microtubules and formation of the spindle in spore mother cells of Equisetum arvense. Cytologia 33: 318-330.

Sanborn, E., P. F. Koen, J. D. McNabb, and G. Moore. 1964. Cytoplasmic microtubules in mammalian cells. Journal of Ultrastructure Research 11: 123-138.

Sato, S. 1958. Electron microscope studies on the mitotic figure. I. Fine structure of the metaphase spindle. Cytologia 23: 383-394.

Sato, S. 1960. Electron microscope studies on the mitotic figure. III. Process of the spindle formation. Cytologia 25: 119-131.

Sax, K. and L. M. Humphrey. 1934. Structure of meiotic chromosomes in microsporogenesis of Tradescantia. Botanical Gazette 96: 353-362.

Schoefl, G. I. 1964. The effects of actinomycin D on the fine structure of the nucleolus. Journal of Ultrastructure Research 10: 224-243.

Schin, K. S. 1965. Core-strukturen in den meiotischen and post-meiotischen Kernen der Spermatogenese von Gryllus domesticus. Chromosoma 16: 436-452.

Schrader, F. 1953. Mitosis. The movement of chromosomes in cell division. 2nd ed. New York, New York, Columbia University Press.

Schwartz, D. 1955. Studies on crossing over in maize and Drosophila. Journal of Cellular and Comparative Physiology 45 (Suppl. 2): 171-188.

Sen, S. K. 1969. Chromatin-organisation during and after synapsis in cultured microsporocytes of Lilium in presence of mitomycin C and cycloheximide. Experimental Cell Research 55: 123-127.

Seshachar, B. R. and S. Bagga. 1963. A cytochemical study of oogenesis in the dragonfly Pantala flavescens (Fabricius). Growth 27: 225-246.

Sheridan, W. F. and R. J. Barrnet. 1969. Cytochemical studies on chromosome ultrastructure. Journal of Ultrastructure Research 27: 216-229.

Shinke, N. 1959. An electron microscopy study of chromonemata in some higher plants. The Nucleus 2: 161-170.

Sotelo, J. R. and O. Trujillo-Cenoz. 1958. Submicroscopic structure of meiotic chromosomes during prophase. Experimental Cell Research 14: 1-8.

Sotelo, J. R. and R. Wettstein. 1966. Fine structure of meiotic chromosomes; comparative study of nine species of insects. Chromosoma 20: 234-250.

Sparrow, A. H., M. J. Moses, and R. Steele. 1952. A cytological and cytochemical approach to an understanding of radiation damage in dividing cells. British Journal of Radiology 25: 182-188.

Sparvoli, E., H. Gay, and B. P. Kaufmann. 1965. Number and pattern of association of chromonemata in the chromosomes of Tradescantia. Chromosoma 16: 415-435.

Steffensen, D. 1959. A comparative study of the chromosome. Brookhaven Symposia in Biology 12: 103-124.

Stempak, J. G. and R. T. Ward. 1964. An improved staining method for electron microscopy. Journal of Cell Biology 22: 697-701.

Stern, H. and Y. Hotta. 1963. Facets of intracellular regulation of meiosis and mitosis. In Harris, R. J. C., ed. Cell growth and cell division. Pp. 57-76. New York, New York, Academic Press, Inc.

Stevens, B. J. 1965. The fine structure of the nucleolus during mitosis in the grasshopper neuroblast cell. Journal of Cell Biology 24: 349-368.

Stubblefield, E. and B. R. Brinkley. 1967. Architecture and function of the mammalian centriole. In Warren, K. B., ed. Formation and fate of cell organelles. Pp. 175-218. New York, New York, Academic Press, Inc.

Stubblefield, E. and W. Wray. 1969. The structure of the Chinese hamster chromosome (Abstract). Journal of Cell Biology 43: 172a.

Swanson, C. P. 1958. Cytology and cytogenetics. Englewood Cliffs, New Jersey, Prentice-Hall, Inc.

Swanson, C. P. and W. J. Young. 1965. Chromosome reproduction in mitosis and meiosis. In Locke, M., ed. Reproduction: Molecular, subcellular, and cellular. Pp. 107-124. New York, New York, Academic Press, Inc.

Swanson, C. P., T. Merz, and W. J. Young. c1967. Cytogenetics. Englewood Cliffs, New Jersey, Prentice-Hall, Inc.

Swift, H. 1959. Studies on nucleolar function. In Zirkle, R. E., ed. A symposium on molecular biology. Pp. 266-293. Chicago, Illinois, The University of Chicago Press.

Swift, H. 1965. Molecular morphology of the chromosome. In Dawe, C. J., ed. The chromosome: Structural and functional aspects. Pp. 26-49. Baltimore, Maryland, The Williams and Wilkins Company. c1967.

Swift, H., Chairman. 1966. Report of the nucleolus nomenclature committee. National Cancer Institute Monograph 23: 573-574.

Swift, H. and B. J. Stevens. 1966. Nucleolar-chromosomal interaction in microspores of maize. National Cancer Institute Monograph 23: 145-166.

Taylor, J. H. 1953. Autoradiographic detection of incorporation of P^{32} into chromosomes during mitosis and meiosis. Experimental Cell Research 4: 164-173.

Taylor, J. H. 1957. The time and mode of duplication of chromosomes. American Naturalist 91: 209-221.

Taylor, J. H. 1958a. The duplication of chromosomes. Scientific American 198: 36-42. June.

Taylor, J. H. 1958b. Sister chromatid exchanges in tritium-labeled chromosomes. Genetics 43: 515-529.

Taylor, J. H. 1959a. Autoradiographic studies of nucleic acids and proteins during meiosis in Lilium longiflorum. American Journal of Botany 46: 477-484.

Taylor, J. H. 1959b. Autoradiographic studies of the organization and mode of duplication of chromosomes. In Zirkle, R. E., ed. A symposium on molecular biology. Pp. 304-320. Chicago, Illinois, The University of Chicago Press.

Taylor, J. H. 1963. The replication and organization of DNA in chromosomes. In Taylor, J. H., ed. Molecular genetics. Part I. Pp. 65-111. New York, New York, Academic Press, Inc.

Taylor, J. H. 1967a. Meiosis. In Ruhland, W., ed. Encyclopedia of plant physiology. Vol. 18. Pp. 344-367. New York, New York, Springer-Verlag.

Taylor, J. H. 1967b. Patterns and mechanisms of genetic recombination. In Taylor, J. H., ed. Molecular genetics. Part II. Pp. 95-136. New York, New York, Academic Press, Inc.

Taylor, J. H., P. S. Woods, and W. S. Hughes. 1957. The Organization and duplication of chromosomes as revealed by autoradiographic studies using tritium-labeled thymidine. National Academy of Sciences Proceedings 43: 122-128.

Teplitz, R. and S. Ohno. 1963. Postnatal induction of ovogenesis in the rabbit (Oryctolagus cuniculus). Experimental Cell Research 31: 183-189.

Uhl, C. H. 1965a. Chromosome structure and crossing over. Genetics 51: 191-207.

Uhl, C. H. 1965b. A model of sister-strand crossing-over. Nature 206: 1003-1005.

Underbrink, A. G., A. H. Sparrow, A. F. Rogers, and V. Pond. 1967a. Observations on the cytology and fine structure of mitosis in the fern. Ophioglossum petiolatum Hook. Cytologia 32: 489-499.

Underbrink, A. G., Y. C. Ting, and A. H. Sparrow. 1967b. Note on the occurrence of a synaptinemal complex at meiotic prophase in Zea mays L. Canadian Journal of Genetics and Cytology 9: 606-609.

Wettstein, R. and J. R. Sotelo. 1965. Fine structure of meiotic chromosomes. The elementary components of metaphase chromosomes of Gryllus argentinus. Journal of Ultrastructure Research 13: 367-381.

Wilson, H. J. 1967. Fine structure of cell centers in the meiotic cells of Tradescantia (Abstract). Journal of Cell Biology 35: 145a.

Wilson, H. J. 1968. The fine structure of the kinetochore in meiotic cells of Tradescantia. Planta 78: 379-385.

Wimber, D. E. and W. Prensky. 1963. Autoradiography with meiotic chromosomes of the male newt (Triturus viridescens) using H^3-thymidine. Genetics 48: 1731-1738.

Wolfe, S. L. 1965a. The fine structure of isolated chromosomes. Journal of Ultrastructure Research 12: 104-112.

Wolfe, S. L. 1965b. The fine structure of isolated metaphase chromosomes. Experimental Cell Research 37: 45-53.

Wolfe, S. L. 1967. The effect of fixation on the diameter of chromosome fiber isolated by the Langmuir trough-critical point method (Abstract). Journal of Cell Biology 35: 145a.

Wolfe, S. L. and J. N. Grim. 1967. The relationship of isolated chromosome fibers to the fibers of the embedded nucleus. Journal of Ultrastructure Research 19: 382-397.

Wolfe, S. L. and G. M. Hewitt. 1966. Strandedness of meiotic chromosomes from Oncopeltus. Journal of Cell Biology 31: 31-42.

Wolfe, S. L. and B. John. 1965. The organization and ultrastructure of male meiotic chromosomes in Oncopeltus fasciatus. Chromosoma 17: 85-103.

Wolfe, S.L. and P. G. Martin. 1967. Strandedness of chromosomes from two species of Vicia. Electron Microscopy Society of America Proceedings 25: 84-85.

Wolstenholm, D. R. and G. F. Meyer. 1966. Some facts concerning the nature and formation of axial core structure in spermatids of Gryllus domesticus. Chromosoma 18: 272-286.

Woollam, D. H. M. and E. H. K. Ford. 1966. The fine structure of the mammalian chromosome in meiotic prophase with special reference to the synaptinemal complex. Journal of Anatomy (London) 98: 163-173.

Wray, W. and E. Stubblefield. 1969. Separation and biochemical analysis of the morphological components of mammalian chromosomes (Abstract). Journal of Cell Biology 43: 160a.

ACKNOWLEDGMENTS

The author wishes to express his appreciation to Dr. C. C. Bowen for his guidance and stimulation throughout this study, Dr. H. T. Horner, Jr. for his valuable suggestions and encouragement, and Dr. N. R. Lersten for his interest and penetrating discussions.

Also, due recognition must be given to fellow graduate students of the "basement group" for their technical assistance and stimulating, often provocative, discussions.

The author is also grateful to his wife, Karen, and son, James II, for their encouragement, understanding, and sacrifices to make this study possible.

This study was supported in part by a National Science Foundation Graduate Fellowship.

APPENDIX A: THIN-SECTIONING--FIXATION, DEHYDRATION, EMBEDMENT, AND STAINING

Fixation

Glutaraldehyde (Sabatini, et al. 1963)

Phosphate buffer

0.1 M KH_2PO_4	0.1 M Na_2HPO_4	pH
25 ml	25 ml	6.80
11	39	7.24
10	40	7.30
8	42	7.42

For 0.05 M solution, dilute 1:1 with distilled water.

Fixative

Mix 0.6 ml 50% v/v glutaraldehyde with 9.4 ml of desired buffer to obtain 10 ml 3% v/v glutaraldehyde fixative.

Fix material for one hour at room temperature (23° C) or for 12-24 hours at 4° C.

Rinse three times, 20 minutes each, with the above buffer.

Postfix in osmium tetroxide (see below).

Glutaraldehyde-Acrolein (modified Sanborn, et al. 1964)

Phosphate buffer as above

Fixative

Mix 0.6 ml 50% v/v glutaraldehyde and 0.3 ml acrolein with 9.1 ml buffer to get 3% v/v glutaraldehyde-3% v/v acrolein fixative.

Fix, rinse, and postfix as with glutaraldehyde.

Osmium tetroxide (Millonig, 1961)

Phosphate buffer as above.

Fixative

Stock solution--dissolve 0.5 g osmium tetroxide in 25 ml double distilled water to get 2% w/v osmium tetroxide.

Dilute stock solution 1:1 with desired buffer to get 1% w/v buffered osmium tetroxide fixative.

Fix specimen for one hour at 4° C or one-half hour at room temperature (23° C).

Dehydrate and embed (see below).

Dehydration and Embedment

Schedule (modified Luft, 1961)

5 minutes	25% ethanol
5	50
5	70
5	95
5	100
5	100
5	100
5	Propylene oxide (PO)
5	" "
5	" "
15	1 resin: 3 PO
30	1 resin: 1 PO
60	3 resin: 1 PO
12 hours	Pure resin

Pour specimens contained in pure resin into plastic pill vial caps and polymerize 1-3 days at 60° C.

Resin mixture (modified Anderson and Ellis, 1965)

Araldite 502	10 g
Epon 812	12 g
DDSA (Dodecenyl succinic anhydride)	28 g
DMP-30	1.5 ml

Staining

Uranyl Acetate (Stempak and Ward, 1964)

Dissolve 5 g of uranyl acetate ($UO_2(CH_3COO)_2 \cdot 2H_2O$) in 50 ml absolute, acetone-free methanol. Filter the solution and store in a tightly stoppered bottle in the refrigerator (4° C) until ready to use.

Schedule

Place staining solution in a small depression plate contained in a petri dish to reduce evaporation.

Immerse grid, section side up, in staining solution for 20 minutes at room temperature.

Wash grid as follows:

absolute methanol	20 dips
100% ethanol	20 dips
95% ethanol	20 dips
50% ethanol	20 dips
distilled water	50 dips
distilled water	50 dips

Remove excess water with filter paper, and store grid on filter paper in petri dish.

APPENDIX B: FREEZE-ETCHING (modified McAlear and Kreutziger, 1967)

Specimen Preparation

1. Squeeze sporocytes from anthers directly into 3% v/v glutaraldehyde (Appendix A), 0.1 M phosphate buffer, pH 6.8, and fix at room temperature for one hour.

2. Pellet the material using a clinical centrifugue, and rinse three times, 20 minutes each, with the above buffer.

3. Infiltrate with ethylene glycol as follows:

7% (v/v in above buffer)		1 hour
15%	"	1 hour
30%	"	3 hours

4. Spin down the sporocytes into a thick suspension using the clinical centrifugue, and draw the suspension via capillary action into a 1 mm diameter by 3 mm length tube rolled from a 400 mesh copper grid.

5. Freeze the specimen in a puddle of liquid propane cooled with liquid nitrogen, quickly blot off the excess propane, and store in a glass vial under liquid nitrogen.

Fracture-Replication

1. Align both shadow (platinum wire) and replica (carbon rod) electrodes with the tunnels in the Berkeley Freeze-Etch Device.

2. Clean all parts of the device with Alconox, rinse well with water, and dry thoroughly with Kimwipes and filtered air.

3. Place the lid and base of the device under liquid nitrogen in a styrofoam bucket.

4. As the lid and base cool, place the specimen holder under liquid nitrogen in a shallow styrofoam dish and insert the frozen specimen into the hole in the specimen holder.

5. Transfer the specimen holder with specimen to the cooled base under liquid nitrogen and place the lid into position.

6. Transfer the entire assembly to the Varian VE-30M vacuum evaporator, and follow the vacuum pumpdown sequence.

7. After reaching a pressure of 10^{-4} Torr or less, degas the electrodes by heating them to red hot for one minute.

8. When the pressure is 6×10^{-6} Torr (approximately 15 minutes from the start of pumpdown), rotate the lid of the freeze-etch device to fracture the specimen and to bring the tunnels in the lid over the fractured specimen and in line with the platinum and carbon electrodes.

9. Allow the specimen to etch by utilizing the heat sink (2-5 minutes).

10. Evaporate the platinum and follow immediately with carbon.

11. Return to atmospheric pressure, and remove the entire assembly from the vacuum evaporator.

Cleaning the Replica

1. Remove the specimen with attached replica from the specimen holder and place in 35% (v/v in phosphate buffer) ethylene glycol in a white porcelain depression plate.

2. Transfer the replica with attached material to standard laboratory dichromate cleaning solution and heat to 60° C for 15 minutes. Transfer the replica to fresh cleaning solution and allow it to return to room temperature.

3. Rinse the cleaned replica six times in double distilled water and pick it up on a 400 mesh copper grid.

APPENDIX C: FIGURES

Figures 1-8. Light micrographs of lacto-aceto orcein squashes used to determine approximate meiotic stages of the anthers prior to fixation for electron microscopy. Line scales = 10 µm. 850 x

Figure 1. Early zygotene

Figure 2. Pachytene

Figure 3. Diffuse diplotene

Figure 4. Late diplotene

Figure 5. Diakinesis

Figure 6. Metaphase I

Figure 7. Anaphase I

Figure 8. Early telophase I

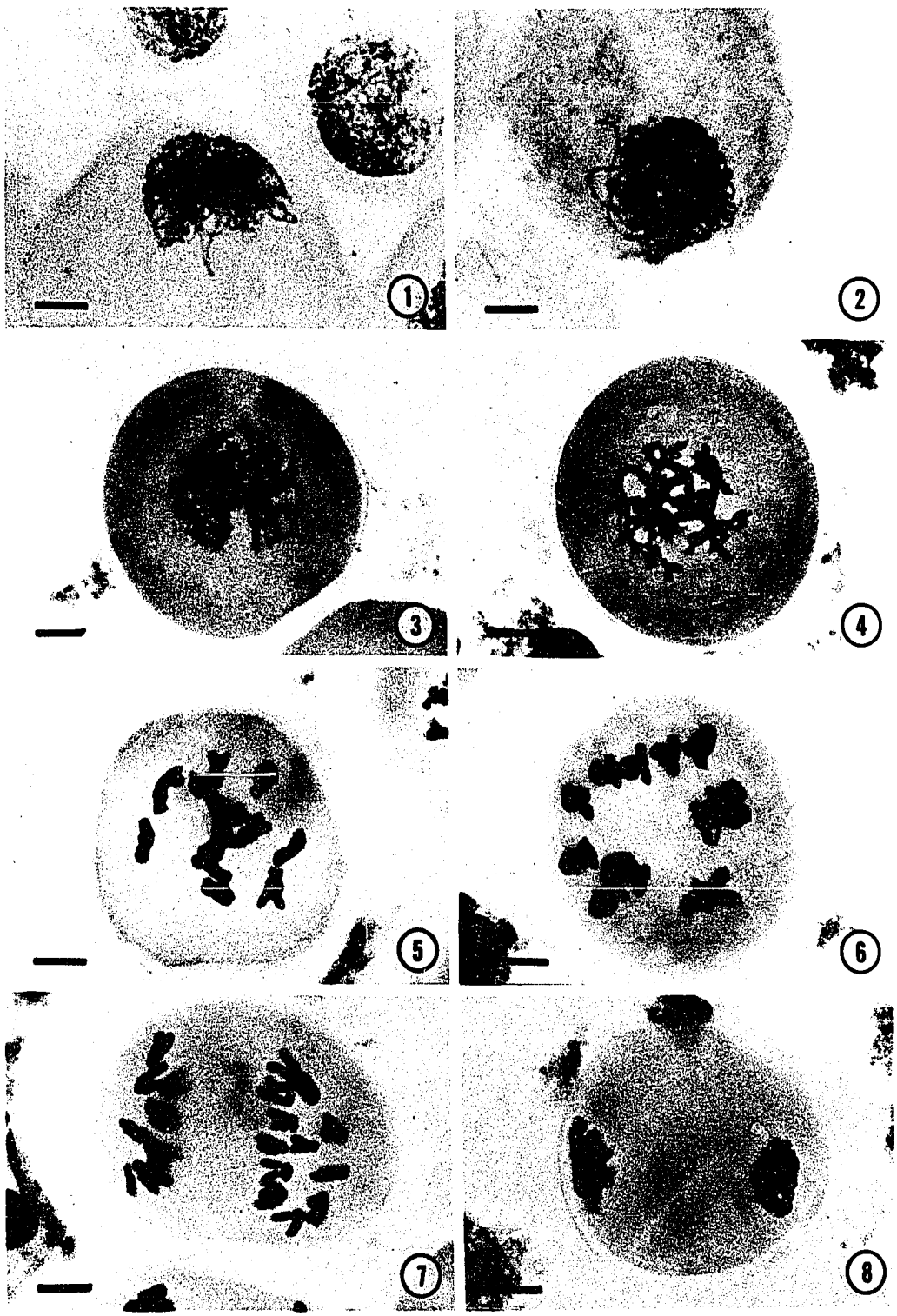
1
2
3
4
5
6
7
8

Figure 9. Zygotene synaptinemal complex (sc). Nucleolus (Nu) is appressed to the nuclear envelope and consists of fine 10-15 nm diameter fibrils (arrows). Glutaraldehyde-acrolein, osmium fixation. Line scale = 0.5 μm. 40,000 x

Figure 10. Pachytene synaptinemal complex (sc) consisting of the lateral complex (L), central region (CR), and central element (CE). Glutaraldehyde-acolein, osmium fixaion. Line scale = 0.5 μm. 40,000 x

Figure 11. Zygotene nucleolar organizer (no) is less electron-dense than both the chromatin (C) and nucleolus (Nu). The structural components of the nucleolar organizer are 7.5-12.5 nm diameter fibrils (arrows). Glutaraldehyde-acrolein, osmium fixation. Line scale = 0.5 μm. 40,000 x

Figure 12. Late diplotene nucleolar organizer (no) is less electron-dense than both the chromatin (C) and nucleolus (Nu). The structural components of the nucleolar organizer are 7.5-12.5 nm diameter fibrils (arrows). Glutaraldehyde-acrolein, osmium fixation. Line scale = 0.5 μm. 40,000 x

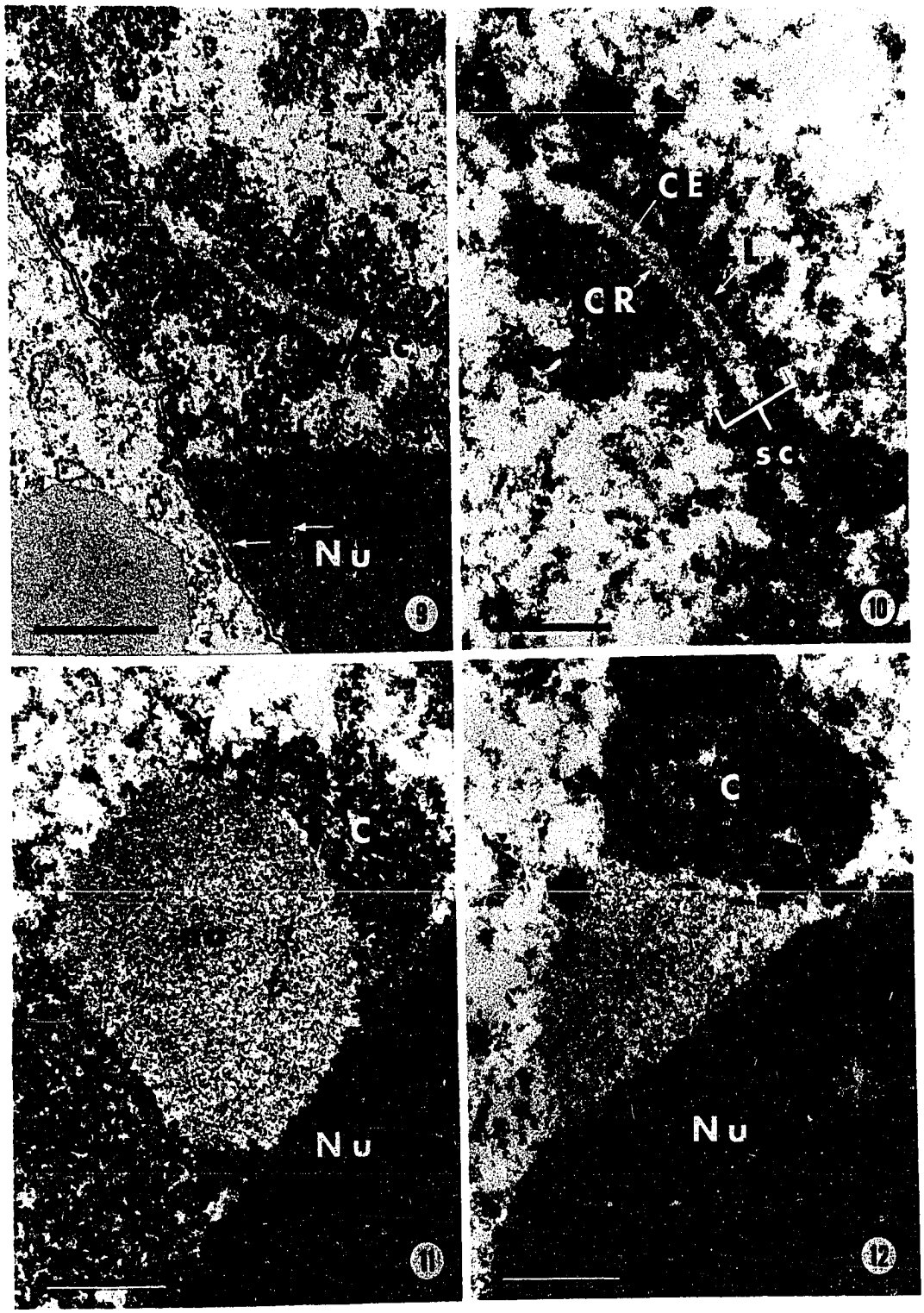
Nu
9
CE
L
CR
SC
10
C
Nu
11
C
Nu
12

Figures 13-16. Nucleoli from several prophase stages. Small arrow indicate relatively electron-transparent "vacuoles". Glutaraldehyde-acrolein, osmium fixation. Line scales = 1 μm. 20,000 x

Figure 13. Zygotene nucleolus appressed to the nuclear envelope (large arrows)

Figure 14. Pachytene nucleolus

Figure 15. Diffuse diplotene nucleolus

Figure 16. Late diplotene nucleolus

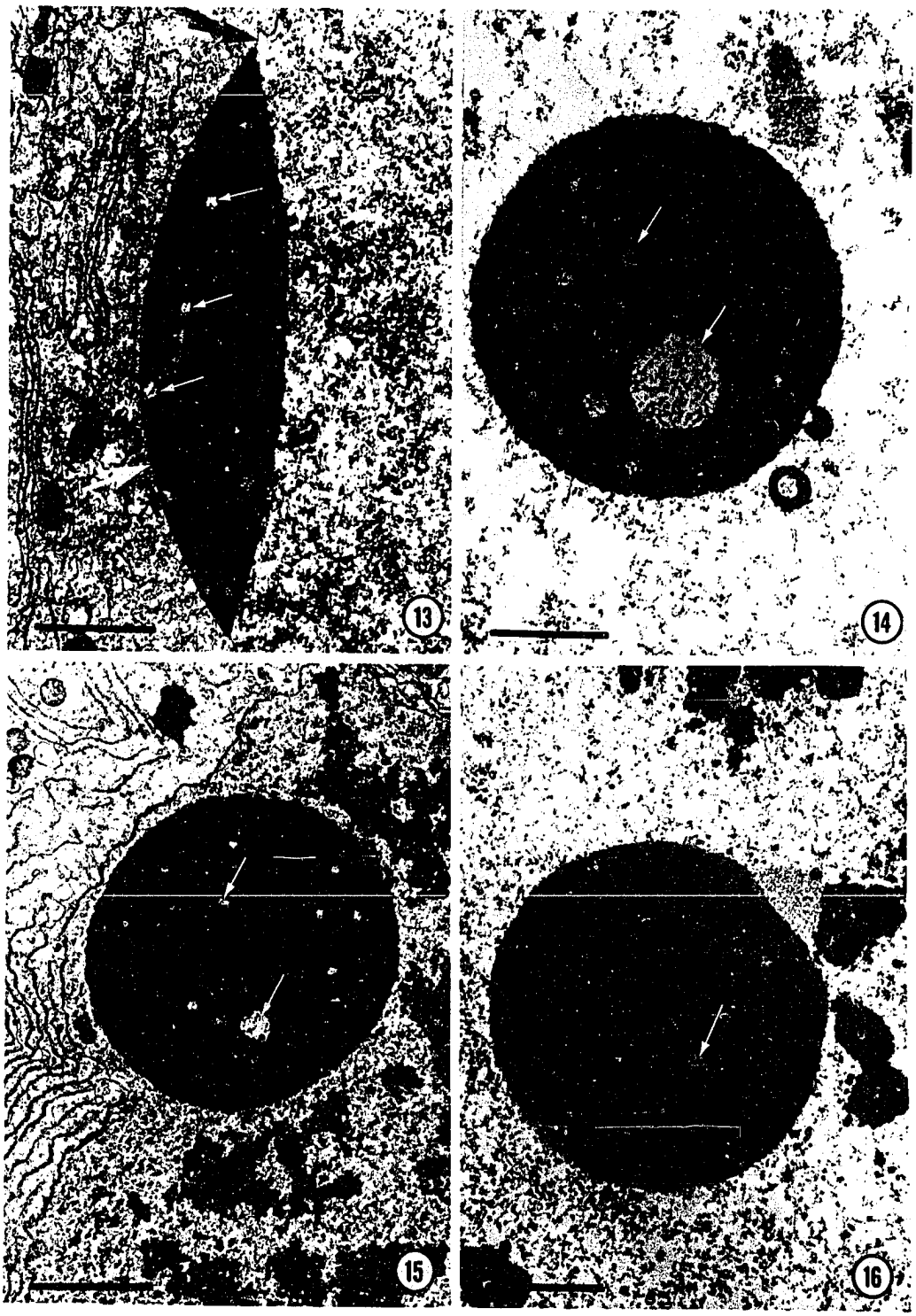
13
14
15
16

Figure 17. Light micrograph of leptotene. Glutaraldehyde-acrolein, osmium fixation. Line scale = 10 µm. 850 x

Figure 18. Area enlarged from rectangle in Figure 20. Compare this untouched micrograph with the interpretations in Figure 19. Glutaraldehyde-acrolein, osmium fixation. Line scale = 0.2 µm. 60,000 x

Figure 19. Interpretation of 20 nm fibril profiles that appear coiled into a 80-120 nm unit. Glutaraldehyde-acrolein, osmium fixation. Line scale = 0.2 µm. 60,000 x

Figure 20. Leptotene chromatin with 300-500 nm chromosome (CH) consisting of paired, twisting 80-120 nm profiles, the chromatids (arrows). Area enclosed in rectangle is shown at a higher magnification in Figures 18 and 19. Glutaraldehyde-acrolein, osmium fixation. Line scale = 0.5 µm. 40,000 x

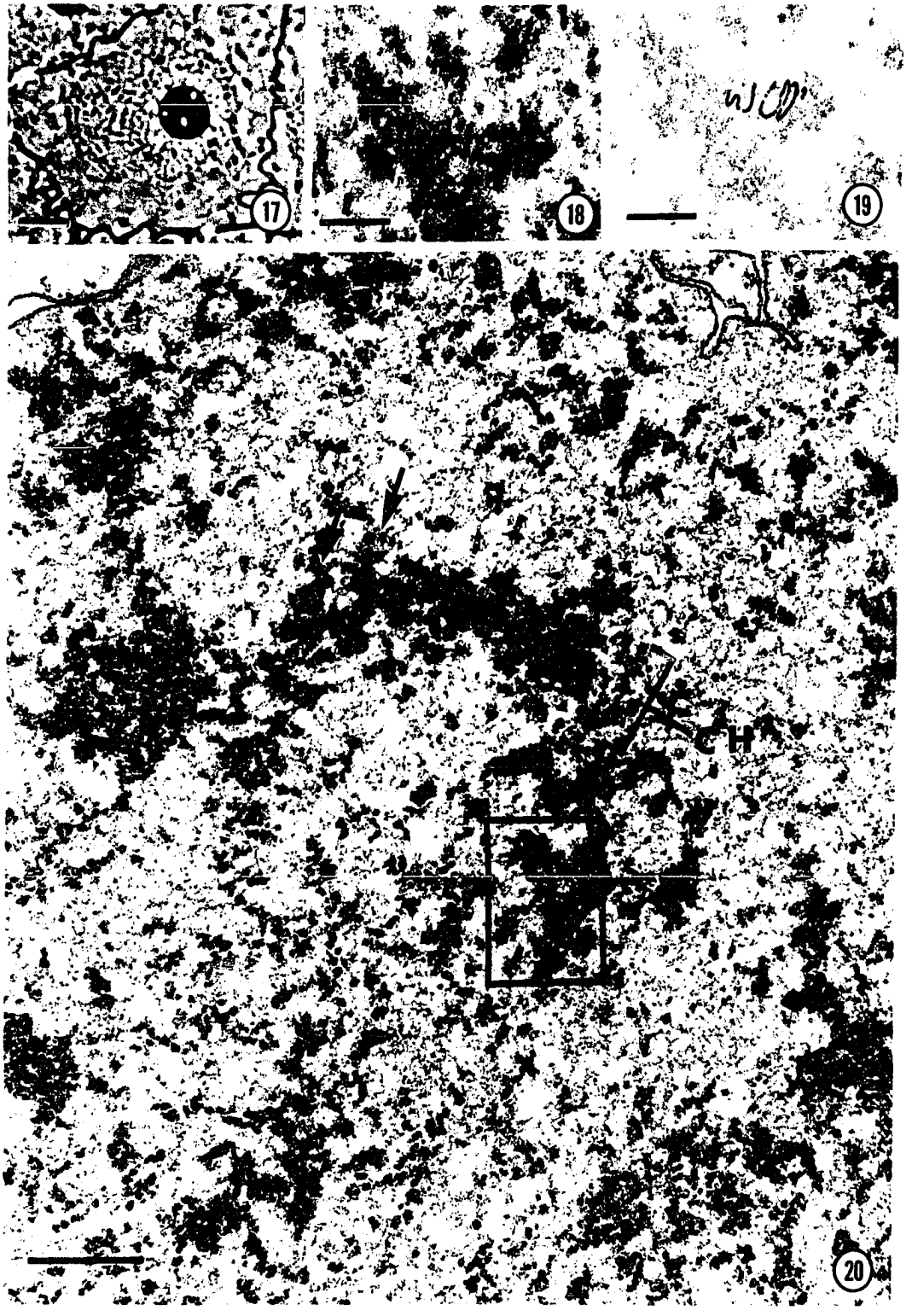
17
18
19
H
20

Figure 21. Light micrograph of zygotene. Glutaraldehyde-acrolein, osmium fixation. Line scale = 10 µm. 850 x

Figure 22. Area enlarged from rectangle in Figure 24. Compare this untouched micrograph with the interpretations in Figure 23. Glutaraldehyde-acrolein, osmium fixation. Line scale = 0.2 µm. 60,000 x

Figure 23. Interpretations of 20 nm fibril profiles that appear coiled into 80-120 nm units (dotted outline). Glutaraldehyde-acrolein, osmium fixation. Line scale = 0.2 µm. 60,000x

Figure 24. Zygotene chromatin. The 500-600 nm chromosomes (CH) lie on each side of the synaptinemal complex (sc). Clear spaces (KS) occur within the chromosomes and delineate 200-250 nm chromatids (CT). Undulating 80-120 nm profiles (small arrows) suggest that the 200-250 nm chromatids are formed from coiled 80-120 nm elements. Area within rectangle is enlarged in Figures 22 and 23. Glutaraldehyde-acrolein, osmium fixation. Line scale = 0.5 µm. 40,000 x

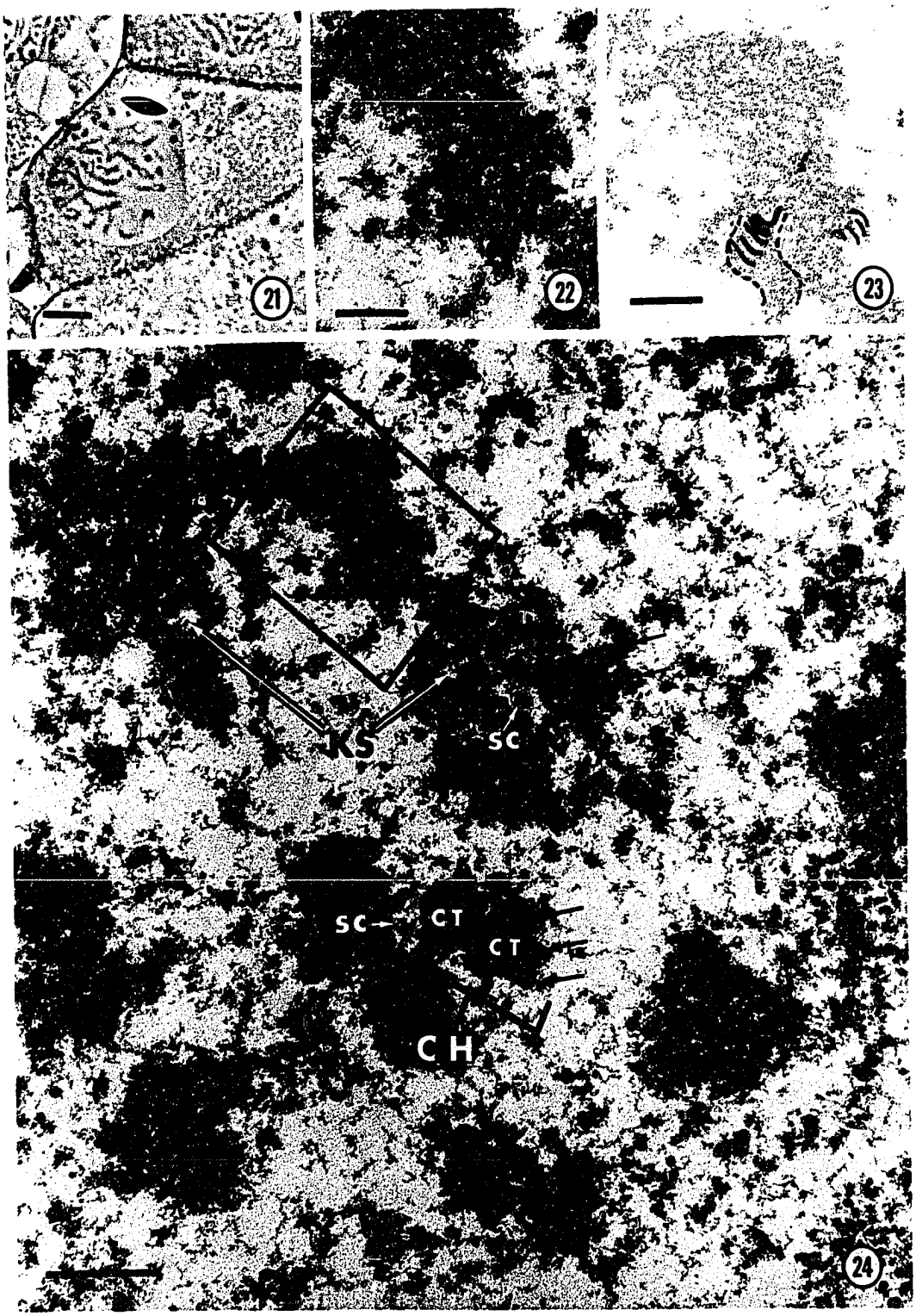
21
22
23
KS
SC
SC
CT
CT
CH
24

Figure 25. Light micrograph of pachytene. Glutaraldehyde-acrolein, osmium fixation. Line scale = 10 μm. 850 x

Figure 26. Area enlarged from rectangle in Figure 28. Compare this untouched micrograph with the interpretations in Figure 27. Glutaraldehyde-acrolein, osmium fixation. Line scale = 0.2 μm. 60,000 x

Figure 27. Interpretations showing profiles of curved 80-120 nm elements (dotted outlines) that appear to be components of the 300 nm chromatids. Profiles of the 20 nm fibrils suggest they are coiled into the 80-120 nm elements. Glutaraldehyde-acrolein, osmium fixation. Line scale = 0.2 μm. 60,000 x

Figure 28. Cross section of pachytene bivalent (1-1.5 μm in diameter) showing dense, amorphous appearing chromatin surrounding the synaptinemal complex (sc). Clear spaces (KS) delineate 300 nm chromatids (brackets) which have undulating profiles suggesting that they are coiled. Area within rectangle is enlarged in Figures 26 and 27. Glutaraldehyde-acrolein, osmium fixation. Line scale = 0.5 μm. 40,000 x

Figure 29. Longitudinal section of pachytene bivalent containing clear spaces (KS) that indicate boundaries between 300 nm chromatids (left bracket) within 500-600 nm chromosomes (right bracket). Synaptinemal complex (sc) occurs in the axis between the homologues. Glutaraldehyde-acrolein, osmium fixation. Line scale = 0.5 μm. 40,000x


25
26
27
SC
KS
28
KS
SC
KS
29

Figure 30. Light micrograph of diffuse diplotene. Glutaraldehyde-acrolein, osmium fixation. Line scale = 10 μm. 850 x

Figure 31. Survey micrograph of nucleus in diffuse diplotene in which bivalents and individual chromosomes are difficult to distinguish. Chromatin units (C) range up to 2-2.5 μm wide, and contain numerous clear spaces (KS) which delineate 500-600 nm profiles (brackets) which are sometimes paired (two large arrows). Twisted profiles of 175-250 nm units (small arrows) appear to compose the 500-600 nm units. A nucleolus (Nu) is also present. Glutaraldehyde-acrolein, osmium fixation. Line scale = 1 μm. 10,000 x

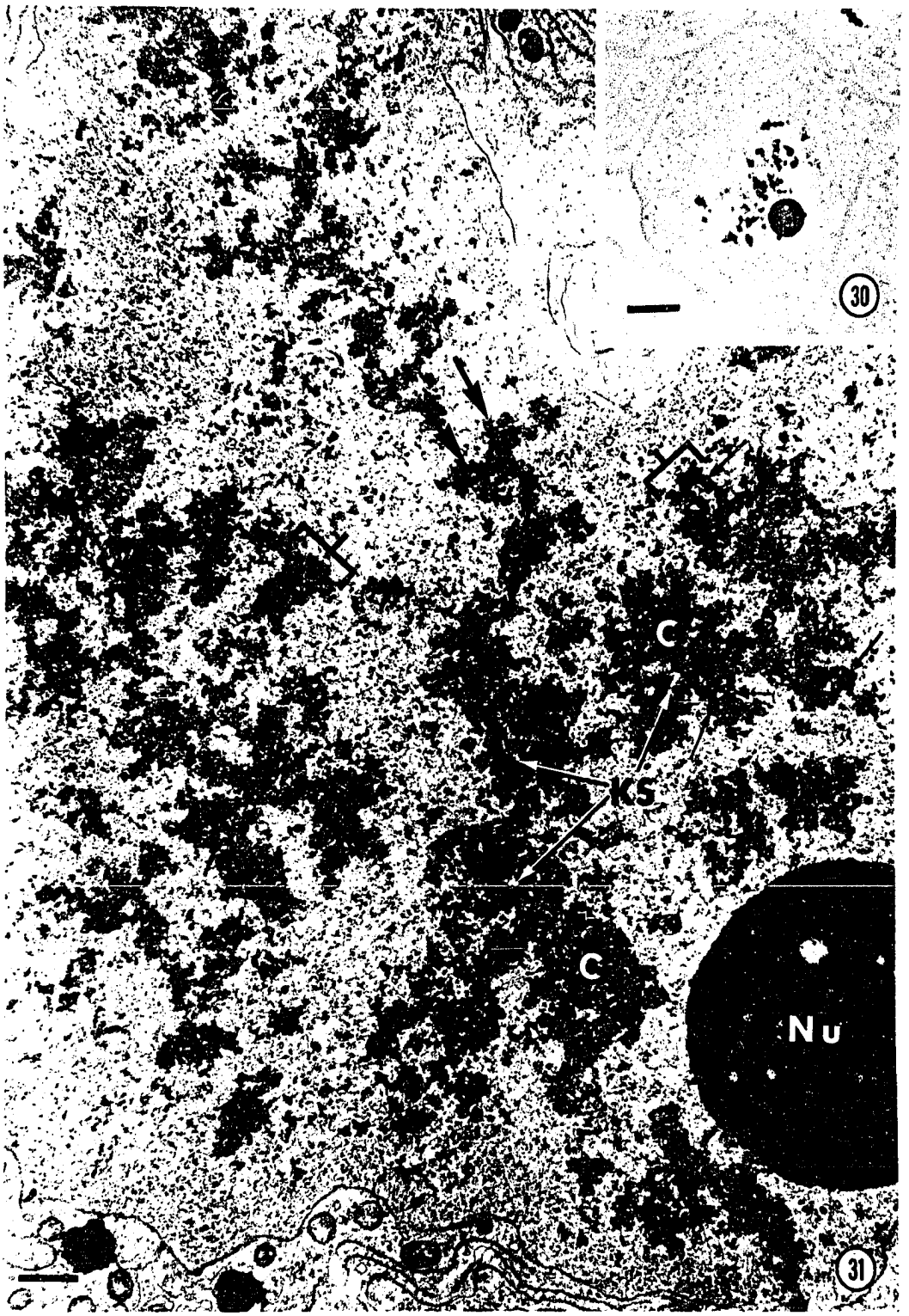
30
C
KS
C
Nu
31

Figure 32. Diffuse diplotene in which the higher structural units are beginning to reappear. The 1.5-1.75 μm chromosome (CH) contains loosely arranged 500-600 nm chromatids (CT), which in turn contain side-by-side 175-250 nm units, apparently subchromatids (SCT). Curved profiles of 80-120 nm elements (small arrows) suggest that they are coiled into the subchromatids. Glutaraldehyde, osmium fixation. Line scale = 0.5 μm. 40,000 x

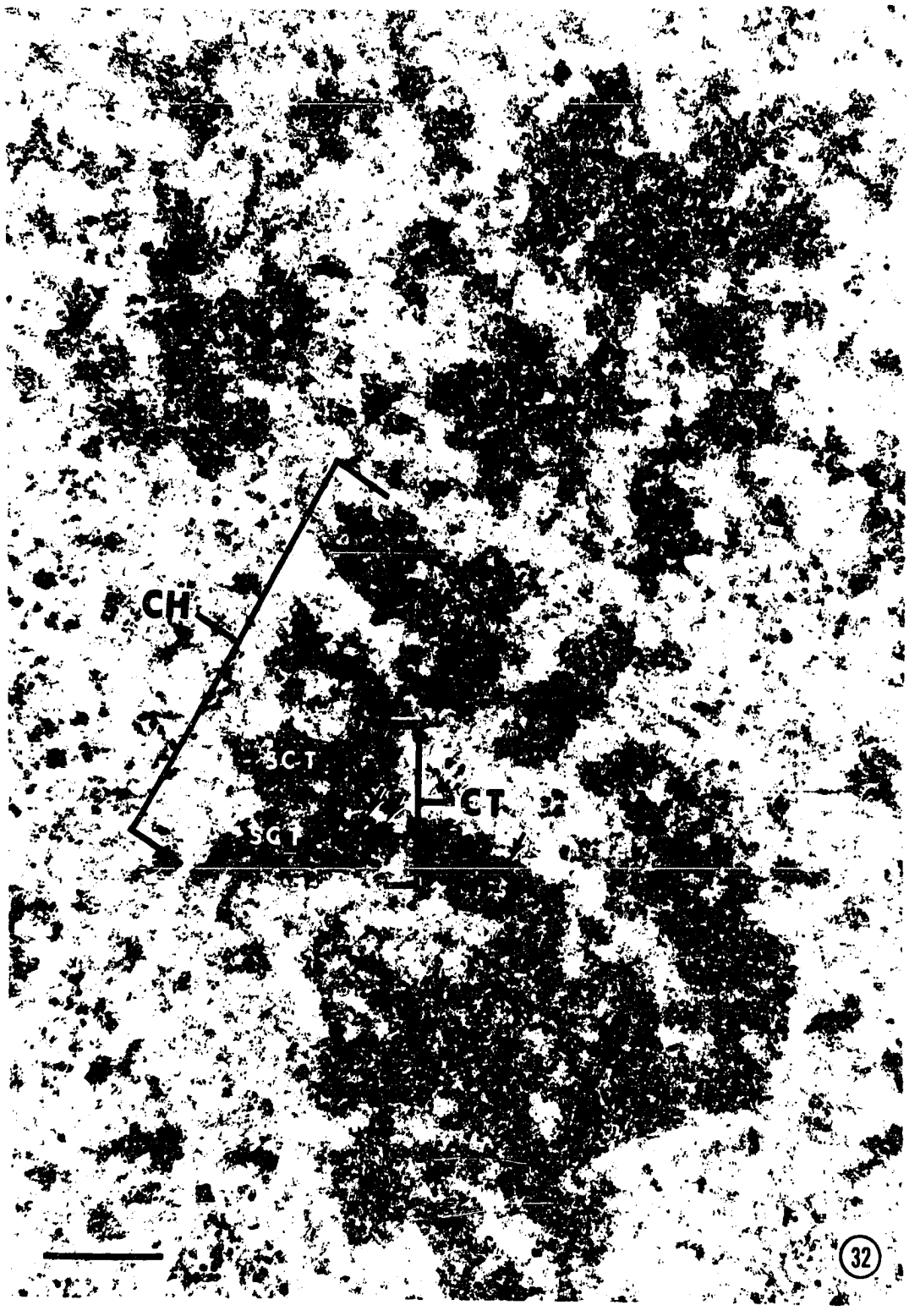
CH
SCT
CT
SCT
32

Figure 33. Late diffuse diplotene chromatid (CT) with clear spaces (KS) delineating two 200-300 nm subchromatids (1 and 2) which appear to be twisted around each other. Bracket on left encloses a undulating 200 nm profile, possibly a grazed subchromatid. Area enclosed in square is enlarged in Figures 40 and 41. Glutaraldehyde, osmium fixation. Line scale = 0.5 µm. 40,000 x


1
2
KS
33

Figures 34-37. Freeze-etch preparations of diffuse diplotene. The elementary chromosome fibrils are approximately 10 nm in diameter and more difficult to delineate than in sectioned material. Arrows in upper left corners indicate the direction of the platinum "shadow".

Figure 34. Chromatin (C) occurs in units up to 600-800 nm across (parallel bars), and stands out above the background (BG). A twisted 300 nm unit is indicated by the bracket. Areas within rectangles are enlarged in Figures 35 and 36. Line scale = 0.5 µm. 50,000 x

Figure 35. Small bracket indicates a 80-120 nm element contained within a 200-300 nm unit (large bracket). Line scale = 0.2 µm. 75,000 x

Figure 36. Loop of chromatin (bracket) 300 nm wide, suggesting a portion of a gyre. Line scale = 0.2 µm. 75,000 x

Figure 37. Chromatin appears in a 80-120 nm element (Bracket Y) and also in a 200-300 nm unit (Bracket Z). Note the nuclear envelope (NE). Line scale = 0.5 µm. 50,000 x

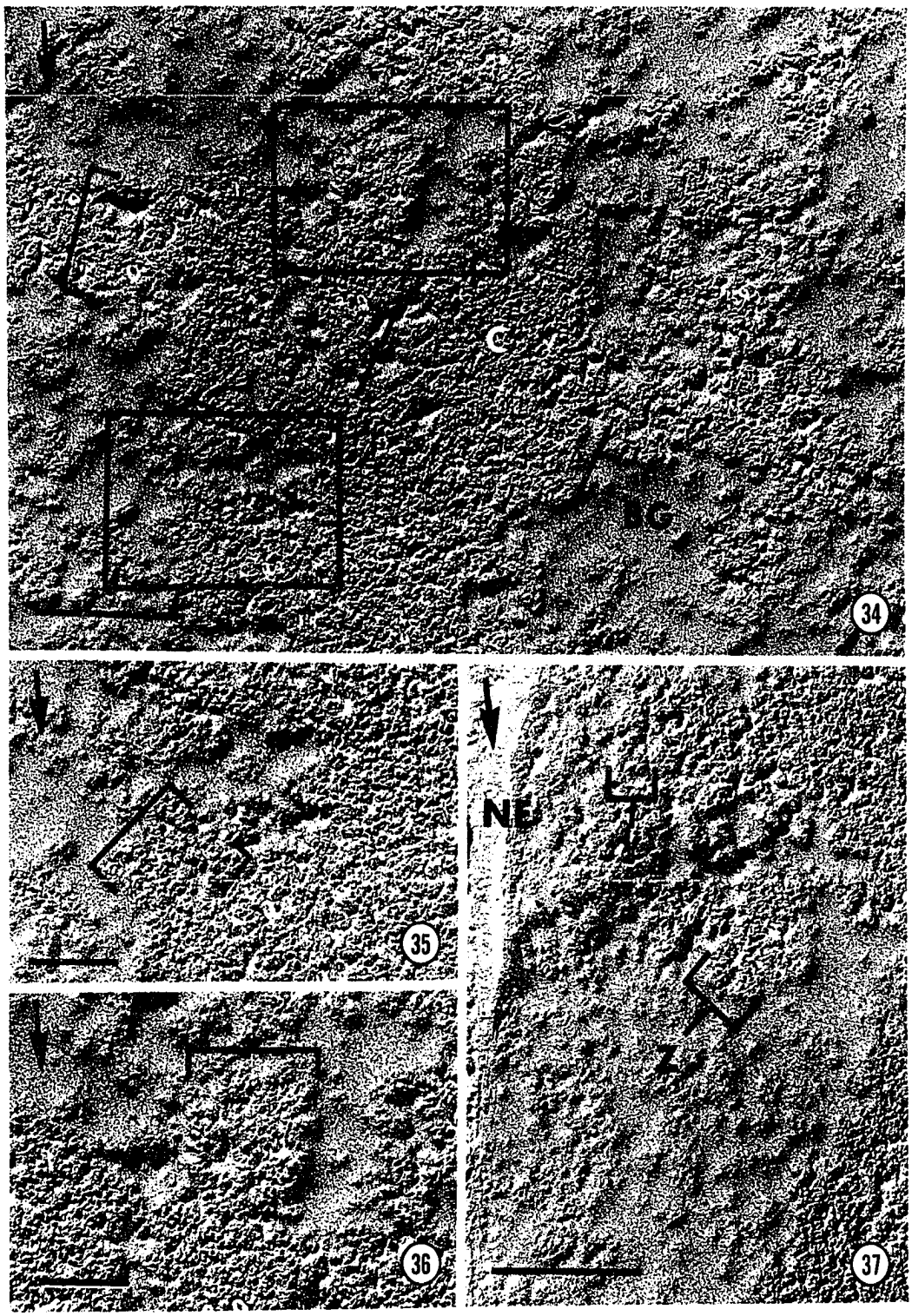
C
NE
34
35
36
37

Figure 38. Light micrograph of late diplotene. Glutaraldehyde, osmium fixation. Line scale = 10 µm. 850 x

Figure 39. Late diplotene bivalent with clear spaces (KS) separating the chromosomes (CH) and the 500-800 nm chromatids (CT) paired within the chromosomes. Subchromatids (SCT), 300-400 nm in diameter, occur side-by-side within the chromatids. Black arrows indicate a 300 nm unit, possibly a grazed subchromatid, composed of a 80-120 nm element folded, or possibly coiled, back onto itself. White arrows point out a subchromatid-size profile continuous between the homologues. Glutaraldehyde, osmium fixation. Line scale = 0.5 µm. 40,000 x

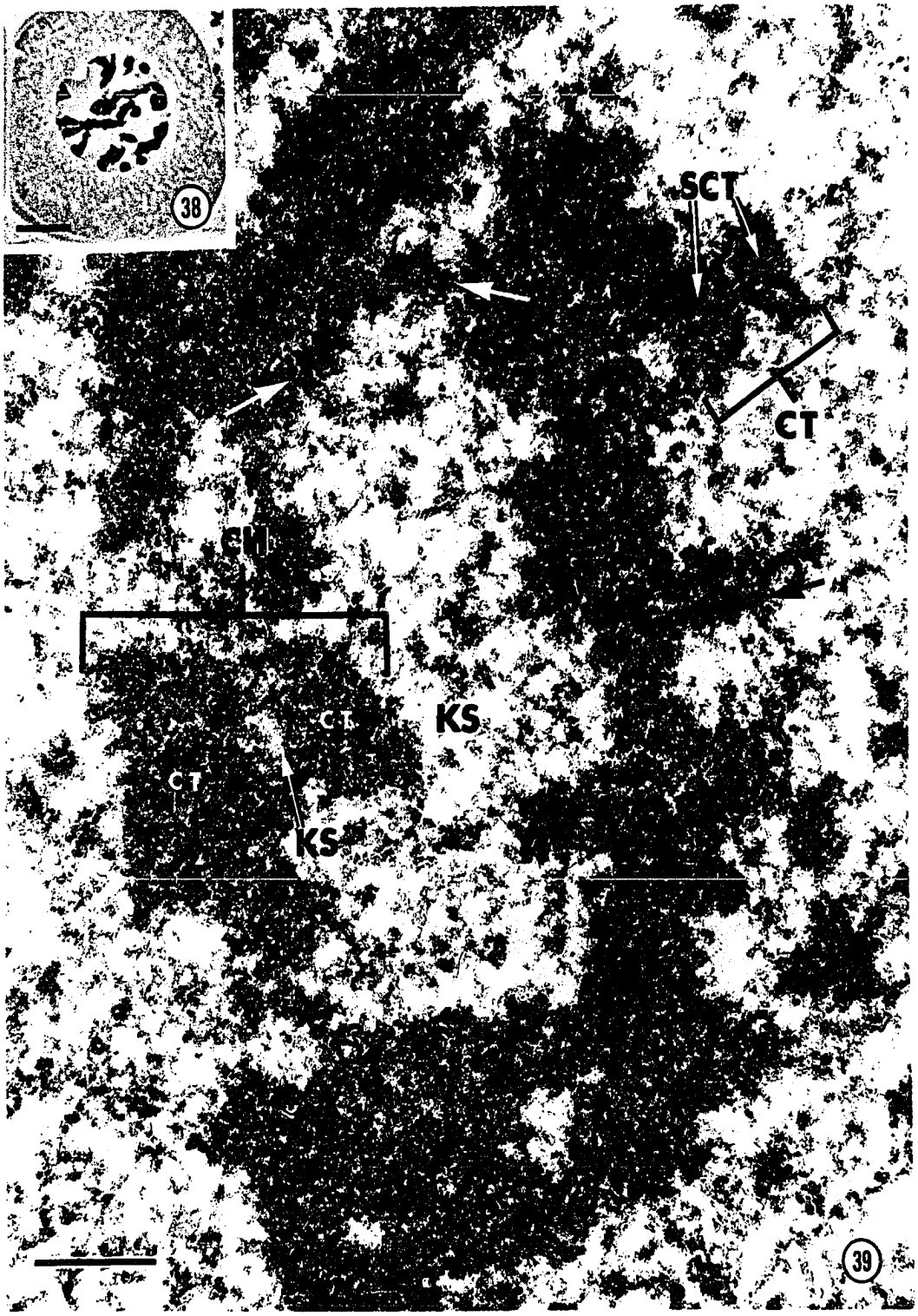
38
SCT
CT
CT
KS
CT
CT
KS
39

Figures 40-47. Micrographs of diffuse and late diplotene chromatin mounted so that interpretation may be presented and compared to the untouched micrographs. Glutaraldehyde, osmium fixation. Line scales = 0.2 μm. 50,000 x

Figure 40. Diffuse diplotene area enlarged from Figure 33. Compare to Figure 41

Figure 41. Interpretation of 20 nm fibril profiles that appear coiled into a 80-120 nm element

Figure 42. Diffuse diplotene. Compare to Figure 43

Figure 43. Interpretations of 20 nm fibril profiles that appear coiled into several 80-120 nm elements

Figure 44. Late diplotene. Compare to Figure 45

Figure 45. Interpretation of 20 nm fibril profiles that appear coiled into a 80-120 nm element

Figure 46. Late diplotene. Compare to Figure 47

Figure 47. Interpretation of 20 nm fibril profiles that appear coiled into a 80-120 nm element

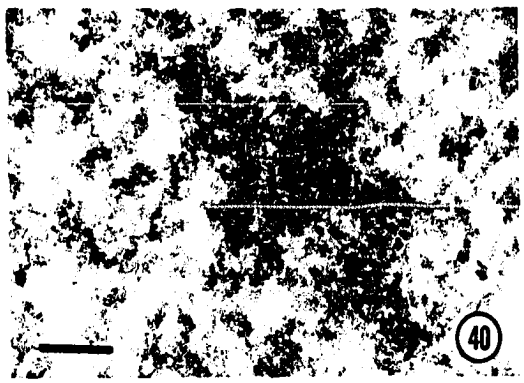
40

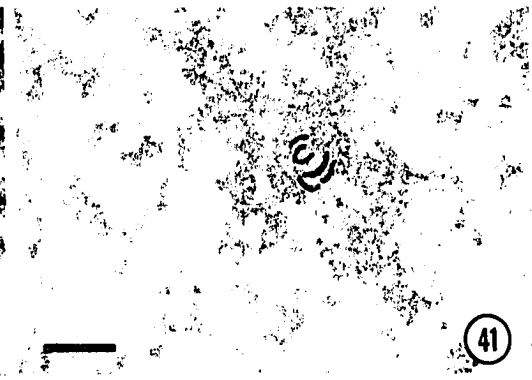
41

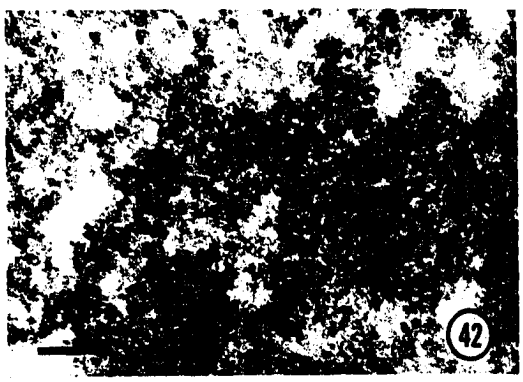
42

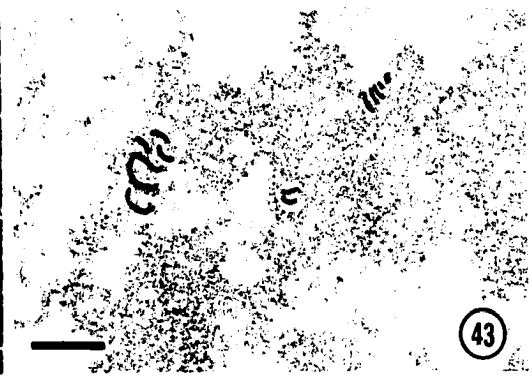
43

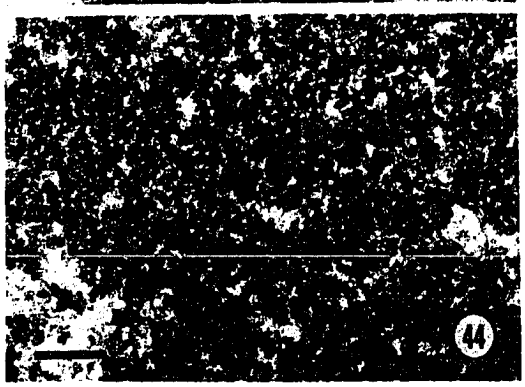
44

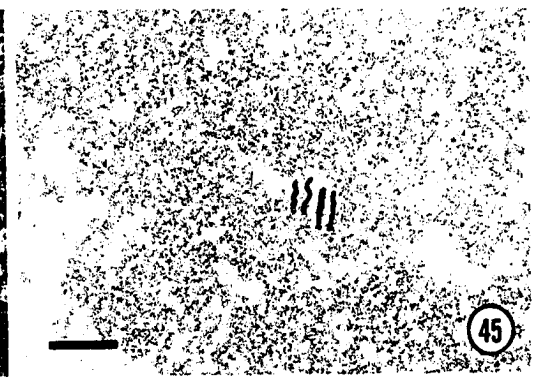
45

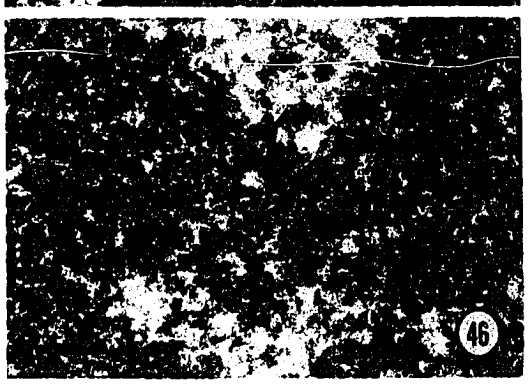
46


47

Figure 48. Light micrograph of diakinesis. Glutaraldehyde-acrolein, osmium fixation. Line scale = 10 μm. 850 x

Figure 49. Bivalent in diakinesis with 2 um diameter chromosomes (CH) widely separated except for their close association at the chiasmata (1 and 2). Clear spaces (KS) delineate 800-900 nm chromatids (CT). Also, 400-500 nm units, apparently subchromatids (SCT), can be seen paired within the chromatids. The kinetochore (K) is less electron-dense than the rest of the chromatin. Glutaraldehyde-acrolein, osmium fixation. Line scale = 1 μm. 26,000 x

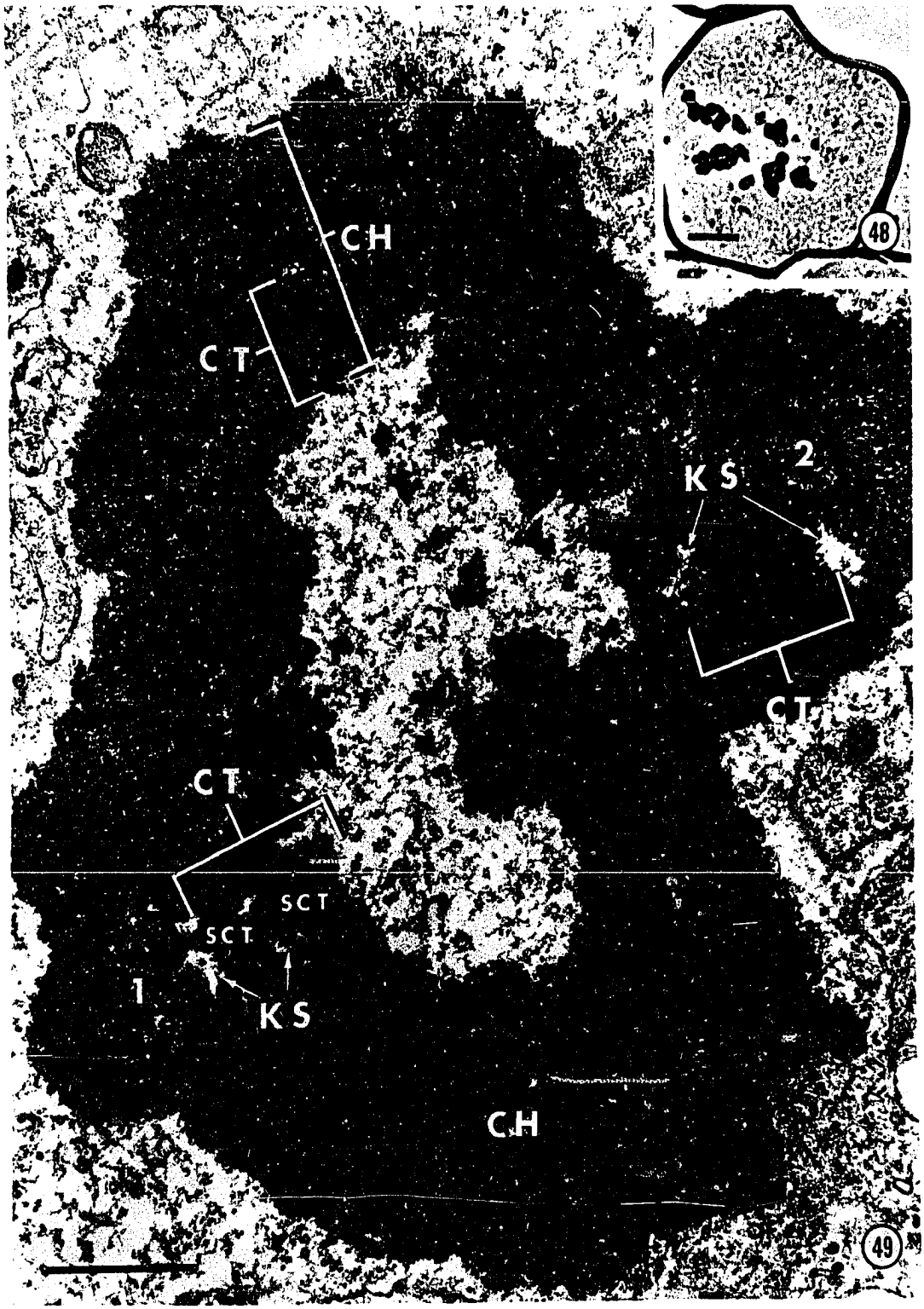
CH
CT
KS
2
CT
CT
SCT
SCT
1
KS
CH
48
49

Figure 50. Near cross sectional view through a chiasma of a bivalent in diakinesis. One of the chromosomes (CH) can be seen to consist of two 800-900 nm chromatids (CT), which contain 400-500 nm subchromatids (SCT). Clear spaces (KS) indicate the boundaries of the above units. Subchromatid size (small arrow) and chromatid size (large arrow) units are continuous between the homologues. Glutaraldehyde-acrolein, osmium fixation. Line scale = 0.5 μm. 40,000 x

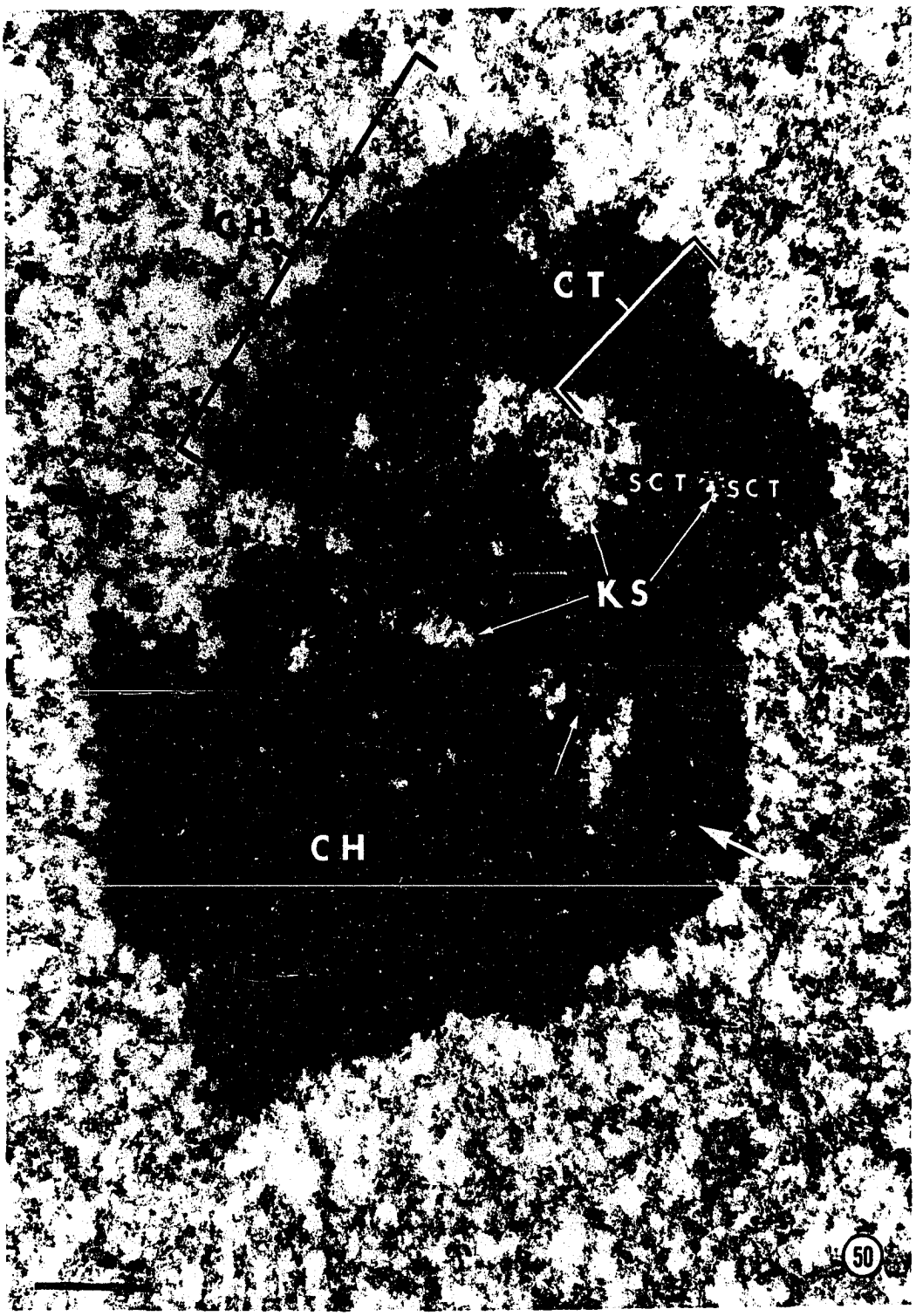
CH
CT
SCT
SCT
KS
CH
50

Figure 51. Light micrograph of metaphase I. Thick section adjacent to area in Figure 52. Glutaraldehyde, osmium fixation. Line scale = 10 μm. 850 x

Figure 52. Metaphase I. Survey micrograph with three bivalents (B) oriented on the metaphase plate. Note the undulating profiles of the bivalents, and also the microtubules (M) connected to the kinetochores (K). One of these kinetochores is shown at a higher magnification in Figure 85. Glutaraldehyde, osmium fixation. Line scale = 1 μm. 9,200 x

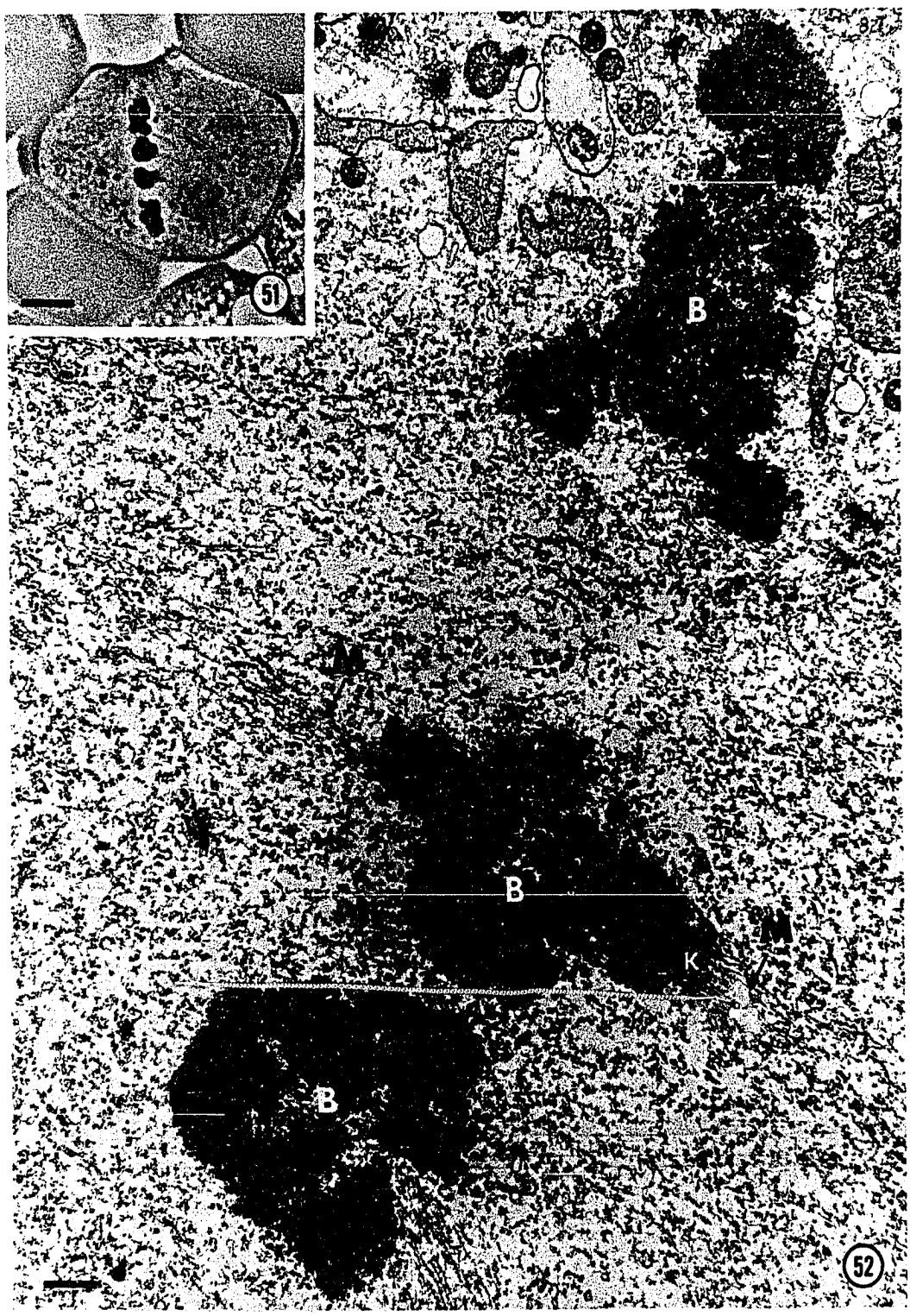
51
B
B
K
B
52

Figure 53. Cross section of metaphase I bivalent showing continuous microtubules (M) passing between the homologues. Clear spaces (KS) mark the boundaries between chromatids (CT), but sub-chromatids cannot be distinguished. Area enclosed in rectangle is enlarged in Figure 56. Glutaraldehyde, osmium fixation. Line scale = 1 μm. 25,000 x

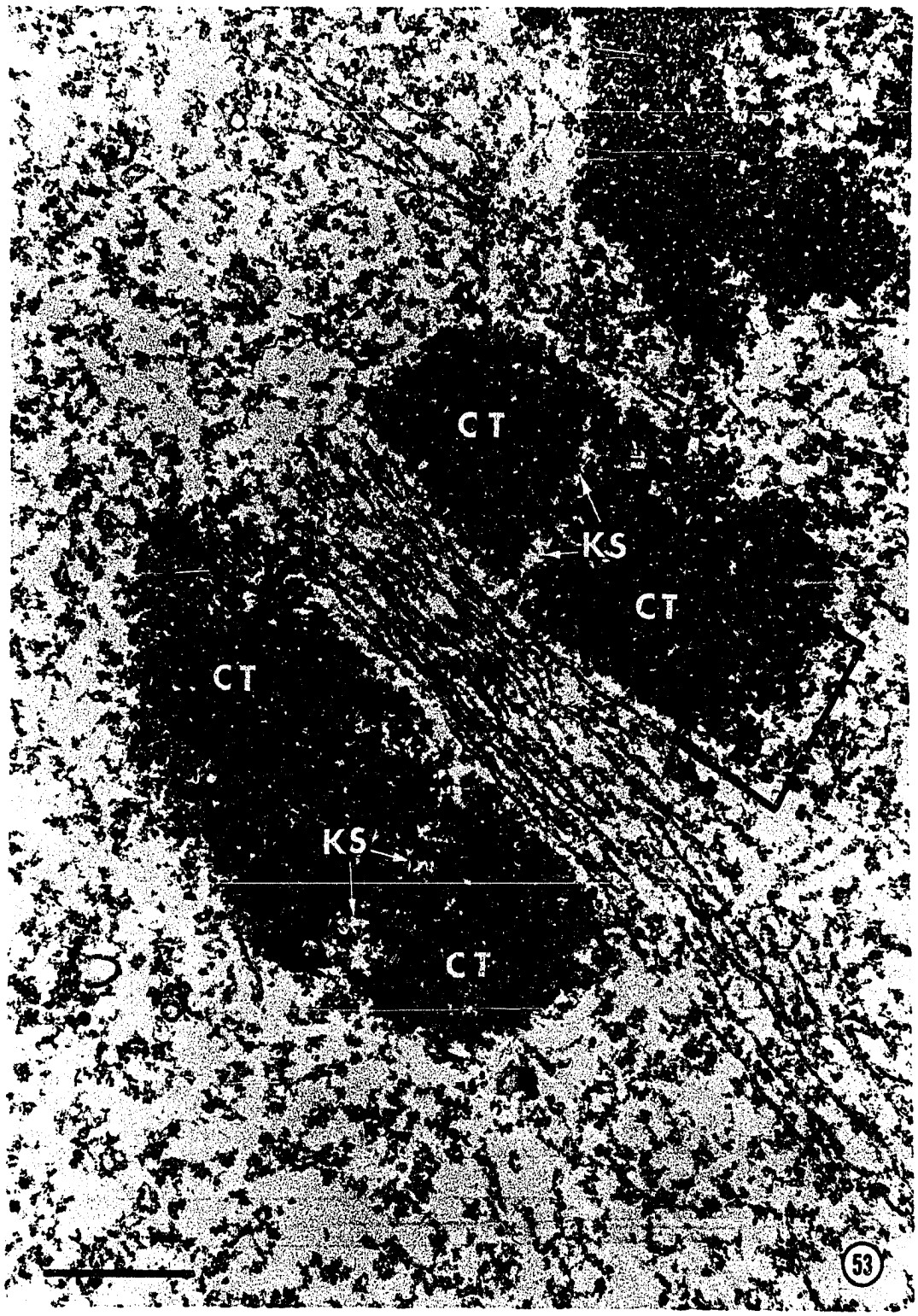
CT
KS
CT
CT
KS
CT
53

Figure 54. Metaphase I bivalent with grazed kinetochore (K), continuous microtubules between the bivalents (white arrow), continuous microtubules between the homologues (black arrow), and a microtubule (double, small white arrows) embedded in the chromatin mass. Area enclosed in rectangle is enlarged in Figure 58. Glutaraldehyde, osmium fixation. Line scale = 1 μm. 20,000 x

Figure 55. Portion of metaphase I bivalent showing a chromatid (CT) with a curved profile suggesting it is a portion of a gyre. Area enclosed in rectangle is enlarged in Figure 59. Glutaraldehyde, osmium fixation. Line scale = 1 μm. 20,000 x

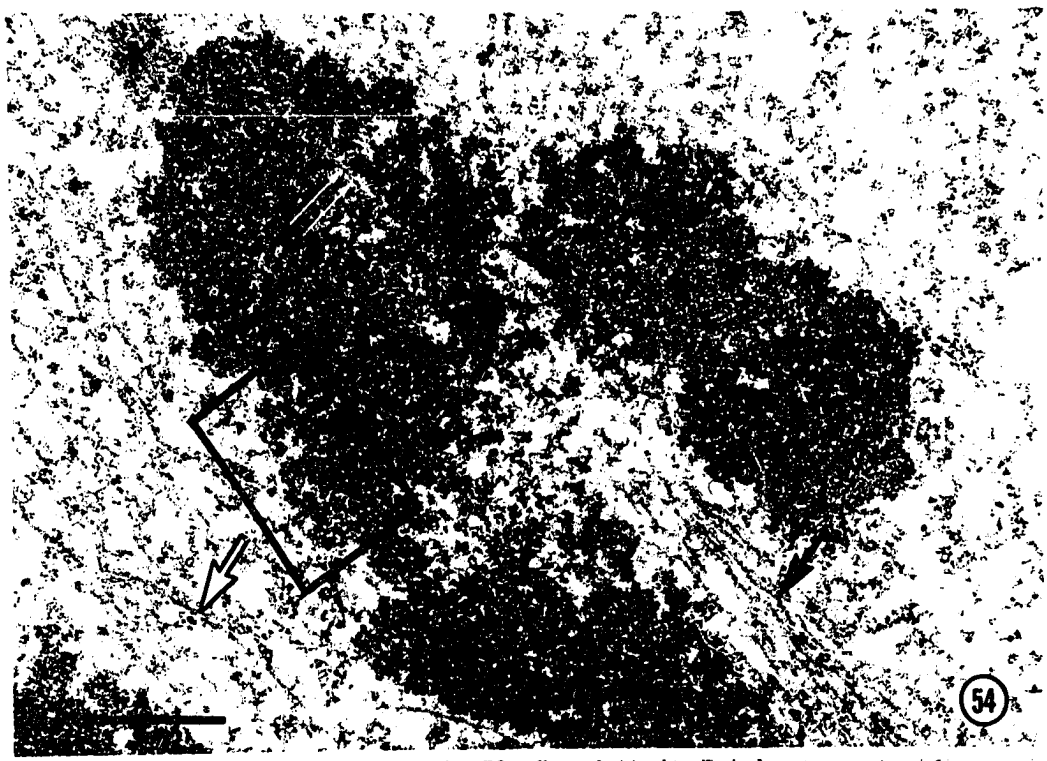
54

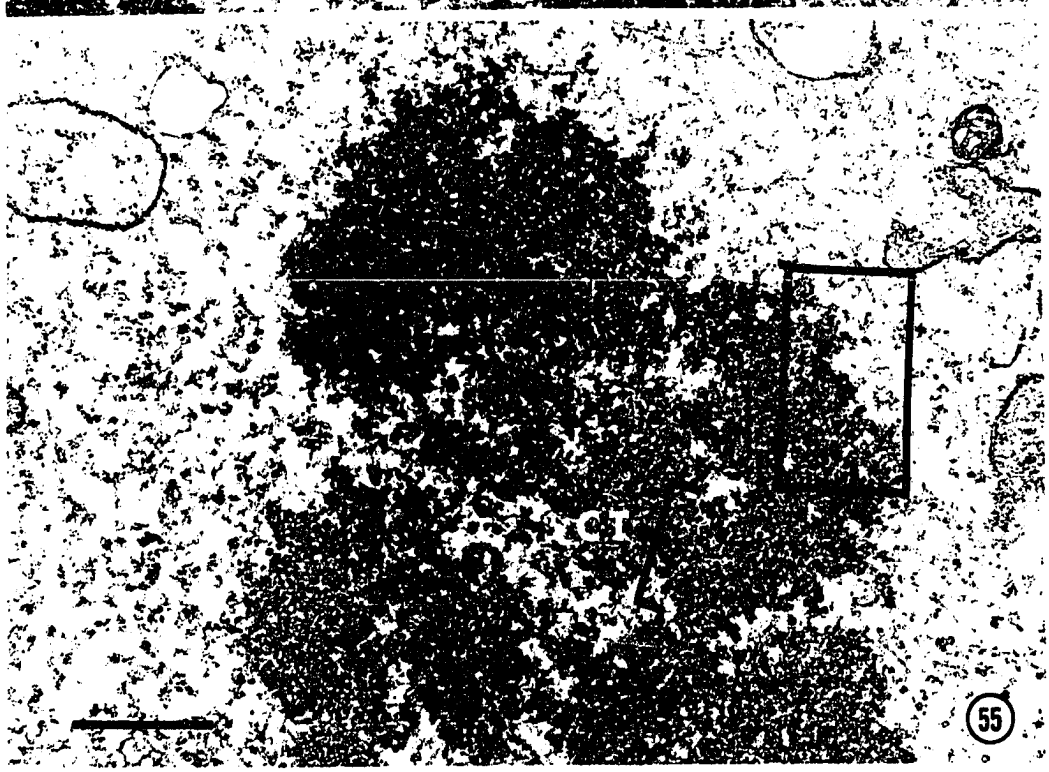
55

Figures 56-59. Metaphase I chromatin. Profiles of 80-120 nm elements (arrows) forming undulations at the edges of the chromosomes. Glutaraldehyde, osmium fixation. Line scales = 0.5 μm. 40,000 x

Figure 56. Area enlarged from Figure 53

Figure 57. Curved profiles of 80-120 nm elements suggest their coiling

Figure 58. Area enlarged from Figure 54

Figure 59. Area enlarged from Figure 55

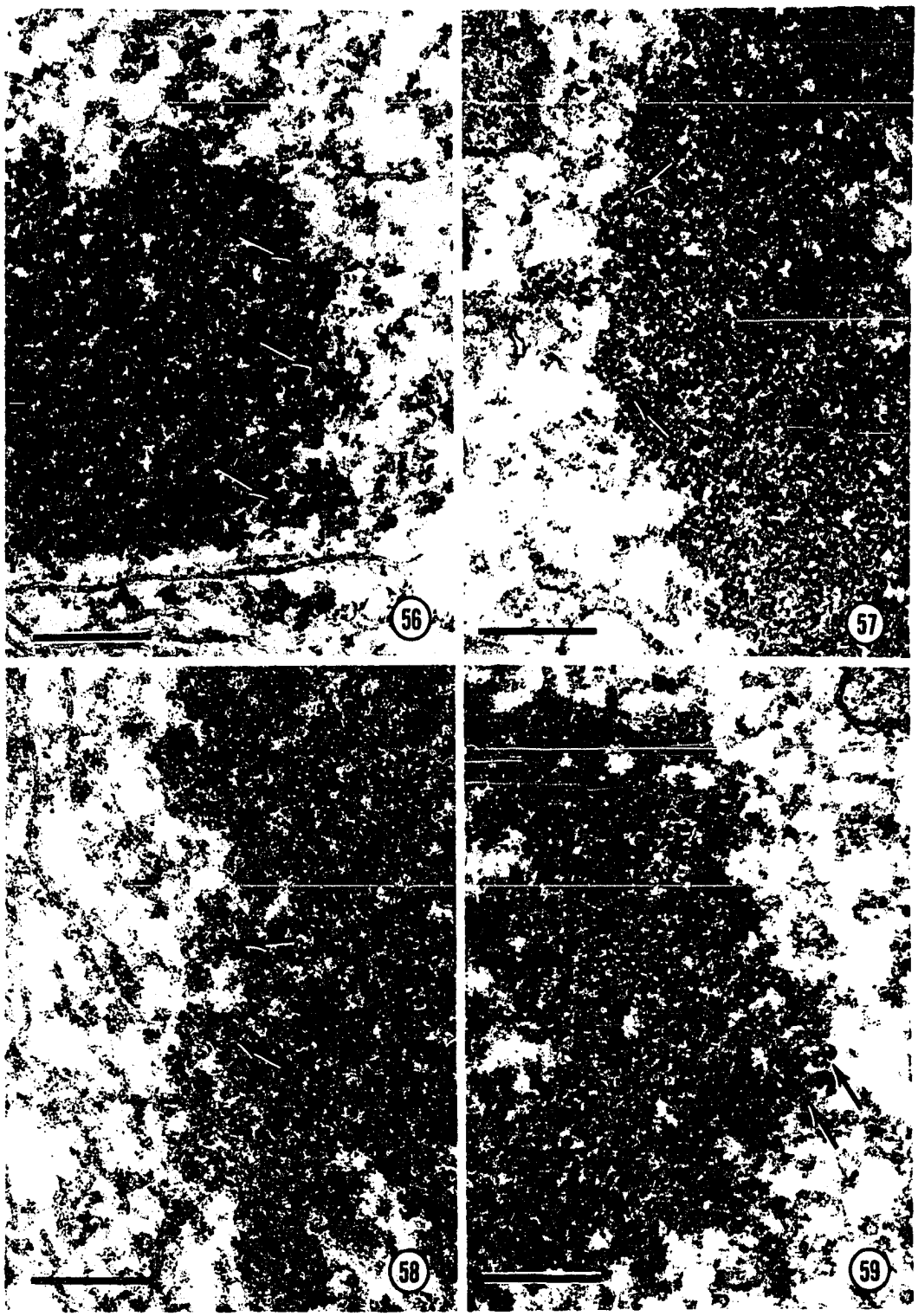
56
57
58
59

Figures 60-63. Sections 1, 14, 40, and 50 of 50 serial sections of a metaphase I bivalent. Chromosome one (CH_1) was the first chromosome in the plane of sectioning (Figure 60), then both chromosomes were equally in the plane of sectioning (Figure 61), and finally the second chromosome (CH_2) was the chromosome in the plane of sectioning (Figure 63). Clear spaces (KS) indicate boundaries between the homologues, between the chromatids (CT), and between subchromatids (SCT). The large clear space between the homologues in Figure 61 is seen to be continuous with the surrounding nucleoplasm in Figure 60 (arrows). No boundaries are evident between the homologues in the regions of chiasmata (1 and 2) in Figure 61. Glutaraldehyde-acrolein, osmium fixation. Line scales = 1 μm. 11,000 x

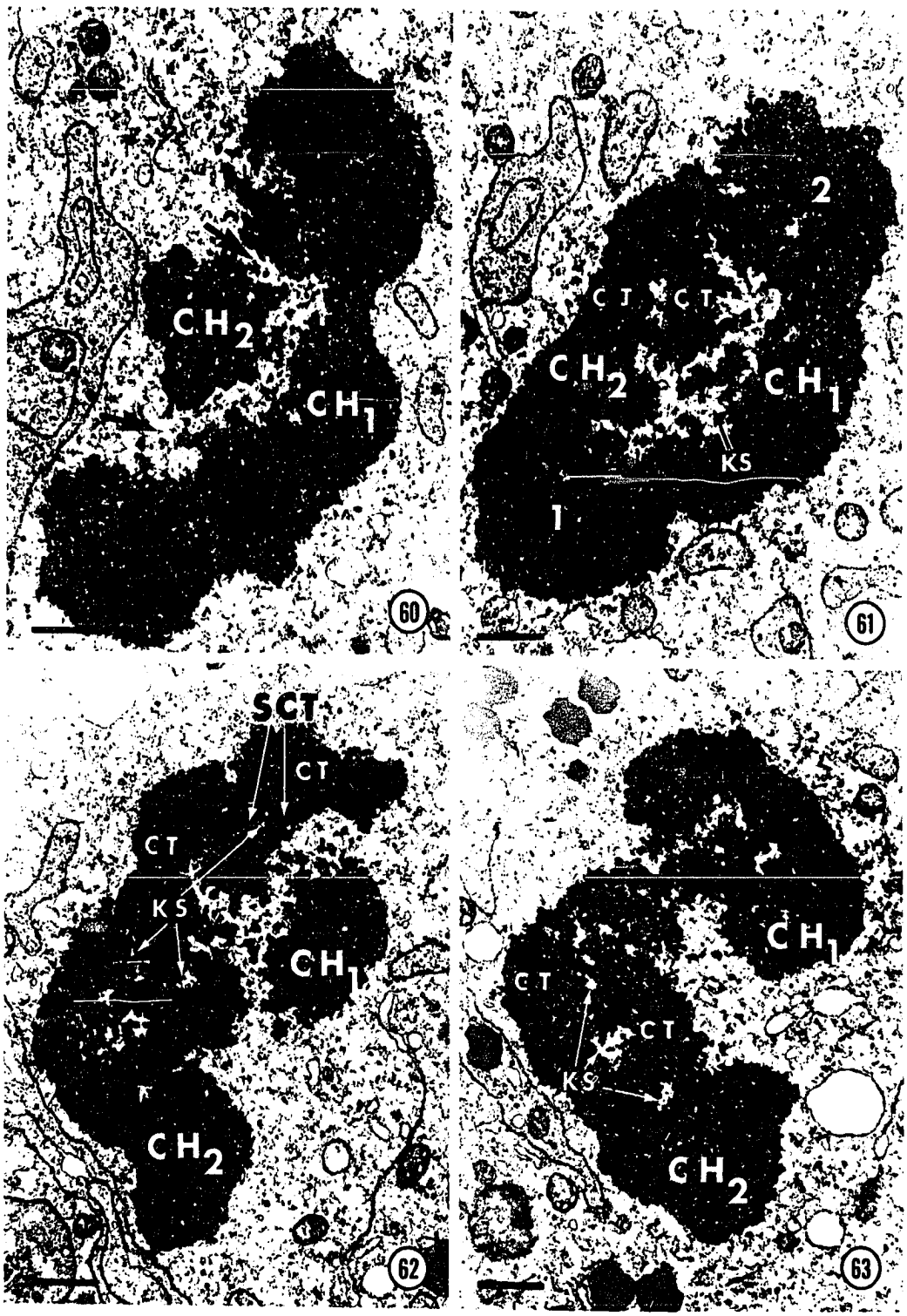
CH2
CH1
60
2
CT
CT
CH2
CH1
KS
1
61
SCT
CT
CT
KS
CH1
CH2
62
CH1
CT
CT
KS
CH2
63

Figures 64-75. Serial sections through portion of a metaphase I bivalent (B). Gaps occur between Figures 66 and 67 (four sections), Figures 67 and 68 (five sections), and Figures 72 and 73 (approximately 10 sections). Chromatids (CT) are delineated within chromosomes (CH) by clear spaces (KS), as are subchromatids (SCT) within chromatids. The clear space on the left in Figure 68 appears isolated with in the chromatin mass, but in Figure 69 it is seen to be continuous (arrow) with the surrounding nucleoplasm. Glutaraldehyde-acrolein, osmium fixation. Line scale = 1 μm. 8,600 x

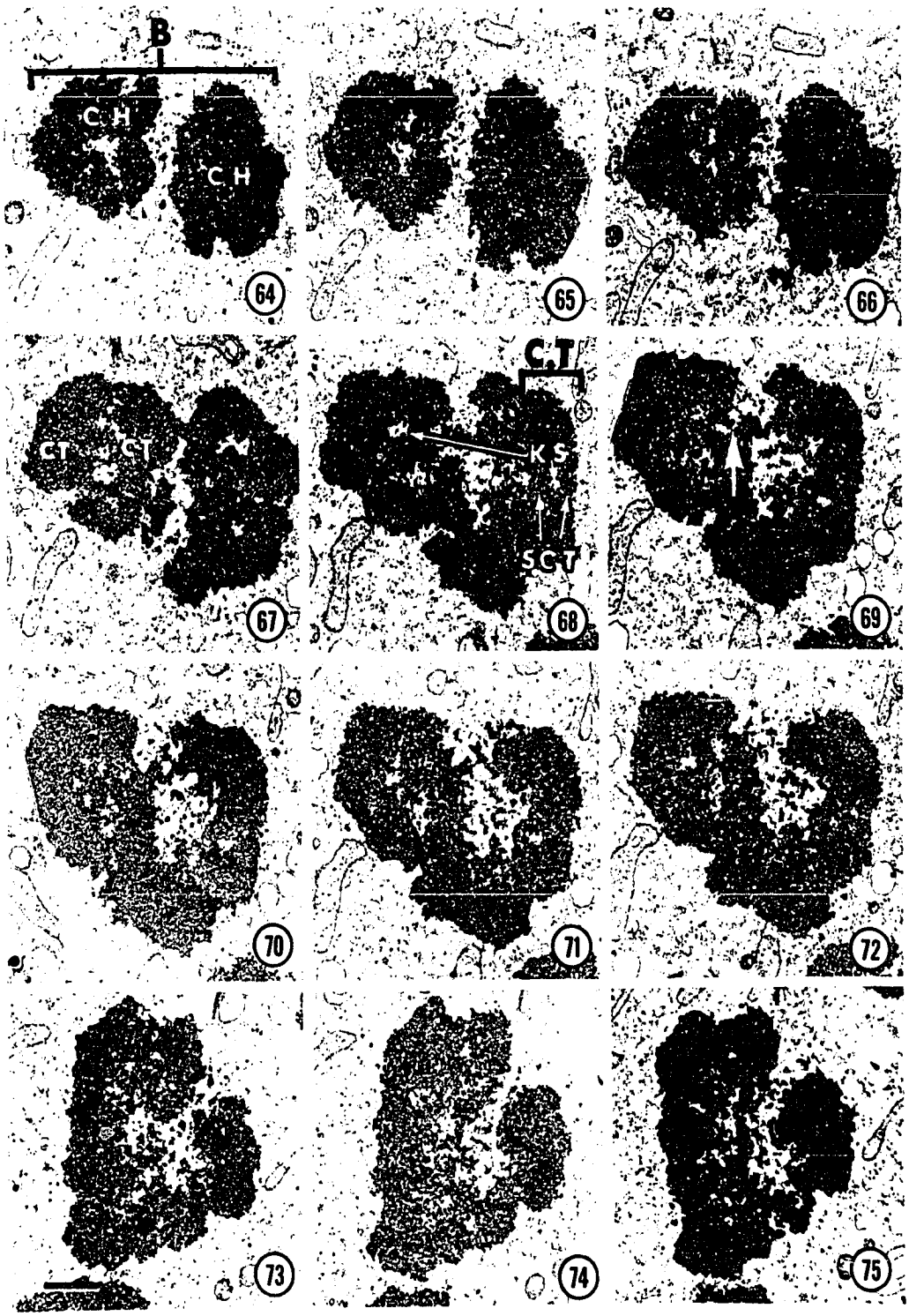
B
C H
C H
64
65
66
C T
C T
67
C T
K S
S C T
68
69
70
71
72
73
74
75

Figures 76-84. Longitudinal serial sections through the telomere region of a metaphase I bivalent (gap of unknown number of sections between Figures 81 and 82). No special structures are observable at the telomeres (small arrows, Figure 79), but two chromatid size units (1 in Figures 76-81, and 2 in Figures 82-84) are continuous between the homologues (CH). Exchange of chromatin between homologues also occurs away from the telomeres, but these units have very irregular profiles ranging from subchromatid size to chromatid size (large arrows in Figures 78 and 84). Glutaraldehyde-acrolein, osmium fixation. Line scale = 1 μm. 8,600 x

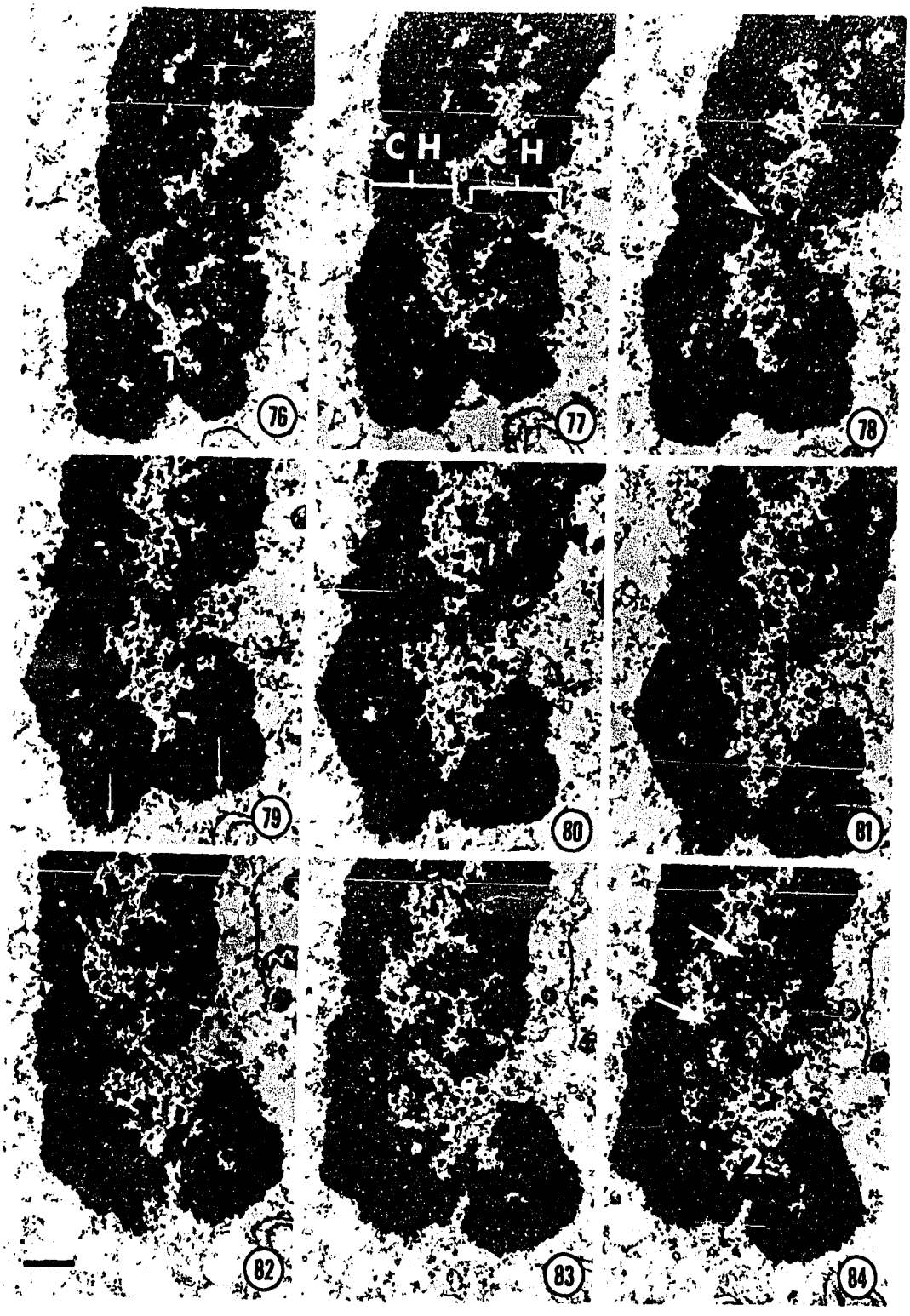
CH
CH
76
77
78
79
80
81
82
83
84

Figure 85. Metaphase I kinetochore (K) enlarged from Figure 52. Microtubules (M) associate with and are embedded in the kinetochore, but no specific attachment sites are evident. Arrow indicates a 7-20 nm diameter kinetochore fibril. Glutaraldehyde, osmium fixation. Line scale = 0.5 μm. 50,000 x

Figure 86. Section adjacent to one in Figure 85. Small arrow indicates an irregular kinetochore fibril. One microtubule (large arrow) grazes the kinetochore and passes into the chromosome mass. A clear space (KS) marks the boundary between the two chromatids (CT) attached to the kinetochore. Glutaraldehyde, osmium fixation. Line scale = 0.5 μm. 50,000 x

Figure 87. Metaphase I kinetochore (K). Arrow indicates a electron-dense chromatin fibril projecting into the relatively lighter kinetochore region. Glutaraldehyde, osmium fixation. Line scale = 0.5 μm. 50,000 x.

Figure 88. Metaphase I kinetochore (K). Arrows indicate electron-dense chromatin fibrils projecting into the lighter kinetochore region. Glutaraldehyde, osmium fixation. Line scale = 0.5 μm. 50,000 x

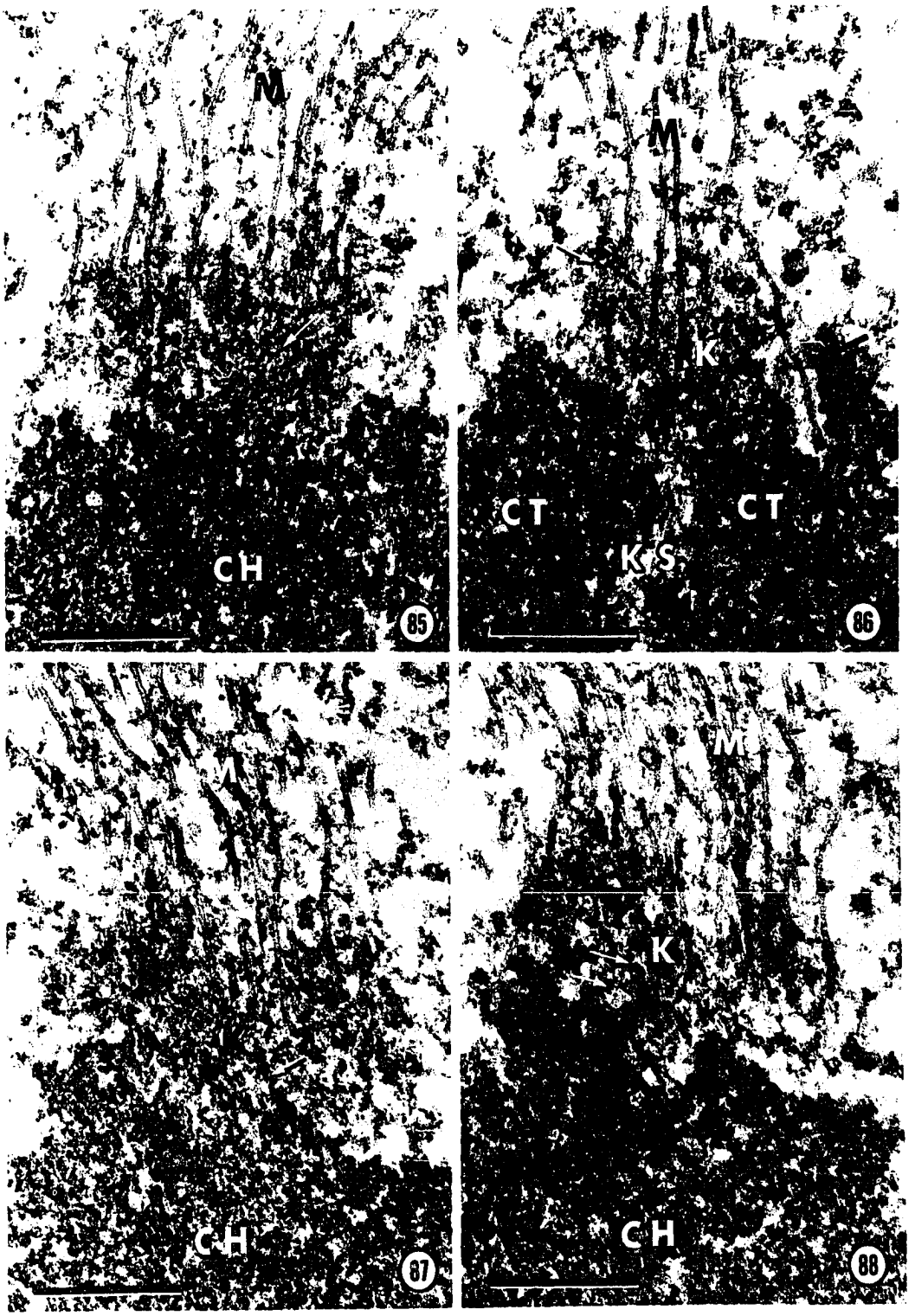
M
CH
85
M
K
CT
CT
K
S
86
M
CH
87
M
K
CH
88

Figures 89-96. Metaphase I chromatin presented with duplicate micrographs side-by-side so that interpretations may be presented and compared to the untouched micrographs. Glutaraldehyde, osmium fixation. Line scales = 0.2 μm. 50,000 x

Figure 89. Compare to Figure 90

Figure 90. Interpretation of 20 nm fibril profiles that appear coiled into a 80-120 nm element

Figure 91. Compare to Figure 92

Figure 92. Interpretations of 20 nm fibril profiles that appear coiled into 80-120 nm elements

Figure 93. Compare to Figure 94

Figure 94. Interpretation of 20 nm fibril profiles that appear coiled into a 80-120 nm element

Figure 95. Compare to Figure 96

Figure 96. Interpretations of 20 nm fibril profiles that appear coiled into 80-120 nm elements

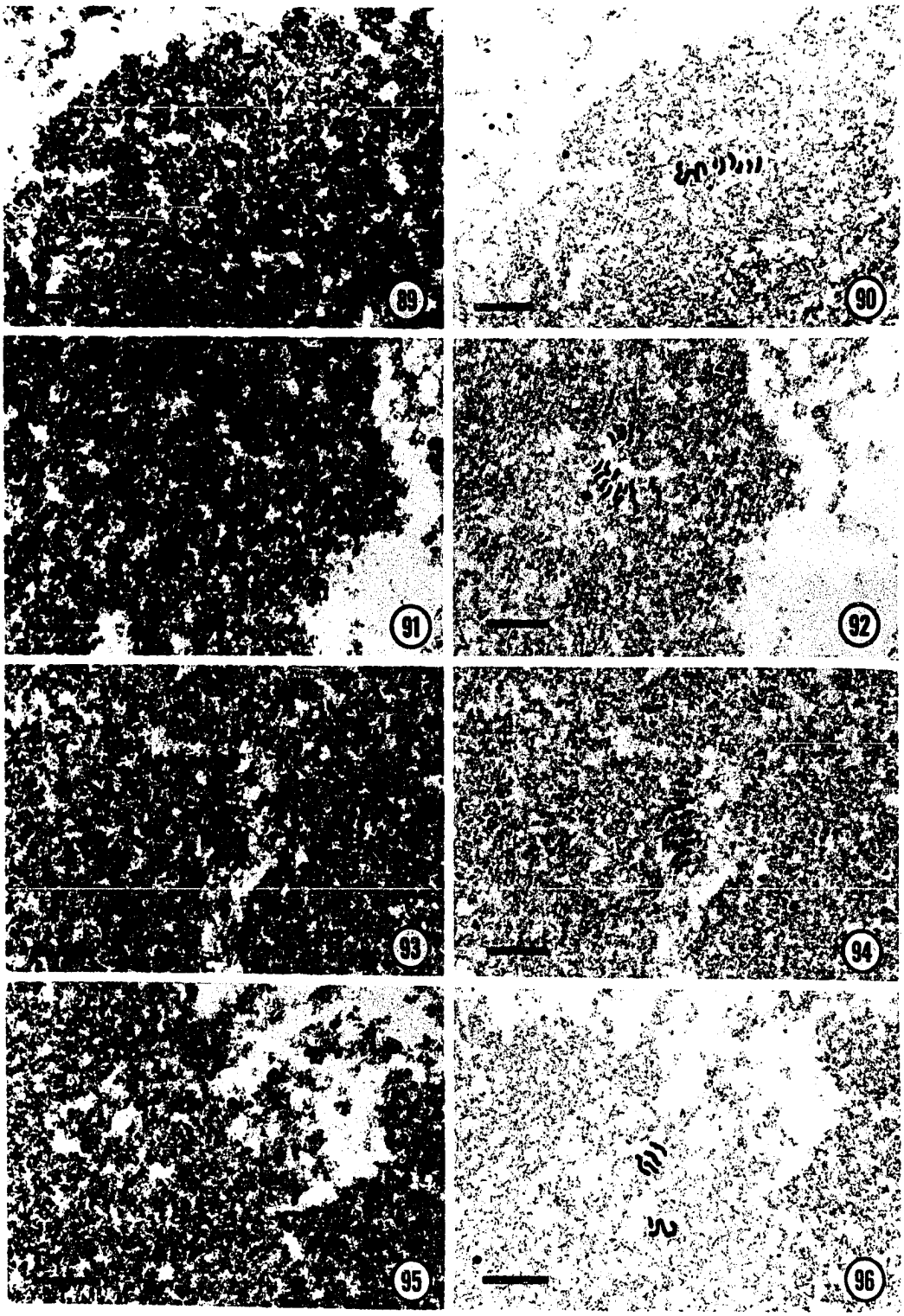
89
90
91
92
93
94
95
96

Figure 97. Light micrograph of anaphase I. Glutaraldehyde, osmium fixation. Line scale = 10 μm. 850 x

Figure 98. Survey micrograph of anaphase I. Each of the arms of the chromosomes actually consist of one chromatid arm (CT). The area enclosed in the rectangle is enlarged in Figure 100, and the kinetochore (K) is enlarged in Figure 103. Glutaraldehyde, osmium fixation. Line scale = 1 μm. 10,000 x


97
98

Figure 99. Anaphase I chromosome with three of the four chromosome arms in the plane of sectioning. Clear spaces (arrows) indicate boundaries between subchromatids (SCT). Kinetochore (K) is less electron-dense than the rest of the chromatin. Glutaraldehyde-acrolein, osmium fixation. Line scale = 1 μm. 25,000 x


SCT
SCT
99

Figure 100. Area enlarged from Figure 98. Clear space (KS) indicates boundary between 800-900 nm subchromatids (SCT). Arrows indicate 80-120 nm elements forming undulating profiles at the edge of the chromosome. Glutaraldehyde, osmium fixation. Line scale = 0.5 μm. 30,000 x

Figure 101. Anaphase I chromatin. Arrows indicate 80-120 nm elements forming undulating profiles at the edge of the chromosome. Glutaraldehyde-acrolein, osmium fixation. Line scale = 0.5 μm. 30,000 x

Figure 102. Anaphase I chromatin. Arrows indicate 80-120 nm elements forming undulating profiles at the edge of the chromosome. Glutaraldehyde, osmium fixation. Line scale = 0.5 μm. 30,000 x

Figure 103. Anaphase I kinetochore (K) enlarged from Figure 98. The kinetochore is less electron-dense than the rest of the chromosome (CH) and consists of 7-20 nm diameter fibrils (arrows). Microtubules (M) connect to and are embedded in the kinetochore, but no specific attachment sites are evident. Glutaraldehyde, osmium fixation. Line scale = 0.5 μm. 50,000 x

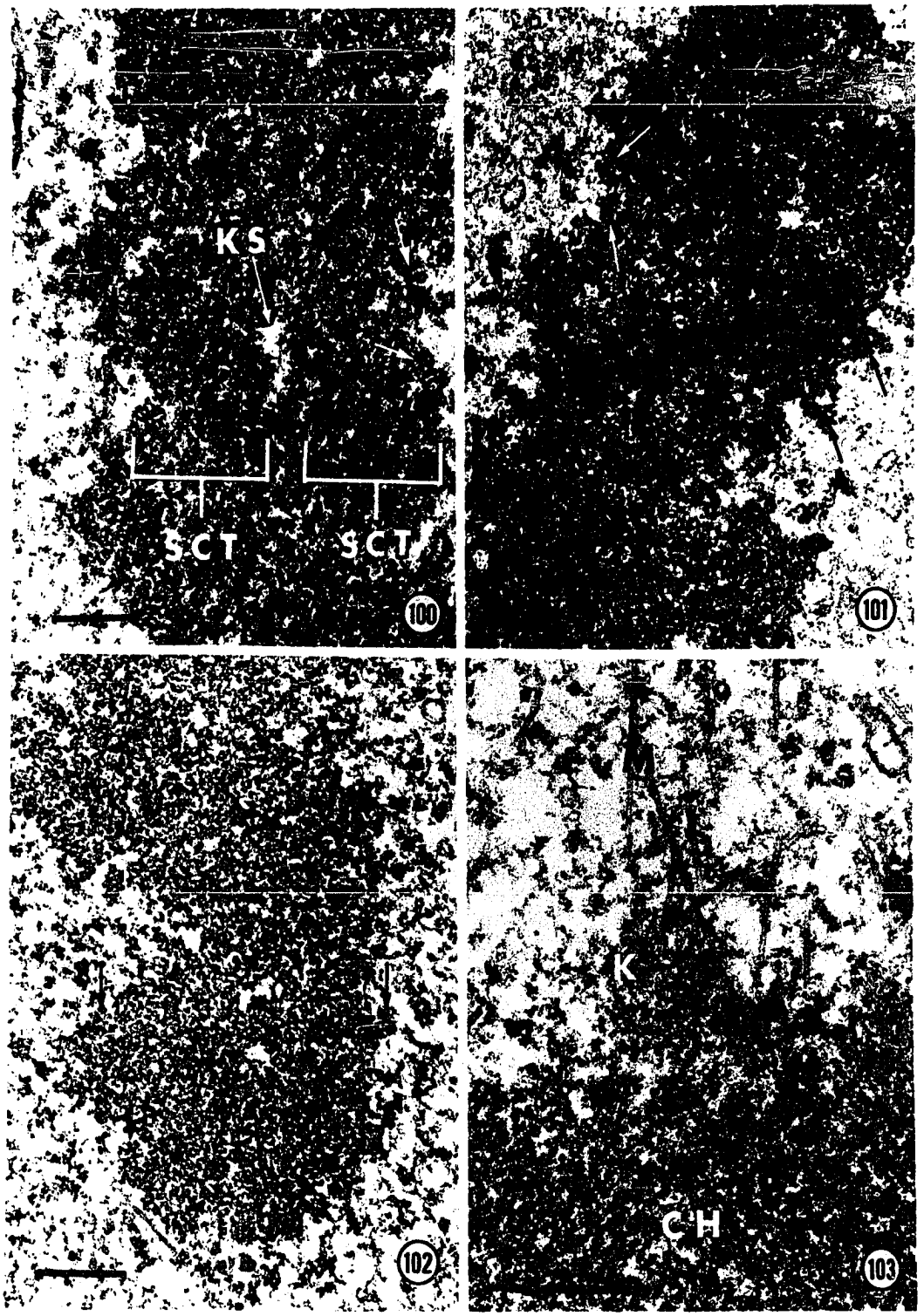
KS
SCT
SCT
100
101
102
K
CH
103

Figure 104. Anaphase I. Light micrograph illustrating same orientation as Figures 105 and 106. Glutaraldehyde-acrolein, osmium fixation. Line scale = 10 μm. 850 x

Figure 105. Survey micrograph of cross section of anaphase I chromosome (chromatid) arms (CT) to be compared to Figure 106. Area enclosed in brackets is enlarged in Figure 108. Glutaraldehyde-acrolein, osmium fixation. Line scale = 1 μm. 10,000 x

Figure 106. Survey freeze-etch micrograph of cross fracture of chromosome (chromatid) arms (CT). Area within brackets is enlarged in Figure 107. Arrow in upper left corner indicates the direction of the platinum "shadow". Line scale = 1μm. 10,000 x

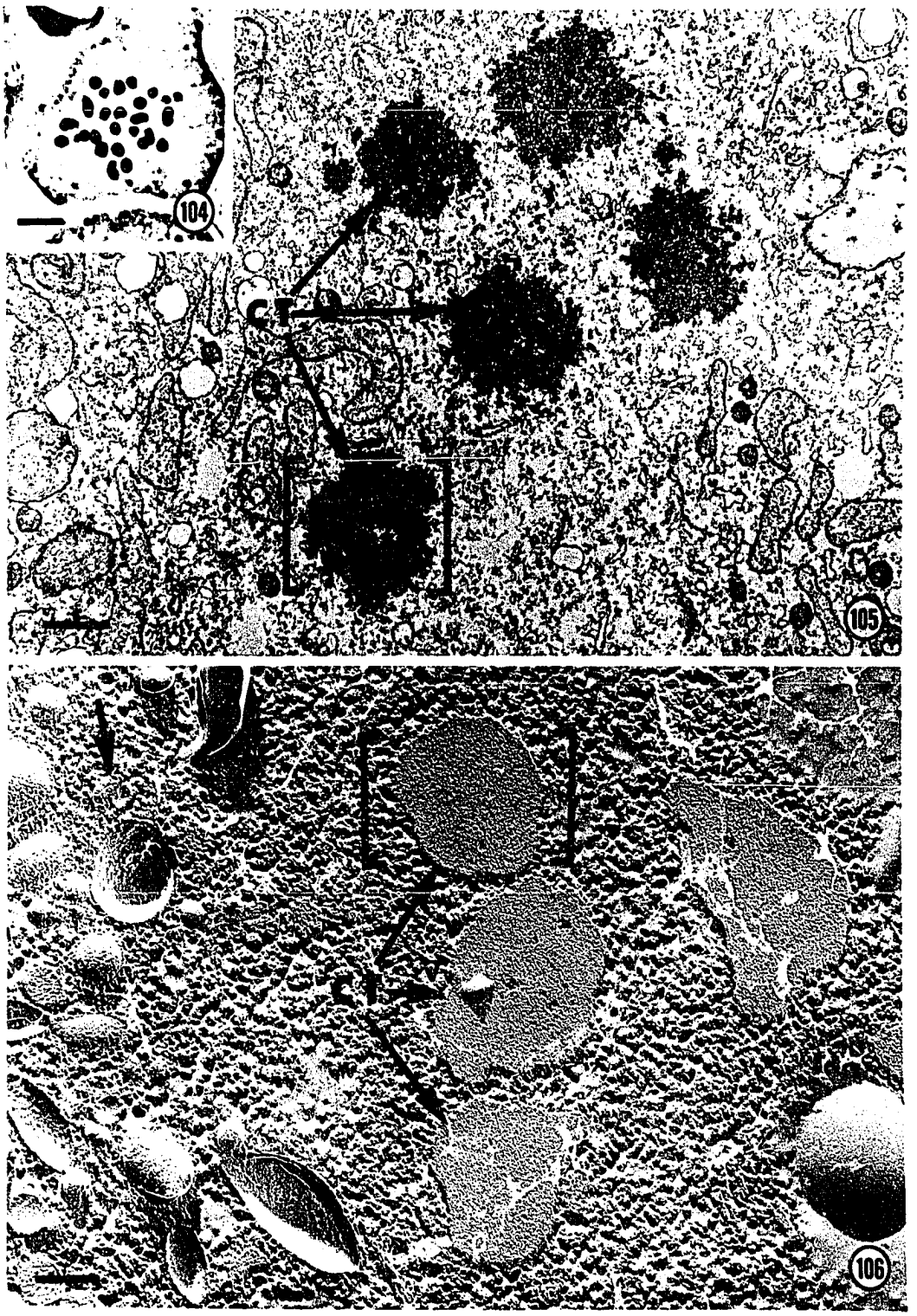
104
105
106

Figure 107. Freeze-etch preparation of cross section of anaphase I chromosome (chromatid) arm enlarged from Figure 106. Small arrows point to areas that may correspond to clear spaces seen in thin sectioned chromatin. Freeze-etched chromatin consists of 10 nm diameter fibrils. The space between this figure and Figure 108 was not routed so that the fibrils in the two types of preparation may be easily compared. Arrow in upper left corner indicates the direction of the platinum "shadow". Line scale = 0.5 μm. 60,000 x

Figure 108. Cross section of anaphase I chromosome (chromatid) arm enlarged from Figure 105. Profiles of the fibrils are 20 nm in diameter. Profiles of 80-120 nm elements (arrows) form undulations (suggestive of coiling) at the edge of the chromatin. Glutaraldehyde-acrolein, osmium fixation. Line scale = 0.5 μm. 60,000 x

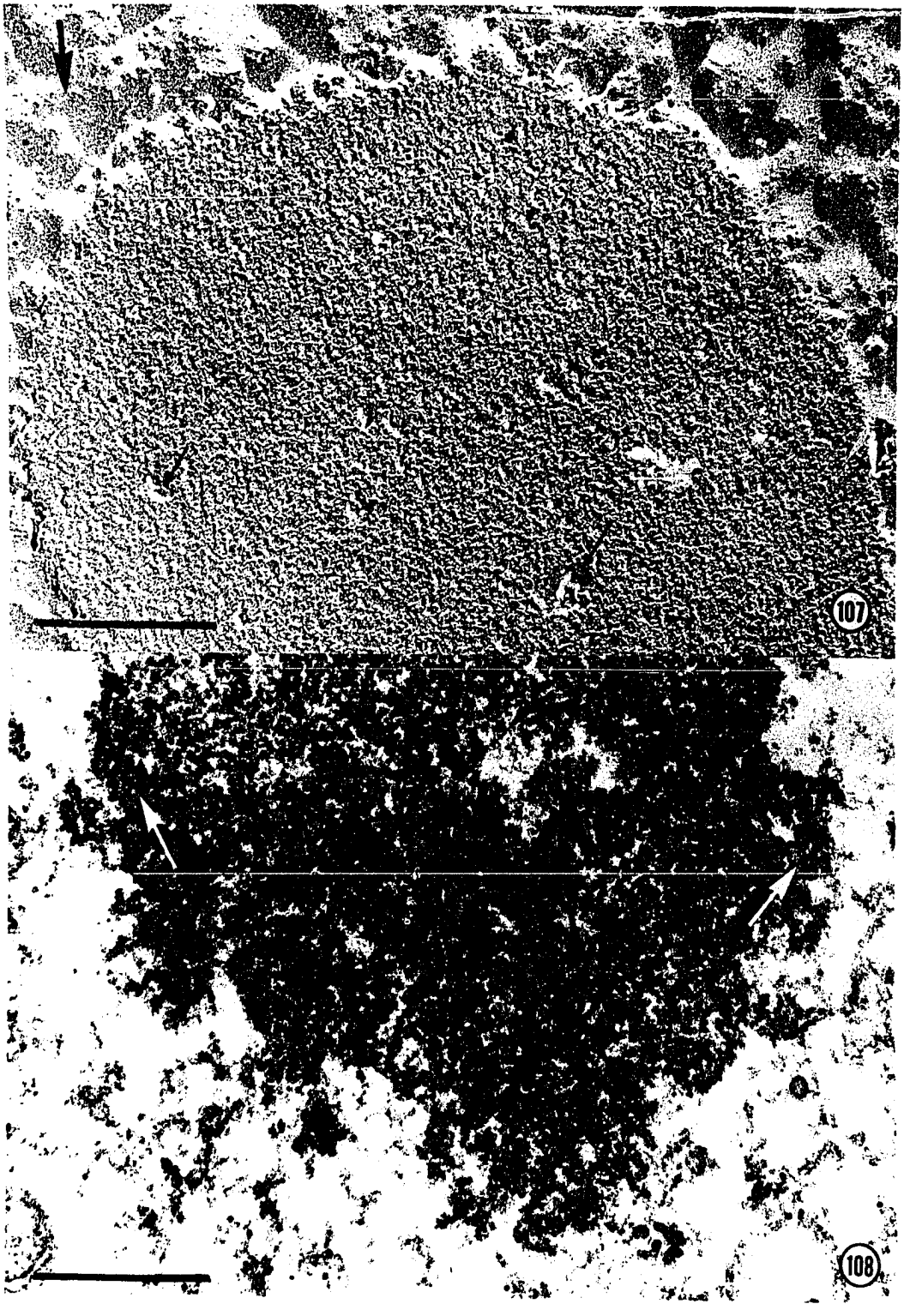
107
108

Figures 109-114. Anaphase I chromatin presented with duplicate micrographs side-by-side so that interpretations may be presented and compared to the untouched micrographs. Glutaraldehyde-acrolein, osmium fixation. Line scales = 0.2 μm. · 50,000 x

Figure 109. Compare to Figure 110

Figure 110. Interpretations of 20 nm fibril profiles that appear coiled into 80-120 nm elements

Figure 111. Compare to Figure 112

Figure 112. Interpretations of 20 nm fibril profiles that appear coiled into 80-120 nm elements

Figure 113. Compare to Figure 114

Figure 114. Interpretations of 20 nm fibril profiles that appear coiled into 80-120 nm elements

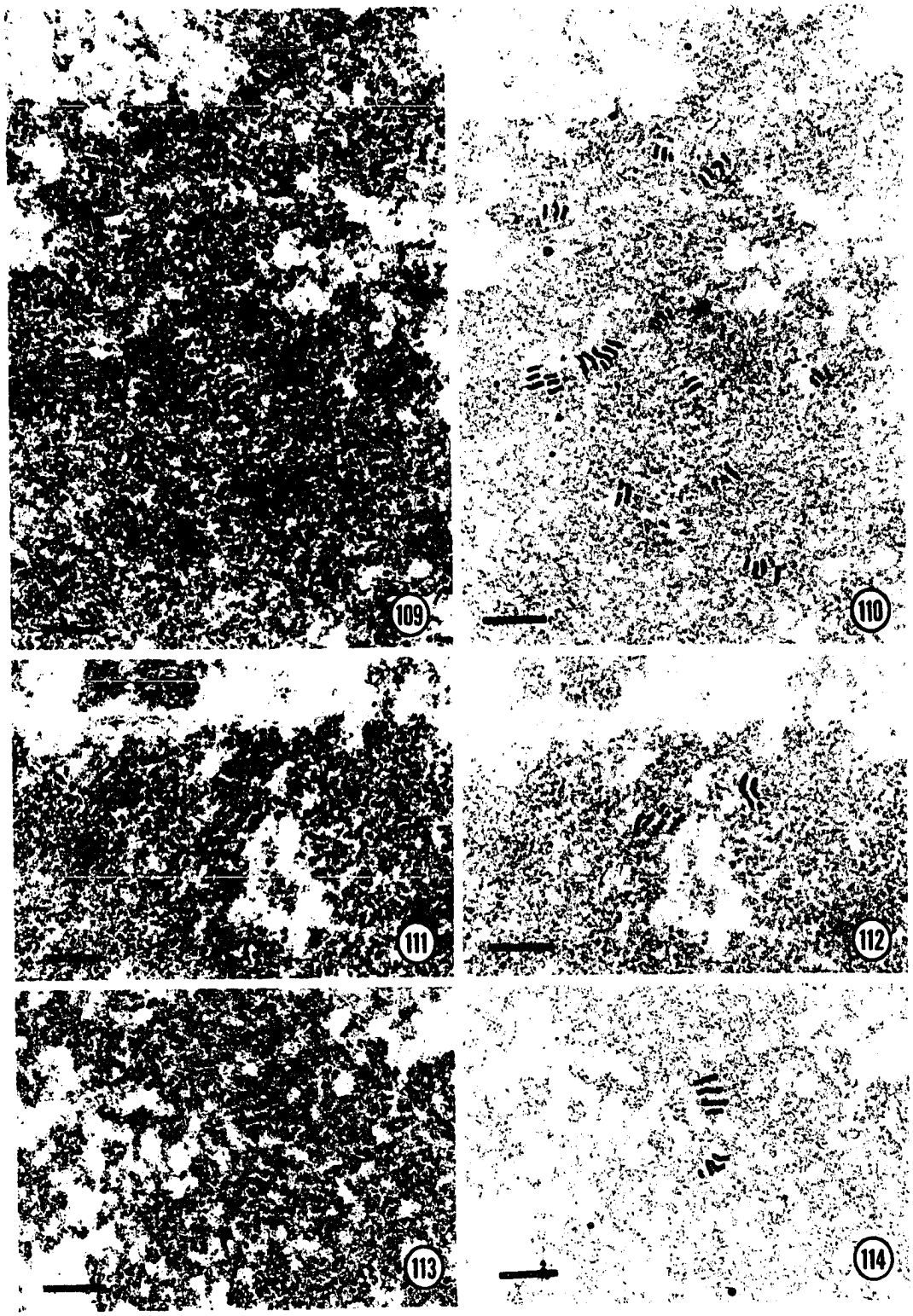
109
110
111
112
113
114

Figure 115. Light micrograph of early telophase I. Glutaraldehyde-acrolein, osmium fixation. Line scale = 10 μm. 850 x

Figure 116. Survey micrograph of telophase I in which the chromosomes have relaxed and the nucleolus (Nu) is reforming. The 400 nm profiles (arrows) are loosely twisted within the chromosomes. Area enclosed within the rectangle is enlarged in Figure 117. Glutaraldehyde-acrolein, osmium fixation. Line scale = 1 μm. 10,000 x

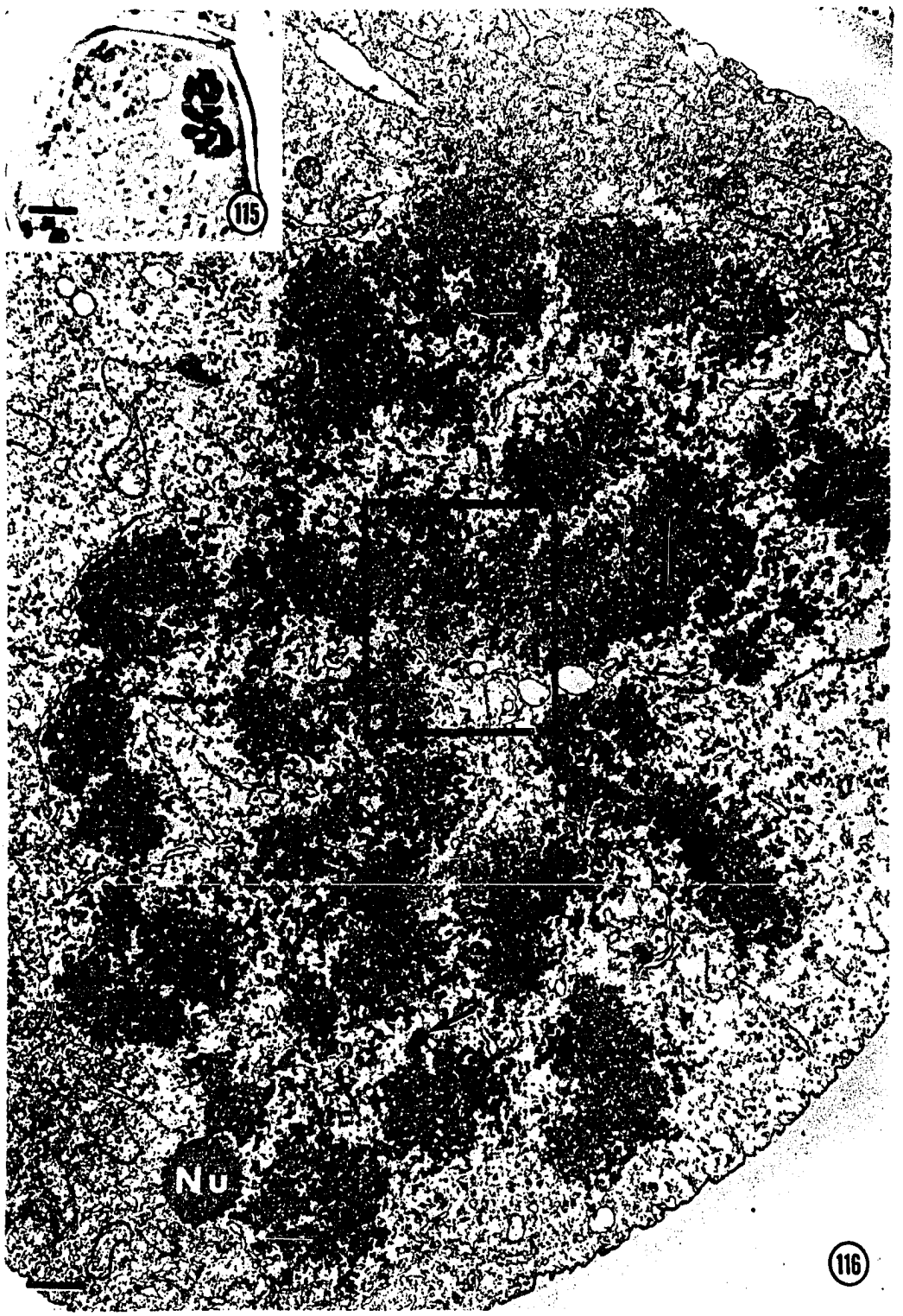
115
Nu
116

Figure 117. Telophase I. Area enlarged from Figure 116. The kinetochore (K) is less electron-dense than the rest of the chromatin and consists of 7-20 nm diameter fibrils (small arrow). A profile of a 80-120 nm element (large arrow) appears coiled into a 400 nm unit. Other 400 nm units (brackets) appear loosely arranged into the chromosomes. Glutaraldehyde-acrolein, osmium fixation. Line scale = 0.5 μm. 50,000 x

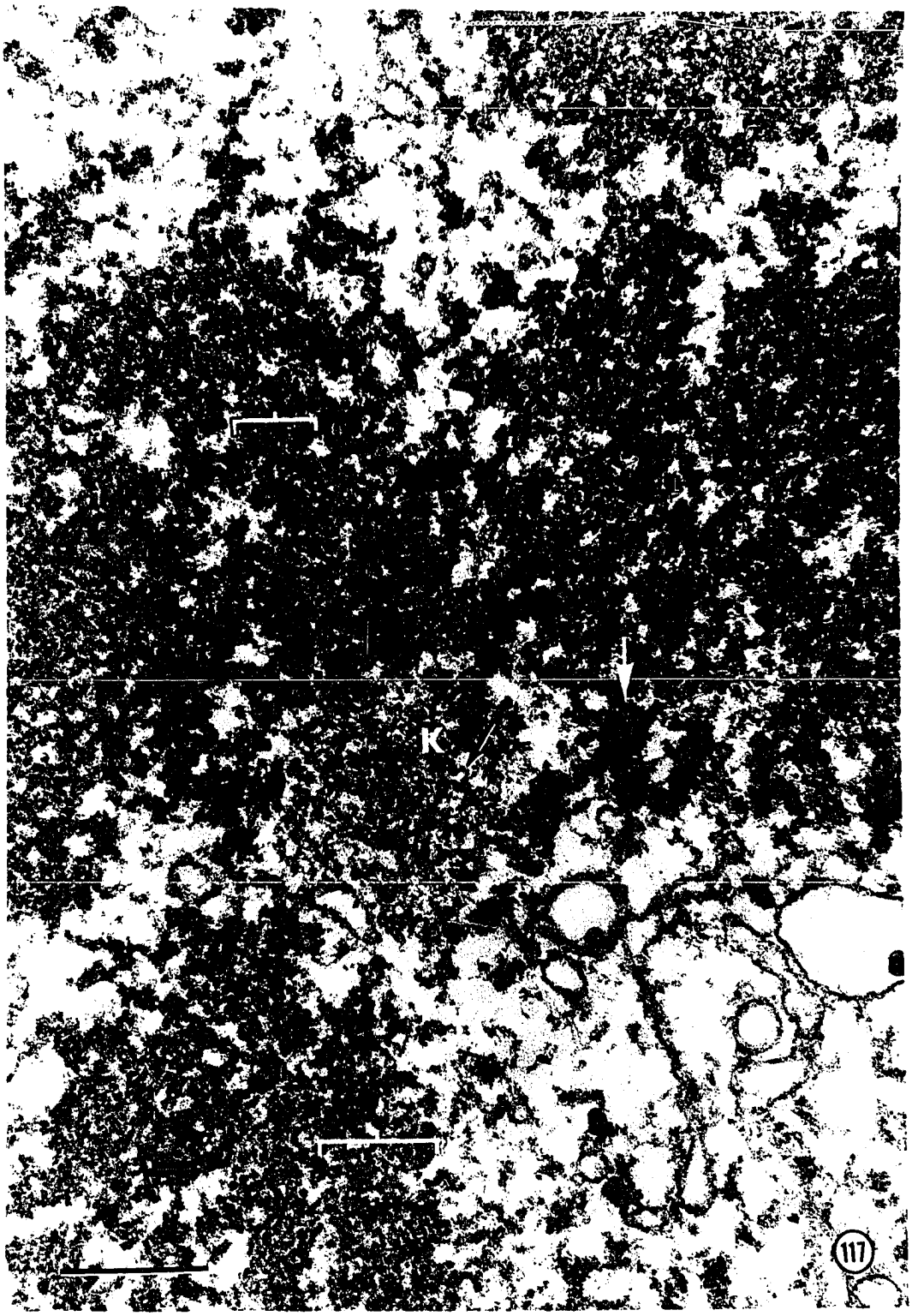
K
117

Figures 118-121. Diagrams to depict author's interpretation of organization and behavior of first meiotic division chromatin of *Lilium*. Line scales approximately = 0.2 μm

Figure 118. Leptotene. Elementary chromosome fibril (ECF) coils to form the first order coil (FOC), which in leptotene is the 80-120 nm chromatid (CT). Two chromatids constitute a 300-500 nm chromosome (CH)

Figure 119. Zygotene. Synapsis begins and the synaptinemal complex (sc) appears. The chromatids, and consequently the chromosomes, thicken due to the supercoiling of the first order coil

Figure 120. Pachytene. Synapsis is completed. First order coil forms 300 nm chromatids. Here, as in the earlier stages, no structures that can be interpreted as subchromatids are evident

Figure 121. Diffuse diplotene. No observable chromatids, chromosomes, or bivalents. First order coils form 175-250 nm elements that often are paired and in later diplotene can be interpreted as subchromatids

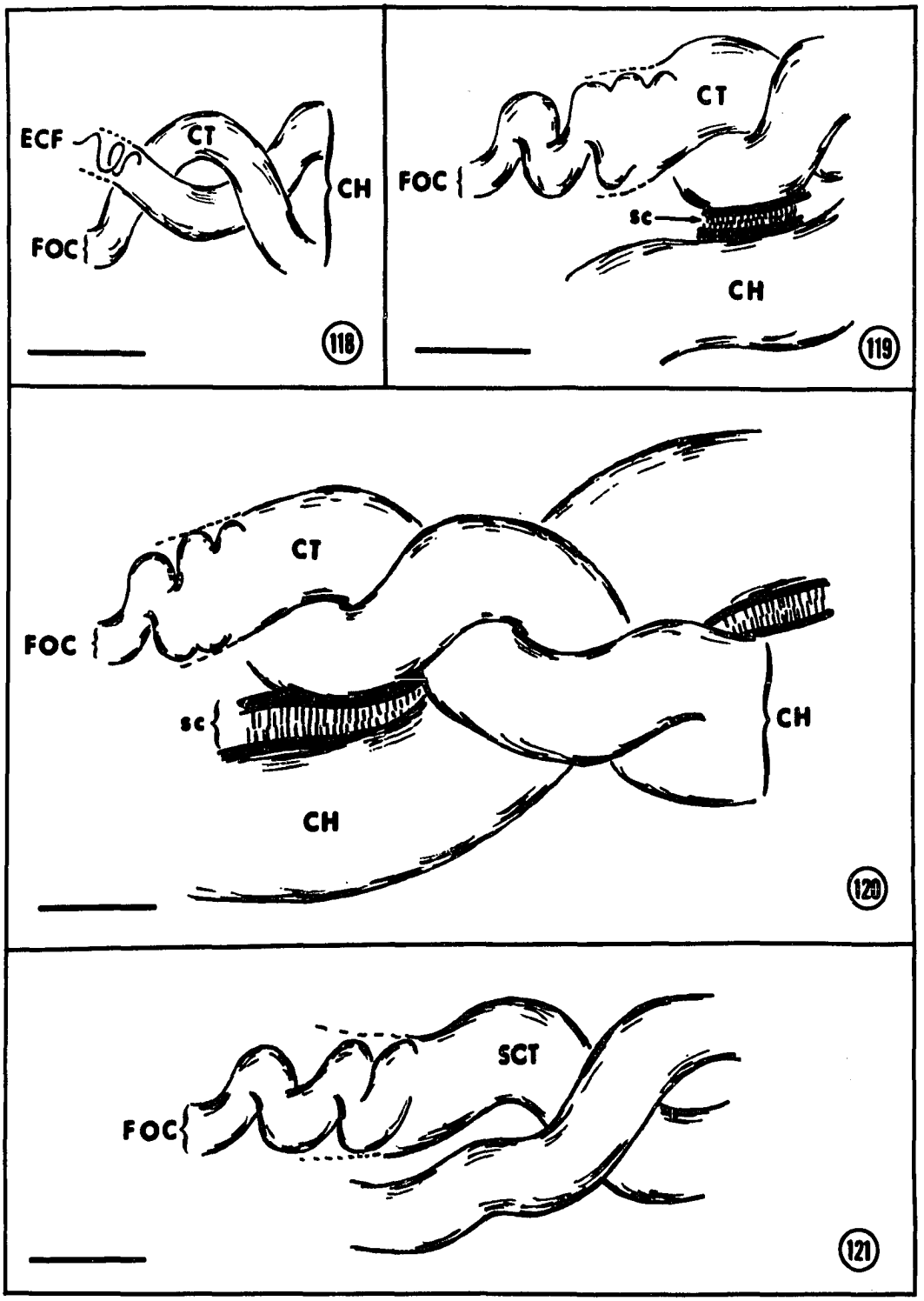
ECF
CT
CH
FOC
118
CT
FOC
sc
CH
119
CT
FOC
sc
CH
CH
120
SCT
FOC
121

Figures 122 and 123. Diagrams to depict author's interpretation of the behavior and organization of first meiotic division chromatin of Lilium. Line scales approximately = 1 μm

Figure 122. Late diplotene. First order coils form 300-400 nm subchromatids which pair to form 500-800 nm chromatids, which in turn pair to form the chromosomes. The homologues are attached to each other only at the chiasmata

Figure 123. Diakinesis. The same levels of organization as in late diplotene, only the various units, except the first order coil, are thicker and more tightly coiled

subchromatid	400-500 nm
chromatid	700-900 nm
chromosome	1.5-2.0 μm

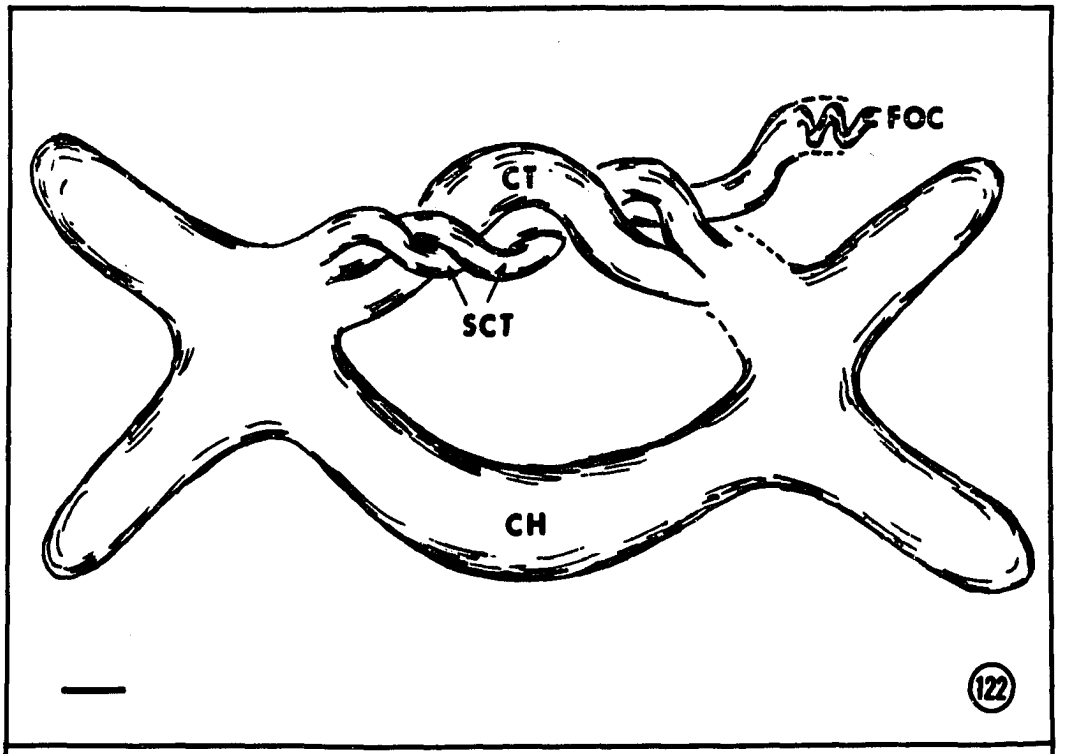
FOC
CT
SCT
CH
122

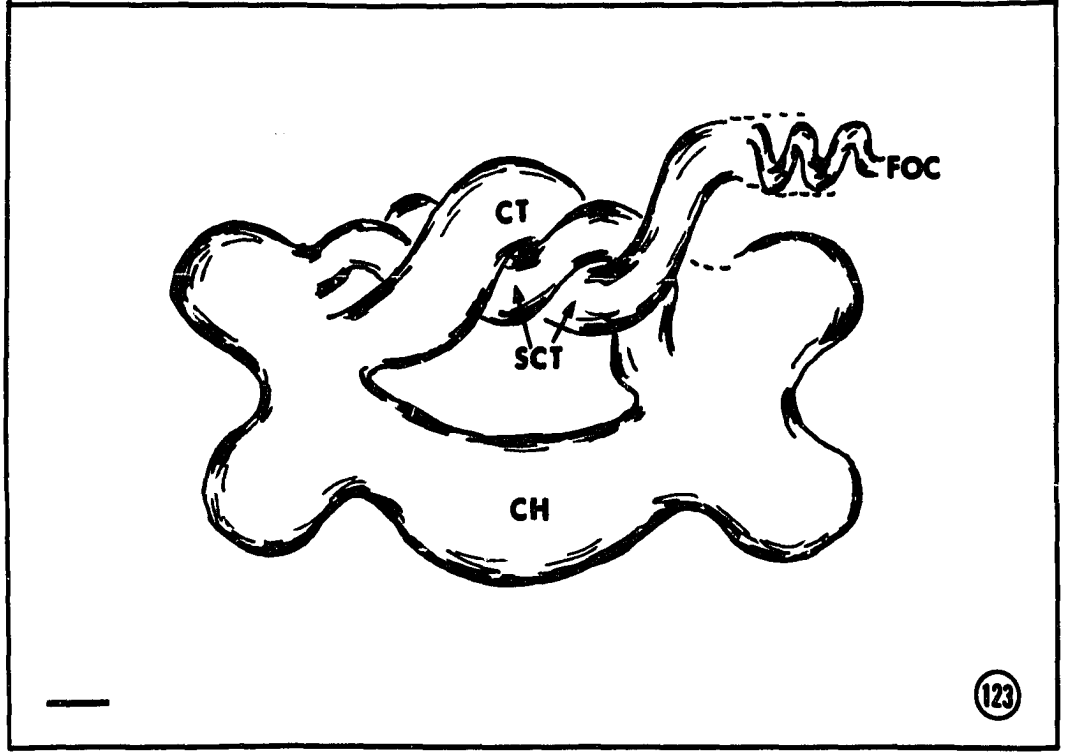
FOC
CT
SCT
CH
123

Figures 124 and 125. Diagrams to depict author's interpretation of the behavior and organization of first meiotic division chromatin of Lilium. Line scales approximately = 1 μm

Figure 124. Metaphase I. The same arrangements and levels of organization as in diakinesis, only the units are thicker and more tightly coiled

subchromatid	400-600 nm
chromatid	800-1000 nm
chromosome	2-2.5 μm

Figure 125. Anaphase I. The chromosome arms (actually chromatid arms) are separate except for their attachment near the kinetochore. The arms are more relaxed than in metaphase and the subchromatids are more easily observed

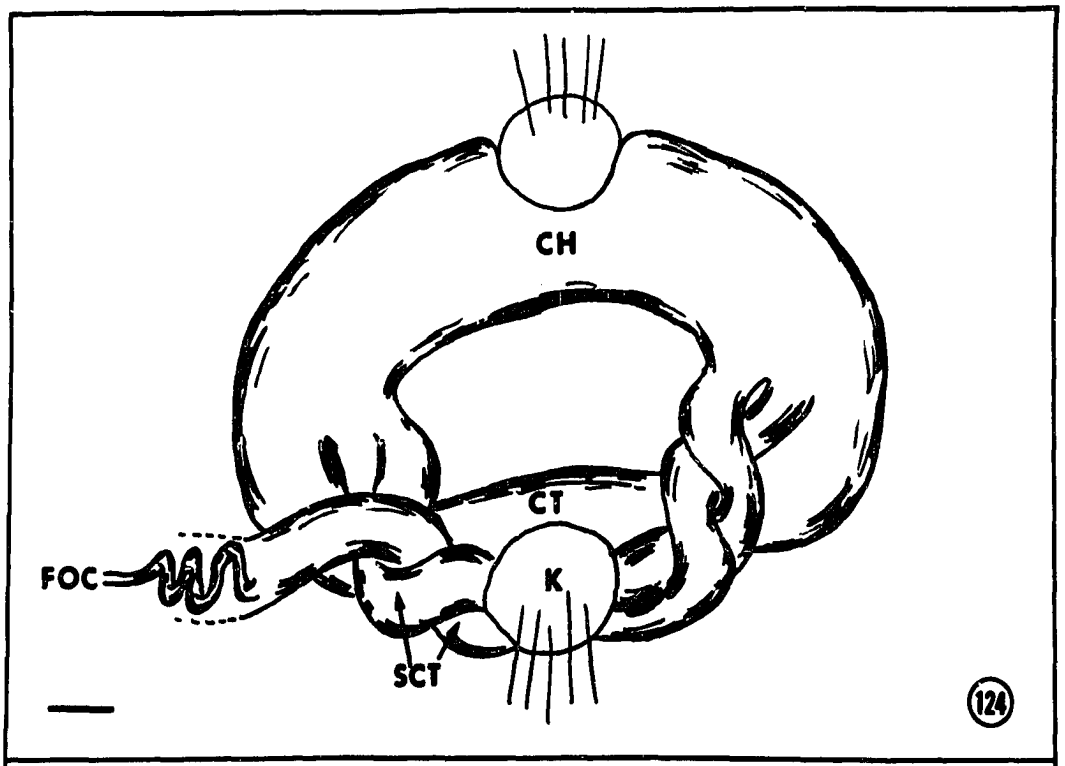

124

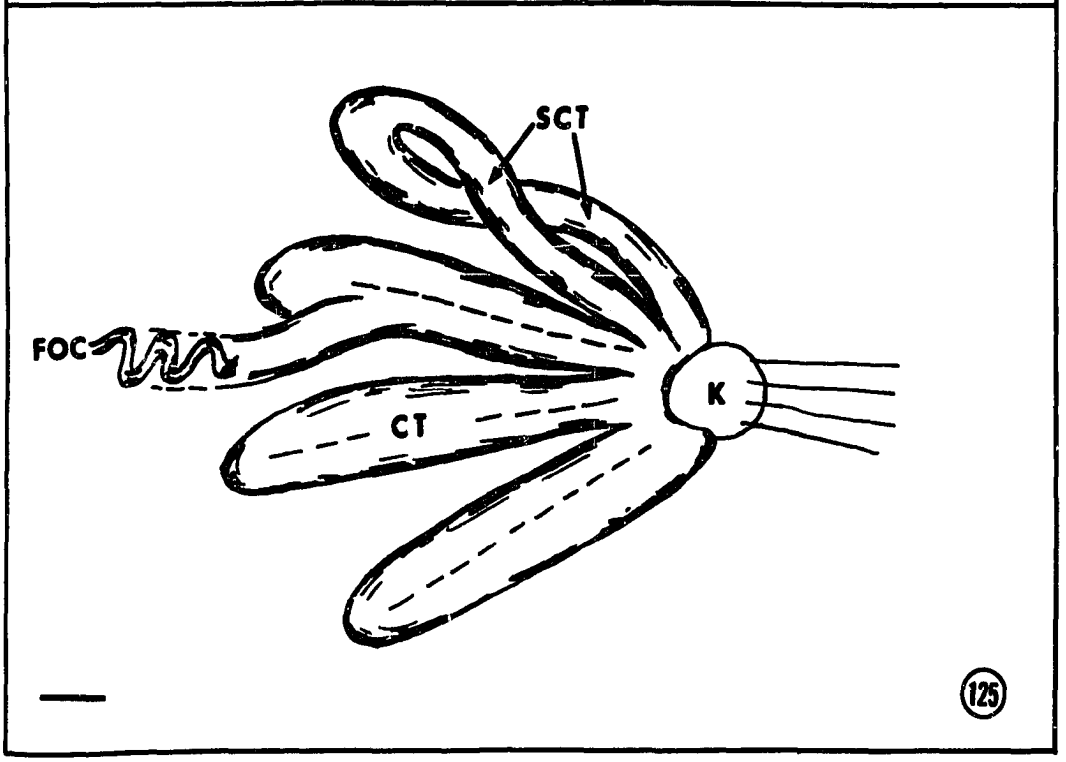

125